

Design of a Planetary-Cyclo-Drive Speed Reducer Cycloid Stage, Geometry, Element Analyses

Växjö, 2012-05-30

15p

Mechanical Engineering/ 2MT00E

Handledare: Hans Hansson, SwePart Transmissions AB

Handledare: Professor Samir Khoshaba, Linnéuniversitetet, Institutuonen för teknik

Examinator: Izudin Dugic

Thesis nr: TEK

Författare : Biser Borislavov, Ivaylo Borisov, Vilislav Panchev

Summary

This project has been assigned by SwePart Transmissions AB. It is about calculation and dimensioning, of the elements in a cycloid stage of a speed reducer. Their idea is to use the results from this project and go into production of such reducer to cover another segment of the market. The company is interested in supplying transmissions for robust systems and for various industrial purposes, where large ratios of speed reduction are needed.

The company has given the necessary input data for the model. They have also provided a real cyclo-drive reducer for further analyses. To obtain the dimensions and forming the geometry of the gears, some parts of Professor Ognyan Alipiev's Phd work have been used. Professor Alipiev is head of "Theory of Mechanisms and Machines" department in University of Ruse "Angel Kanchev", Bulgaria. For the determination of forces on the elements, models and drawings has been used Solidworks (SW) CAD software and SW simulation environment. The resultant calculation process can be used for designing the geometry and determination of the properties regarding the cycloid reducer.

Keywords: cyclo drive, cycloid speed reducer, epicycloid reducer

Acknowledgements

This project has been carried through during the spring semester 2012 at the Linnaeus University and with the assistance of SwePart Transmissions AB.

We would like to present our gratitude to the following:

- Professor Ognyan Alipiev (Angel Kunchev University, Faculty of Mechanical and Manufacturing Engineering, Ruse) for providing us with all the necessary theoretical data and also responding to the questions we had. Thank you!
- Samir Khoshaba (Linnaeus University, School of Engineering, Växjö) for supervision of the project and all the good times. Thank you!
- Hans Hansson (SwePart Transmissions AB, Liatorp) for introducing the problem and providing us with the necessary data and also his time. Thank you!
- Assistant Filip Genovski (Linnaeus University, School of Engineering, Växjö) Thank you!
- Our parents for the support. Thank you!
- Li Yawei and Wu Yuanzhe, for the group work we did together on this project. Thank you!
- The ERASMUS student exchange program. Thank you!
- The Swedish education system. Thank you!

CONTENTS

1. INTRODUCTION.....	1
1.1 Background.....	1
1.2 Task/Problem Description.....	6
1.3 Limitations.....	6
2. THEORY.....	7
2.1 Geometry.....	7
2.1.1 The epicycloid curve.....	7
2.1.2. Geometry of modified epicycloid gears.....	8
2.1.3. General concept of eccentric tool meshing.....	9
2.1.4. Basic dimensions of epicycloidal gears.....	14
2.1.5. Equations for teeth profile and curvature radius.....	17
2.1.6 Forming of the epicycloidal gear transmission.....	22
2.1.7. Action line. Contact Points.....	24
2.1.8 Distinctive Meshing Angles.....	26
2.1.9 Contact ratio.....	28
2.2. Cycloid gearbox design.....	31
2.2.1 Forces and Force distribution in the cycloid gear.....	31
2.2.2. Designing the holes and the thickness of the cycloid discs.....	33
3. METOD.....	37
3.1 Modeling in SolidWorks.....	37
3.2. Getting the results.....	37
3.3 Making Assembly and Simulation.....	38
4. RESULTS.....	40
4.1. Total ratio.....	40
4.2 SolidWorks Simulation Results.....	40
4.2.1.Cycloid Gear Results.....	41
4.2.2 Input Shaft Results.....	47
4.2.3. Output Shaft Results.....	53
4.2.4. Eccentric Shaft Results.....	60
5. ANALISYS.....	67
6. CONCLUSION.....	70
7. REFERENCES.....	71
8. APPENDIX.....	72

1. Introduction

The main aspects of the project are presented in this chapter. The background will give a general overview of the basic features about the product. The main aspects of the task are described in the problem description sub-chapter.

1.1. Background

The project has been performed in cooperation with SwePart Transmission AB. The company is a leading supplier of spare parts and transmissions for vehicles and industry. They have an idea to design a gearbox, that can replace a model of a planetary-cycloid gearbox, used in many industries such as robust systems, mines, metallurgy, chemical, and textile and in situations where high speed reduction is needed. The high ratio is provided because of the planetary and cycloid stages of speed reduction. The project is divided in two parts carried out by different groups. In this paper part one is presented, tough some data has been used from the other group's calculations. SwePart are primarily interested to know more about the general equations for calculating the properties of the second reduction stage (e.g. cycloidal stage).

This paper shows the geometrical knowledge for producing the special geometry required to draft the cycloid gear wheel. Calculated example based on the provided input data is presented (Appendix 1). The cycloid reducer is a speed reducer (shown in Figure 1 below).

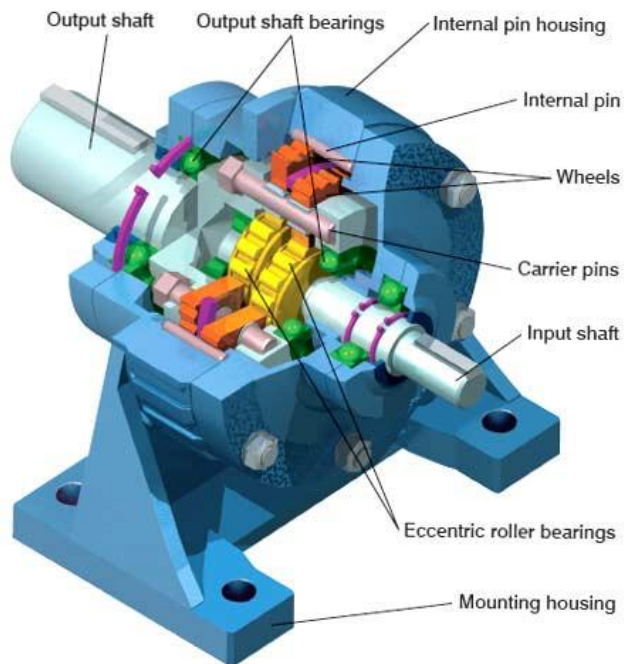


Figure 1. Cycloid reducer (<http://www.ohiobelting.com/images/shimpo4.jpg>)

It consists of four main components: an input and output shaft, cycloid discs and housing with internal pins. The input shaft has two eccentric roller bearings (eccentrically mounted cams), fitting into the eccentric roller bearing of the wheels (discs). This eccentricity causes the center of the disc to rotate in the housing. The wheels' (discs') teeth are less than the housing's pins, causing the reverse orbit rotation within the housing. If a fixed point of the circumference of the cycloid wheel (disc) is traced, the

resulting path will describe a curve called a *hypocycloid*. The rotary motion is converted via the disc rolling over within the housing, which accommodates the pins. The ratio of the gearbox depends on the relative dimensions of the disc and the housing.

Engineers use gear reducers in mechanized industry and/or industrial-automation applications. Over the time two types of reducers became a desired standard, because of their advantages, naming: cycloid and planetary speed reducers. Using high speed engines for general purposes and for precise machines working with servomotors; these machines require in many cases the rotation speed to be reduced and the torque to be increased. The smallest and most compact gear used to achieve this task is the cyclo-planetary gear (CPG) shown on Figure 2.

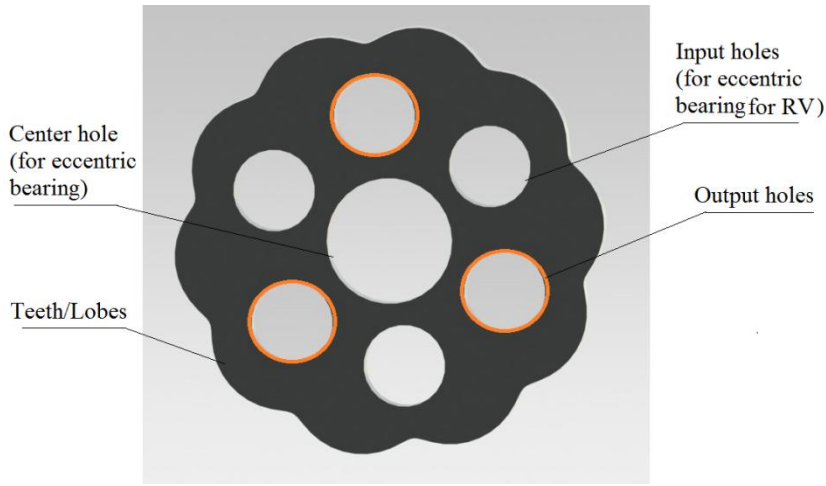


Figure 2. Cyclo Planetary Gear (CPG)

As mentioned, the reducer unit consists of four basic parts: the high-speed input shaft, a single or compound cycloid planetary gear, an eccentric cam (eccentric bearing) and a slow-speed output shaft. In Figure 3 is shown the exploded view of the assembly. In a lot of cases the design and terminology of the components can vary .On this figure are also shown the other parts like the shielding, the bearing, spacer, the ring gear housing also the slow shaft (output shaft) and shaft rollers. The input shaft is connected to the eccentric cam, through a key connection. This rigid connection creates the eccentric cycloid gear rotation i.e. cycloid motion. This motion causes the discs to roll over the ring gear rollers, mounted in the ring gear housing (also later referred to as pins). The output shaft is connected to the cycloid disc via shaft rollers. From the figure it can be observed that the shaft rollers are situated into the cycloid disc's perimeter holes (look at Figure.2). The torque is transferred from the perimeter holes, as the disc rotates to the output shaft. These holes are bigger than the slow shafts rollers; which causes the output pins to move around in the holes. Steady rotation of the output shaft is achieved from the wobbling movement of the disc. The direction of rotation of the output shaft is the opposite of the direction of the input shaft.

According to Darali drives (2012,homepage) and Sumitomo drives (2012,homepage) single stage efficiency approaches 93%, double stage 86% and the reduction rate of a single stage reducer is up to 199:1 and double stage up to 7569:1.

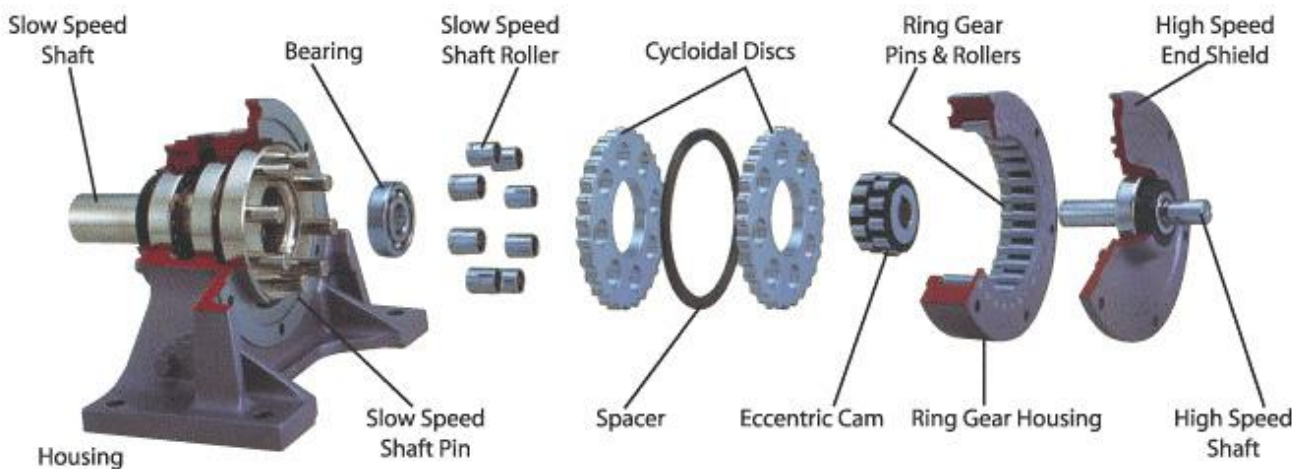


Figure 3. Exploded View of a Cycloid Speed Reducer
[\(<http://www.gearmotor.com.my/wp-content/uploads/2010/02/cyclo-drive-spare-parts.jpg>\)](http://www.gearmotor.com.my/wp-content/uploads/2010/02/cyclo-drive-spare-parts.jpg)

Gear ratio is designated by this expression:

$$i = \frac{z_2 - z_1}{z_1} \quad (\text{Eq 1.})$$

Where i – reduction rate

z_1 – number of teeth(lobes) on the cycloid disc

z_2 – number of pins in the housing .

Both cycloid and planetary reducers can be implemented in any industry where servo, stepper or variable frequency drives are used (D'Amico, 2012). Both have their advantages in comparison, the author has made this brief Table1 shown below:

Table 1. Reducer advantages in comparison (www.machinedesign.com)

Benefits of planetary gearboxes	Benefits of cycloidal gearboxes
High torque density	Zero or very-low backlash stays relatively constant during life of the application
Load distribution and sharing between planet gears	Rolling instead of sliding contact
Smooth operation	Low wear, Quiet operation
High efficiency	Shock-load capacity
Low input inertia	Torsional stiffness
Low backlash	Flat, pancake design
Low cost	Ratios exceeding 200:1 in a compact size

-RV-type cyclo-drive

So far the main principles for the cycloid mechanism have been explained, regarding the concept where the eccentric bearing is located in the center of the discs. The RV type in particular is a plano-eccentric reduction gear mechanism working on the same “cyclo” principle.

The reducer is shown in Figure 2 in Appendix 2, and also has the advantages, the concept offers. Note that the designed reducer differs from the one shown in the figures. Although as mentioned the principle of speed reduction and power transfer are the same.

The RV is a 2-stage speed reducer which includes: a spur gear stage with involute teeth and an epicyclic gear reduction stage. The first stage has an input gear (sun gear) coupled with in this case three satellite gears. They are connected to the crankshafts via splines. The first stage can be modified to change the overall unit ratio.

The crankshafts are driven by the spur gears. On the crankshafts are mounted the eccentric bearings, which cause the eccentric (cycloidal) motions of the two discs. They are offset 180 degrees from one another for equally balancing the load. The cycloid gear, driven by the eccentric shafts engages with the pins in the case. The transferred power then is directed to the output shaft. The gear rotates the opposite direction comparing to the input shaft. In fig.4 is shown how this works.

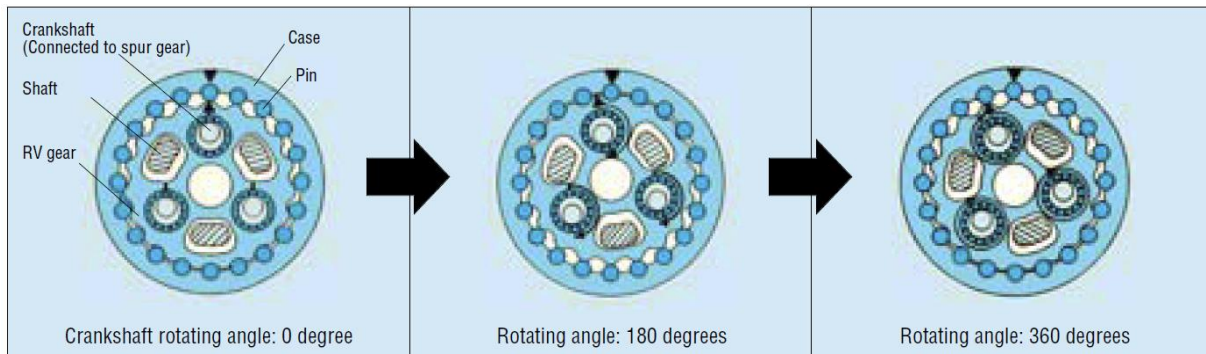


Figure 4. RV Principle (www.nabtesco.com)

The mechanism block diagram below in Figure 5 shows the whole reducer and its components. On the right side is shown the kinematic scheme, and on the left the cycloid stage.

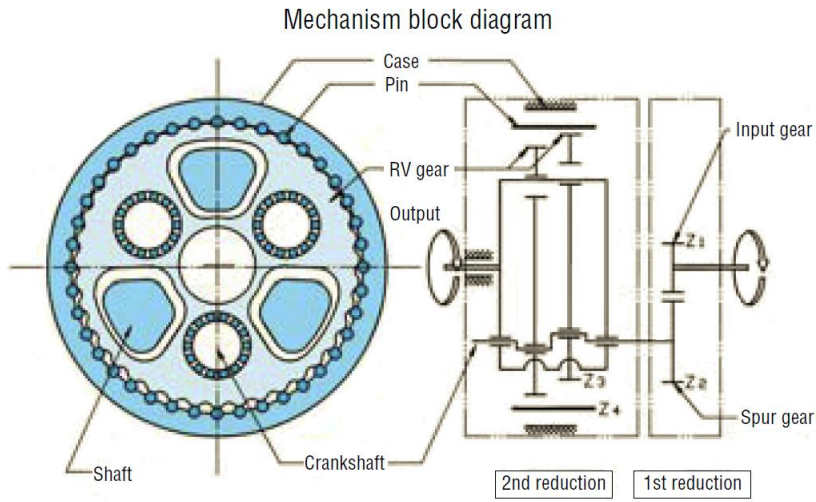


Figure 5. Mechanism Block Diagram (www.nabtesco.com)

The overall reduction ratio of the reducer can be determined from the following equation:

$$i = \frac{1}{1 + \frac{Z_2}{Z_1} Z_4} \quad (\text{Eq 1.1})$$

Where here i - is the reduction ratio, Z_1 - is the number of teeth on the sun gear, Z_2 – number of teeth on the satellite gears, Z_4 – number of pins in case.

In Figure 3 in Appendix 2 are shown some examples where these reducers are often used.

1.3 Task/Problem Description

The main aim of the project is to design a planetary-cyclo-drive speed reducer. SwePart Company is interested in a certain type of these reducers, consisting of two stages: a planetary and cycloid reduction stages. Our assignment is to design the cycloid stage of the reducer. This includes generating the equations for the geometry of a cycloid gear and analysis of the parts related to the motion (shafts : input, output and eccentric bearing shaft) also dimensioning and testing the epicycloid gear. The other group designed the shafts, the shaft related parts, in this paper have their designs have been tested and evaluated in Solidworks simulation. Input data (rotational speed and torque) has been received from the other group.

The work in this paper is divided in two main parts:

- Geometry
- Design

Geometry part consists of generating equations for the teeth profile, equations for the specific features (number of teeth, modification, module, radius of the pins) and equations for the basic diameters.

Design part is about creating the real reducer with the input data given from the company. It is shown what are the criteria's that the parts should meet in order to function properly. This paper proposes a simple and exact approach for the profile design of the cycloid gear and gearing, as the main part of the reducer.

Design example is shown with the input data given from SwePart AB:

Ratio: $i = 240$

Output Torque: $T_2 = 6300 \text{ Nm}$

Frequency of Rotation: $n_2 = 4,3 \text{ rpm}$

Safety factor (SF) ≥ 2

Material: Case hardened steel 20MnCr6

1.4 Limitations

Because of the time, needed to go further and deeper into the subject the paper shows only the main concepts. Therefore only static analyses have been made. Also a big issue was finding the right terminology for these transmissions in English since they are not standardized. Another limitation is also the computers that were used, because the simulations take a lot of time.

2. Theory

In this chapter are explained the main equations for the geometry of cycloid gears and transmissions. The chapter is focused on epicycloid formation, main dimensions and teeth/lobe profiles of the gears and transmission parameters.

2.1 Geometry

2.1.1 The epicycloid curve

Table 2. Used symbols

Symbol	Explanation	Dimension	Note
r_o	Radius of the epicycle	mm	
e_o	Epicycloids epicycle	mm	
r_c	Pins radius	mm	
φ	Angle of rotation of the epicycle	mm	
r_1	Pitch circle radius	mm	

The definition for an epicycloid is - a curve, produced by tracing the path, generated by a chosen point of a selected circle, called epicycle. This is rolling without slipping around another fixed circle.

There are three types of epicycloids - normal, shortened and extended (not shown because it has no practical value here). On Figure 6 (a) can be observed the normal, on (b) the shortened epicycloid curve. Here will be explained how the path is formed.

Looking at Figure 6 (a) – to generate the profile of the normal epicycloid, point O_c is rigidly connected on the circle with radius r_o . The circle will be rolling without slipping around the guiding circle with radius r_1 . In this case it is shown that: $e_o = r_o$.

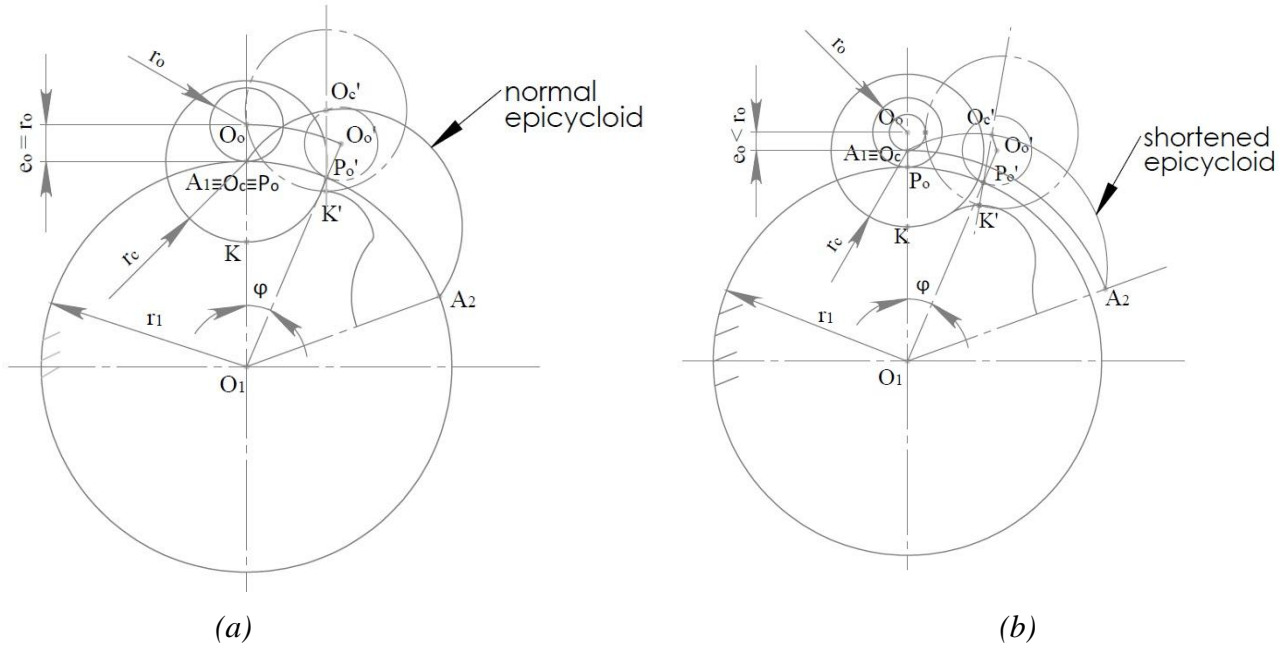


Figure 6. Curve generating (Alipiev, 1988)

In Figure 6(b) can be seen a shortened epicycloid, the curve is also called in mathematics an epitrihoid. The geometry is produced the same way as a normal epicycloid. The difference here is that the point O_c

lies in the perimeter of the rolling circle. Here can be written that for a epicycloid to be shortened it has to satisfy the following: $e_o < r_o$.

All epicycloid gears have a theoretical and working profile. The theoretical profile is needed to help define the actual working profile. The epicycloid (normal or shortened) is the theoretical profile, and the working profile is an equidistant curve. To obtain the working profile a circle with radii r_c (shown in Figure 8) is presented. Its centre is related to point O_c . Here point K is the contact point between the working profile and a circle with radii r_c . Generating the working profile here has been significantly simplified because of the use of Solidworks CAD environment.

2.1.2 Geometry of modified epicycloid gears

Table 3. Used symbols

Symbol	Explanation	Dimension	Note
a_w	Center distance	mm	
r_2	Radius of the pitch circle	mm	
r_{W_1}	Radius of the centrole of the epicycloid	mm	
r_{W_2}	Radius of the centrole of the pins circle	mm	

The cycloid drive shown in Figure 7, consists of a epicycloid gear 1 with teeth (also called lobes) and 2 internal housing with pins. The profile itself has the shape of an equidistant curve (later referred to as working profile) to the epicycloid curve (normal or shortened).

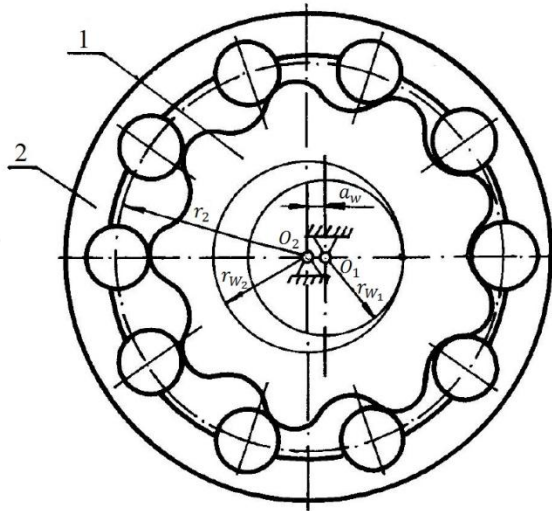


Figure 7. Corrected cycloid drive (Alipiev, 1988)

Here is observed a transmission with difference in the number of teeth z_2 and z_1 , between the housing and the gear equal to one, expressed by:

$$z_2 - z_1 = 1$$

The centroles (circles with common centers) of the epicycloid gear and housing are circles with radii naming r_{W_1} and r_{W_2} . Making distinguish in function of the location of the centrole to the tooth profile, corrected and not corrected gears will be recognized.

With not addendum modified gears we will refer to those, which centrode circle of the epicycloid gearing is matching the circle over which the centers of the pins are located ($r_{W_2} = r_2$). On the other hand the case where $r_{W_2} \neq r_2$ the gearing is modified. Not modified, epicycloid gearing with teeth difference $z_2 - z_1 \gg 1$ is used in modern solutions. According to (Alipiev, 1988) it is better to use modified. Actually modification is a necessity, as explained further in the paper. In this case the circle on which the centers of the pins (of the housing) are located, is bigger than the centrode of the cycloid gear ($r_2 > r_{W_1}$). When the drives have difference in teeth equal to 1 - the modification is completely necessary, meaning that $r_2 > r_{W_2}$.

2.1.3. General concept of eccentric tool meshing

Table 4. Used symbols

Symbol	Explanation	Dimension	Note
ω_0	Angle of velocity of the instrument	deg	
ω_1	Angle of velocity of the cycloid	deg	
r_{W_0}	Radius of the instrument	mm	
p	Length of the module circle step	mm	
m	Module	-	
r_c^*	Coefficient of the radius of the profile generating circle	-	
e	Center distance between module and profile generating circles	mm	
X	Modification	mm	
x	Coefficient of modification	-	

-Instrument meshing

In Figure 8 can be observed the eccentric tool meshing scheme. With O is marked the instrumental wheel and with 1 the epicycloid gear/disc. The cutting instrument with radii r_c is rotating with an offset from its original axis. This creates an eccentric motion around O_o . The cutting tool and the blank are rotating in opposite directions. The proportion of the angular velocities determines the number of lobes/teeth on the cycloid disc. With ω_o is marked the velocity of the tool and with ω_1 the velocity of the disc, e.g. :

$$\frac{\omega_o}{\omega_1} = z_1.$$

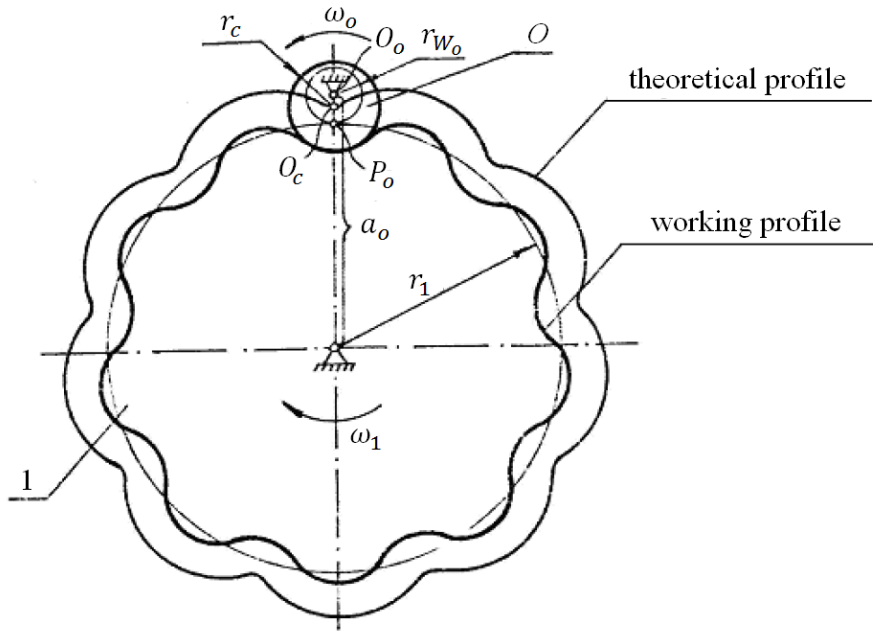


Figure 8 Eccentric Tool Meshing (Alipieva, 1988)

Point P_o meets the radius of the cutting instrument's base circle and wheel's: naming r_{W_o} and r_1 . This point is referred to as tool meshing point. Circle r_{W_o} rotates without slipping over circle r_1 . On the other hand point O_c lies in the perimeter of r_{W_o} . The same while rotating around O_o will generate the theoretical profile, while the circle with radii r_c will generate (cut) the working profile.

-Profile cutting instrument

One of the most important factors laying the foundations of modern technology is interchangeability. Interchangeability could exist only if standardization is available. The gears are one of the most difficult and accurate machine details to manufacture. Thus the standardization of some of the parameters of the gears is the main task in order to produce accurate gears.

To cut the cycloid disc a special instrument is introduced. It has been called a profile generating contour (shown on Figure 9, page 11).

When cutting an involute spur gear, a rack-cutter is used to generate the profile, but when cutting a cycloid gear using a rack is not possible because of the following reasons:

1. If we use a rack-cutter, the generating profile would be a very complicated and non-technological curve;
2. Using the rack we cannot express the displacement in any way.

On Figure 9 is introduced the *module circle* with radius r_0 and *profile generating circle* with radius r_c . The module circle is used as a base, so that the parameters of the *profile cutting instrument* and cycloid gear have standard values. The module is actually the diameter of its module circle:

$$m = 2r_0 \quad (\text{Eq 2.1.1})$$

The module m is measured in millimeters and its values are strongly regulated by standards. The circumference p of the modular circle r_0 is called a *pitch of the profile cutting instrument*. The module is determined by:

$$m = \frac{p}{\pi} \quad (\text{Eq 2.1.2}).$$

The radius of the *profile generating circle* is given with the following equation:

$$r_c = r_c^* m, \quad (\text{Eq 2.1.3})$$

Where r_c^* is the *coefficient of the circle radius*. Its value is equal to 1, according to (Alipiev, 1988). The radius r_c is equal to the radii of the pins of the cycloid housing and the center of the profile generating circle O_c is lying on the module circle.

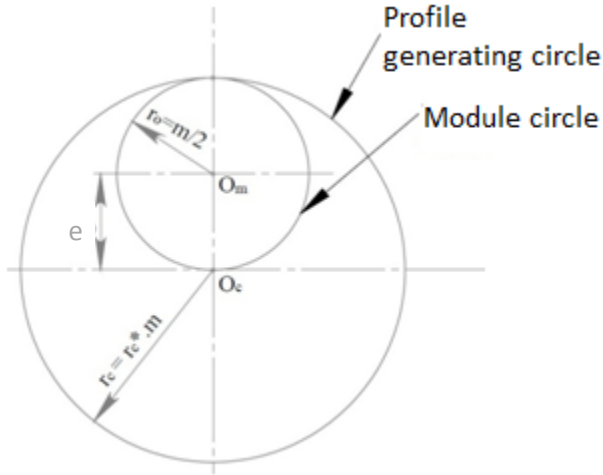


Figure 9. Profile Generating Contour (Alipiev, 1988)

The distance between the centers of both, profile generating circle and module circle is designated by e and is called eccentricity of the *profile cutting instrument*. It can be determined with the module according to the following equation:

$$e = \frac{m}{2} \quad (\text{Eq 2.1.4})$$

The dimensions of the profile cutting instrument can be determined by two independent from each other parameters. The module which acts like a scale factor, and coefficient of the profile generating circle (r_c^*). These parameters will directly determine the cycloid gears dimensions.

In particular the profile generating tool has an eccentric contour which has a determined pivot (Figure 10). In addition to the profile cutting instrument, with eccentricity e_0 and radius r_{w0} is added the original circle. The eccentricity is equal to the distance from the pivot O_0 and the center of the profile generating circle O_c . The original circle's radius is equal to the radius of the modular circle ($r_{w0} = r_0 = \frac{m}{2}$), but in general they are not coincident.

In summary the *module circle* and the profile generating circle as main components of the profile cutting instrument do not change their mutual position. What changes is the location of the profile cutting instrument over initial circle. This change is called *addendum modification*. The displacement is measured from one pre-selected nominal position (O_o).

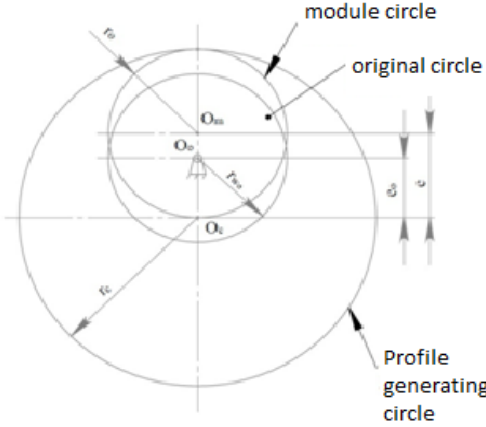


Figure 10. Profile cutting instrument (Alipiev, 1988)

-Addendum Modification

In Figure 11 can be seen the process of forming the teeth on the blank 1 by the teeth forming circle. The resultant teeth are with determined geometric form. With r_{wo} and r_1 are designated respectively the radius of the circles which belong to the cutting tool. As mentioned above r_{wo} is equal to the radius of the module circle, r_1 is the radius of the pitch circle of the epicycloidal wheel. In all the four schemes in Figure 11 the center distance is the same $a_0 = r_{wo} + r_1$. The only difference is the position of the profile cutting instrument. The location of the profile cutting instrument affects the form, size and disposal of the teeth.

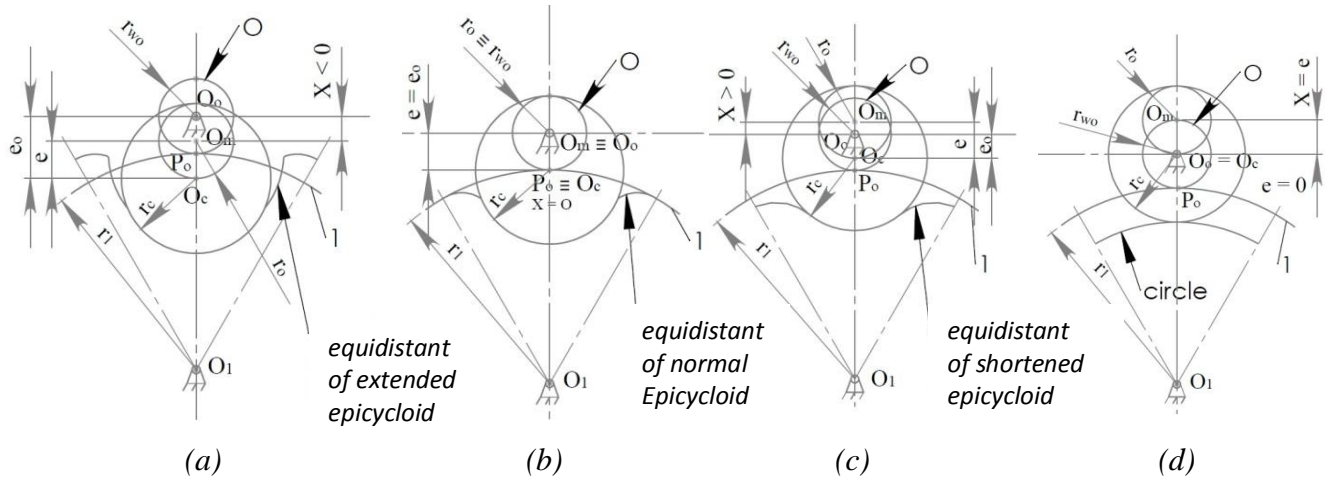


Figure 11. Forming Process (Alipiev, 1988)

The position of the *profile cutting instrument* in which the *module circle* coincides with the *original circle* and simultaneously touches the *pitch circle* of the epicycloidal wheel is called *nominal position*

(see Figure 11 (b)). Any other position is formed by displacing (modifying its position) the profile cutting instrument. The epicycloidal wheel formed in a nominal position is called unmodified wheel.

If the profile cutting instrument is displaced from the nominal position in which the module circle is not touching the pitch circle the result would be an *unmodified wheel*.

The modification of the profile cutting instrument is the difference between the eccentricity of the profile cutting instrument and the eccentricity of the generating circle i.e.:

$$X = e - e_0 \quad (\text{Eq 2.1.5})$$

Apparently according to (Eq 2.1.5) the eccentricity could be positive, negative or nominal. If $e > e_0$ then the displacement is positive (see Figure 11 (c)), if $e < e_0$ then it is negative (look at Figure 11 (a)) and if $e = e_0$ (the modification is equal to zero) the condition is called nominal. There is a fourth condition $X = e$, the modification is equal to zero ($e_0 = 0$) and it is called a boundary condition (see Figure 11 (d)).

The modification of the profile cutting instrument can be expressed by the following equation

$$X = x \frac{m}{2} \quad (\text{Eq 2.1.6})$$

Where x is the *coefficient of modification*. It can be either positive or negative, so the following modifications are possible:

1. $x = 0$ - without modification
2. $1 > x > 0$ – positive gears
3. $x < 0$ – negative gears
4. $x = 1$ – border gears

When looking at a transmission with a difference of teeth equal to one, practical value have only positive modifications (see Figure 11 (c)). Also positive modification is a necessity otherwise the tooth/lobe profile will result to be undercut.

From Figure 11 can be summarized the information so far: that all the basic parameters needed to define the dimensions of the gear are:

- a) The module – m ;
- b) Coefficient of the radius of the profile generating circle $r_c^* = 1$;
- c) Coefficient of modification of the profile cutting instrument - x ;
- d) Number of teeth of epicycloidal wheel z_1 .

2.1.4. Basic dimensions of epicycloidal gears

Table 5. Used symbols

Symbol	Explanation	Dimension	Note
s	Length of the pitch of the epicycloid wheel	mm	
r_{Tf_1}	Theoretical radius of the dedendum circle	mm	
r_{Ta_1}	Theoretical radius of the dedendum circle	mm	
r_{f_1}	Radius of the dedendum circle	mm	
r_{a_1}	Radius of the addendum	mm	
h_1	Tooth depth	mm	
λ	Coefficient of the epicycloid shortening	-	
a	Center distance	mm	

All the dimensions of the epicycloidal gears will be defined using Figure 1 in Appendix 2. All the basic dimensions are derivatives of the basic parameters as it has been shown.

- Step of the pitch circle

Pitch - according to the theory of mechanisms, it is the distance between two homonymous profiles. In the process of cutting the epicycloidal gear the tool is rolling without slipping on the pitch circle. From the general definition for pitch, follows that it is in this case the length of the enclosed curve divided by the number of teeth.

Therefore, if we designate with p the pitch of the epicycloidal wheel on its pitch diameter and if we use the relation $m = \frac{p}{\pi}$ we can write down the following:

$$p = \pi m \quad (\text{Eq 2.1.7}).$$

The module of the generating circle, which has formed a certain wheel is called module of epicycloidal wheel.

- Pitch diameter

The circumference s of the pitch can be defined with the help of the following formulas:

$$s = 2\pi r_1 \quad (\text{Eq 2.1.8})$$

$$s = z_1 p \quad (\text{Eq 2.1.9})$$

If we substitute p from (Eq 2.1.7) and (Eq 2.1.8) in (Eq 2.1.9) and for the radius of the pitch diameter is obtained the following equation:

$$r_1 = \frac{mz_1}{2} \quad (\text{Eq 2.1.10})$$

For the diameter of the pitch circle we can write the following

$$d_1 = mz_1 \quad (\text{Eq 2.1.11})$$

- Diameter of the theoretical dedendum circle

From Figure 1 in Appendix 2 can be observed that the section $\overline{PO_c}$ is equal to X of the profile cutting instrument. If we take that into consideration for the radius of the theoretical dedendum we can write down the following formula:

$$r_{Tf_1} = r_1 + X \quad (\text{Eq 2.1.12})$$

When we substitute (Eq 2.1.6) and (Eq 2.1.10) for the radius of the theoretical dedendum we receive:

$$d_{Tf_1} = m(z_1 + x) \quad (\text{Eq 2.1.13})$$

- Diameter of theoretical addendum circle

According to the distances in Figure 1 in Appendix 2 for r_{Ta_1} we can write:

$$r_{Ta_1} = r_{Tf_1} + 2e_0 \quad (\text{Eq 2.1.14})$$

And if we take into consideration equations (Eq 2.1.12) and $e_o = m/2(1 - x)$ for the radius we obtain:

$$r_{Ta_1} = m\left(\frac{z_1}{2} + 1 - \frac{x}{2}\right) \quad (\text{Eq 2.1.15})$$

Respectively the formula for the diameter is:

$$d_{Ta_1} = m(z_1 + 2 - x) \quad (\text{Eq 2.1.16})$$

- Diameter of the working profile dedendum circle

Since the real profile of the teeth of the epicycloidal wheel is actually an equidistant to the theoretical profile the following formula for the radius can be presented:

$$r_{f_1} = r_{Tf_1} - r_c \quad (\text{Eq 2.1.17})$$

The radius of the dedendum circle is defined when we substitute equations (Eq 2.1.12) and (Eq 2.1.3) in (Eq 2.1.17)

$$r_{f_1} = \frac{m}{2}(z_1 + x - 2r_c^*) \quad (\text{Eq 2.1.18})$$

From where for the diameter of the dedendum circle will be:

$$d_{f_1} = m(z_1 + x - 2r_c^*) \quad (\text{Eq 2.1.19})$$

- Diameter of the working addendum circle

Similar to the working dedendum, the radius of the addendum is defined as difference of r_{Ta_1} and r_c radii i.e.:

$$r_{a_1} = r_{Ta_1} - r_c \quad (\text{Eq 2.1.20})$$

When we substitute equations (Eq 2.1.14) and (Eq 2.1.3) for the radius and diameter respectively we have

$$r_{a_1} = \frac{m}{2}(z_1 + 2 - x - 2r_c^*) \quad (\text{Eq 2.1.21})$$

$$d_{a_1} = m(z_1 + 2 - x - 2r_c^*) \quad (\text{Eq 2.1.22})$$

- Teeth depth

The depth of the teeth h_1 can be determined as the difference between the radii of the addendum and dedendum circles. But from Figure 1 in Appendix 2 is observed that:

$$h_1 = 2e_0 \quad (\text{Eq 2.1.23})$$

And after substituting the equation for $e_0 = \frac{m}{2}(1 - x)$ and (Eq 2.1.23) for h_1 we receive the following:

$$h_1 = m(1 - x) \quad (\text{Eq 2.1.24})$$

- Coefficient of shortening of the epicycloids

The coefficient of shortening the epicycloid is designated by λ and is defined with the help of the following relation :

$$\lambda = \frac{e_0}{e} \quad (\text{Eq 2.1.25})$$

Also

$$\lambda = 1 - x \quad (\text{Eq 2.1.26})$$

- Center distance

Center distance a is the distance $\overline{O_1O_0}$. According to Figure 1 in Appendix 2:

$$a = r_1 + r_{w0} \quad (\text{Eq 2.1.27})$$

If we take into consideration equations (Eq 2.1.10) and that $r_{w0} = r_0 = \frac{m}{2}$ for the pitch center distance we obtain the following equation:

$$a = \frac{m}{2}(z_1 + 1) \quad (\text{Eq 2.1.28})$$

The center distance is not dependable on the displacement of the profile cutting instrument and is permanent for epicycloidal wheel with a certain module and number of teeth.

- Influence of the modification on the geometry of the teeth

The analyses of the formulas lead to the following conclusions:

- The modification of the profile cutting instrument does not change the diameter of the pitch circle of the epicycloidal wheel;
- Diameter of the addendum circle d_{0_1} decreases when the coefficient of the modification - x of the profile cutting instrument is increased;
- The diameter of the dedendum circle d_{f_1} increases when the coefficient of the modification is increased;
- When the coefficient of the modification of the profile cutting instrument is increased the tooth depth of the epicycloidal gear decreases;
- The addendum and the dedendum circles coincide and the tooth depth is equal to zero when the coefficient of the displacement is equal to 1.

The mention above is illustrated in Figure 12 below.

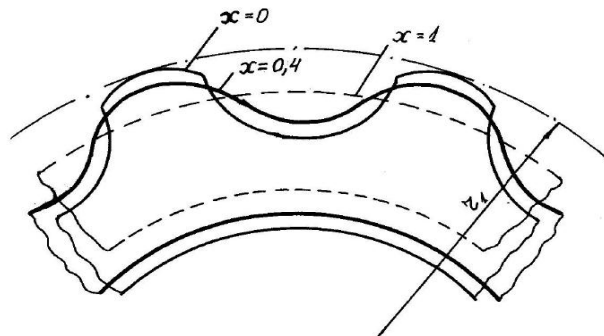


Figure 12. Lobes Modification (Alipiev, 1988)

2.1.5. Equations for teeth profile and curvature radius.

Table 6. Used symbols

Symbol	Explanation	Dimension	Note
ξ	Coordinates of the different points	-	
η	Coordinates of the different points	-	
ψ	Angle of rotation of the generating wheel	deg	
ρ	Radius of curvature	mm	
ρ_T	Radius of the theoretical curvature	mm	
ρ^*	Coefficient of the radius of the theoretical curvature	-	
ρ_p	Radius of the working curve	mm	
r_l	Radius of the position of the inflection point l	mm	
r_n	Radius of the position of the inflection point n	mm	
r_{a_2}	Radius of the addendum of the pin wheel	mm	

- Determination of the theoretical and working profile of the epicycloid

The teeth profile can be determined by formation of a profile generating circle q , which will move in relative motion. In order to do that, it is needed to form two movable Cartesian coordinate systems (shown in Figure 13) : $\xi O_0\eta$ is the first one and it is in connection with profile generating circle , XO_1Y is the second one which is connected with the epicycloid circle. The equation of the profile generating curve in $\xi O_0\eta$ coordinate system is:

$$\xi^2 + (\eta + e_0)^2 = r_c^2 \quad (\text{Eq 2.1.29})$$

Where ξ and η are the coordinates of profile generating circle points.

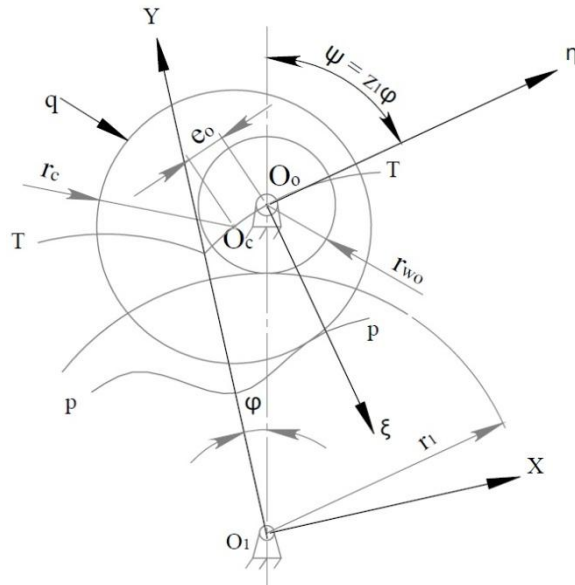


Figure 13. Theoretical and Working Profile (Alipieiev, 1988)

The centrododes of the profile generating curve are: r_1 for epicycloid circle and r_{wo} for generating circle. When the generating circle turns on an angle (ψ), the epicycloid circle will turn on an angle (φ). These angles are in relation:

$$\frac{\psi}{\varphi} = \frac{r_1}{r_{wo}} = z_1 \quad (\text{Eq 2.1.30})$$

The relation between $\xi O_0\eta$ and XO_1Y coordinate system is:

$$\xi = X \cos(\varphi + \psi) - Y \sin(\varphi + \psi) + \alpha \sin \psi \quad (\text{Eq 2.1.31})$$

$$\eta = X \sin(\varphi + \psi) + Y \cos(\varphi + \psi) - \alpha \cos \psi \quad (\text{Eq 2.1.32})$$

There is a connection between φ , ψ and z_1 :

$$\psi = z_1 \varphi \quad (\text{Eq 2.1.33})$$

Before finding the working profile p-p, first the theoretical profile T-T must be found. In this case the radius of the generating circle will be equal to 0 ($r_c=0$), which means that:

$$\xi = 0 \quad (\text{Eq 2.1.34})$$

$$\eta = -e_0 \quad (\text{Eq 2.1.35})$$

Using the information from above the equations for theoretical profile will be:

$$X_T = \frac{m}{2} [(z_1 + 1) \sin \varphi - (1 - x) \sin(z_1 + 1) \varphi] \quad (\text{Eq 2.1.36})$$

$$Y_T = \frac{m}{2} [(z_1 + 1) \cos \varphi - (1 - x) \cos(z_1 + 1) \varphi] \quad (\text{Eq 2.1.37})$$

These equations for shortened epicycloid are valid in case of: $0 < x < 1$

The working profile is an equidistant curve of the theoretical profile. The equations for equidistant curve in respect of the theoretical profile are:

$$X_W = X_T + \frac{r_c Y_T}{\sqrt{X_T^2 + Y_T^2}} \quad (\text{Eq 2.1.32})$$

$$Y_W = Y_T + \frac{r_c X_T}{\sqrt{X_T^2 + Y_T^2}} \quad (\text{Eq 2.1.33})$$

Where X_W and Y_W are the coordinates of working profile; X_T and Y_T are the coordinates of theoretical profile.

After differentiation of X_T and Y_T – the equations for the working profile can be written:

$$X_W = \frac{m}{2} \left[(z_1 + 1) \sin \varphi - (1 - x) \sin(z_1 + 1) \varphi + \frac{2r_c^*[(1-x) \sin(z_1+1)\varphi - \sin \varphi]}{\sqrt{1-2(1-x) \cos z_1 \varphi + (1-x)^2}} \right] \quad (\text{Eq 2.1.34})$$

$$Y_W = \frac{m}{2} \left[(z_1 + 1) \cos \varphi - (1 - x) \cos(z_1 + 1) \varphi + \frac{2r_c^*[(1-x) \cos(z_1+1)\varphi - \cos \varphi]}{\sqrt{1-2(1-x) \cos z_1 \varphi + (1-x)^2}} \right] \quad (\text{Eq 2.1.35})$$

- Curvature radius

The differentiation geometry shows that every curve radius can be built by the following equation:

$$\rho = \frac{(\dot{X}^2 + \dot{Y}^2)^{3/2}}{\dot{X}\ddot{Y} - \dot{Y}\ddot{X}} \quad (\text{Eq 2.1.36})$$

Where $\dot{X}, \dot{Y}, \ddot{X}$ and \ddot{Y} are in function of φ .

Like the teeth profile before finding the working curvature radius, it is needed to find the theoretical curvature radius ($\rho_T = \rho_T(\varphi)$). And after transforming and calculating the equations of theoretical teeth profile and the above equation, the equation for theoretical curvature radius will be:

$$\rho_T = \frac{m}{2} (z_1 + 1) \frac{[1+(1-x)^2 - 2(1-x) \cos z_1 \varphi]^{\frac{3}{2}}}{1+(1-x)^2(z_1+1)-(1-x)(z_1+2) \cos z_1 \varphi} \quad (\text{Eq 2.1.37})$$

Where it is obvious that ρ_T is depending only on x, z_1 and m .

The connection between the working curvature radius ρ_p and the theoretical curvature radius ρ_T is :

$$\rho_p = \rho_T - T_c = m(\rho^* - r_c^*) \quad (\text{Eq 2.1.38})$$

Where $\rho^* = \rho_T/m$.

- Distinctive points of teeth profile

The teeth profile is formed by two sections: bulge section (Figure 14 (a)) and concave section (Figure 14 (b)). There are four distinctive points, which are important for the working profile (see Figure 15):



Figure 14. Profile section (Alipiev, 1988)

- *Start point* – f – is located on the dedendum circle and it has a diameter d_f (respectively radius r_f)
- *Addendum point* – a – is located on the addendum circle and it has a diameter d_a (respectively radius r_a)
- *Inflex point* – l – at this point the teeth profile transforms from concave section to bulge section.
- *Border point* – n – is the point where the profile has least radius. It is located on bulge section.

The exact location of l and n points can be found by the equations for their radii in function of φ .

$$r_p = \sqrt{X_W^2 + Y_W^2} \quad (\text{Eq 2.1.39})$$

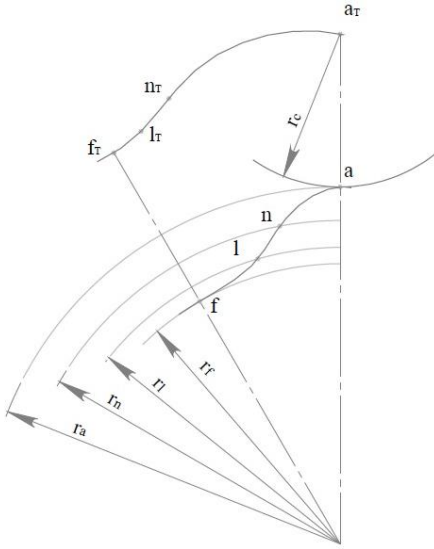


Figure 15. Distinctive points of the profile (Alipieiev, 1988)

After transforming and calculating the equations of working teeth profile and the above equation, the l point radius and n point radius will be:

$$r_l = \frac{m}{2} \left[(z_1 + 1)^2 + (1 - x)^2 + 4r_c^{*2} - 2 \frac{1+z_1+(1-x)^2(z_1+1)^2}{z_1+2} - \frac{4r_c^{*2}z_1x(2-x)}{\sqrt{1+(1-x)^2-2\frac{1+(1-x)^2(z_1+1)}{z_1+2}}} \right]^{1/2} \quad (\text{Eq 2.1.40})$$

$$r_n = \frac{m}{2} \left[(z_1 + 1)^2 + (1 - x)^2 + 4r_c^{*2} - 2(z_1 + 1) \frac{1-z_1+(1-x)^2(2z_1+1)}{z_1+2} - \frac{8r_c^{*2}z_1x(2-x)}{\sqrt{1+(1-x)^2-2\frac{1-z_1+(1-x)^2(2z_1+1)}{z_1+2}}} \right]^{1/2} \quad (\text{Eq 2.1.41})$$

With these equations it is easy to find the radii of l and n points, without calculating the coordinates of them. It is obvious that the radii are only depending on x , z_1 , m and r_c^* .

There is one limitation - the profile generating circle r_c should be less or equal than the curvature radius $\rho_{T \min}$.

$$r_c = r_c^* m \leq \rho_{T \min}; r_c^* \leq \frac{3(z_1+1)\sqrt{3z_1x(2-x)}}{2(z_1+2)^{3/2}} \quad (\text{Eq 2.1.42})$$

In this case the module m will not influence over the result.

2.1.6 Forming of the epicycloidal gear transmission

Table 7. Used symbols

Symbol	Explanation	Dimension	Note
γ	Angle of motion transmission	deg	
l	Coefficient of non-centroidality	-	
Δ	Correction coefficient of r_c^*	-	

- Gearing conditions

Every epicycloidal gear meshes correctly if:

1. The radius of the circle on which the centers of the pins are located r_2 is equal to the pitch center distance;
2. The radius of the pins r_c is equal to the form generating circle;
3. The difference between the number of teeth of the epicycloidal wheel and the number of pins must be equal to 1;
4. The center distance a_w is equal to the eccentricity e_0 i.e.

$$a_w = e_0 = \frac{m}{2}(1 - x) \quad (\text{Eq 2.1.43})$$

On Figure 16 is shown an epicycloidal gearing, where r_{w_1} and r_{w_2} are respectively the radii of the centrolede circles of the epicycloidal and the circle on which the pins are located. These circles are starting circles.

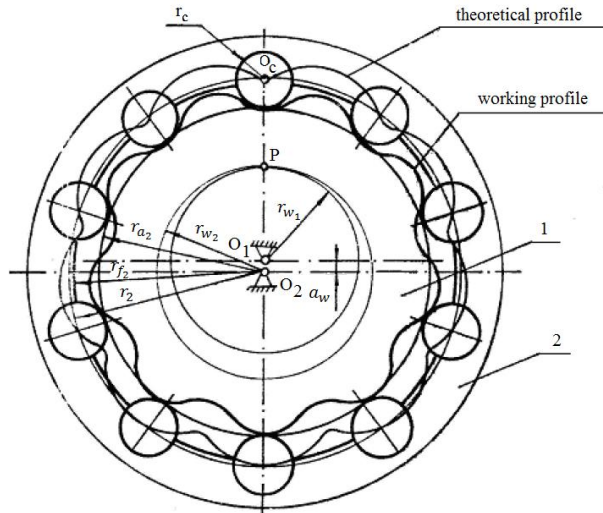


Figure 16. Corrected epicycloid transmission (Alipieva, 1988)

Since :

$$\frac{r_{w_1}}{r_{w_2}} = \frac{z_1}{z_2}, \quad (\text{Eq 2.1.44})$$

for the radii of the base circles we have :

$$r_{w_1} = a_w z_1 \quad (\text{Eq 2.1.45})$$

$$r_{w_2} = a_w z_2 \quad (\text{Eq 2.1.46})$$

After taking into consideration the equation (Eq 2.1.43) we can determine the formulas for the radii of the base circles

$$r_{w_1} = \frac{mz_1}{2}(1 - x) \quad (\text{Eq 2.1.47})$$

$$r_{w_2} = \frac{mz_2}{2}(1 - x) \quad (\text{Eq 2.1.48})$$

- Dimensions of the housing

All these dimension can be determined only with the basic parameters m , r_c^* , x , z_1 .

Diameter of pitch circle r_2 . It is the radius on which all the pins are located. Since $r_2 = r_1 + r_{w_0}$ and $r_1 = \frac{mz_1}{2}$ and $r_{w_0} = \frac{m}{2}$ for the radius of the pitch circle we can write down

$$r_2 = \frac{mz_2}{2} = \frac{m(z_1+1)}{2} \quad (\text{Eq 2.1.49})$$

If we compare the radii of the pitch and initial circles of the epicycloid plate when $1 > x > 0$ it's obvious that $r_2 > r_{w_1}$. They are equal when $x = 0$.

Diameter of the pins. The radius and the diameter of the pins can be calculated with the following formulas:

$$r_c = r_c^* m \quad d_c = 2r_c^* m \quad (\text{Eq 2.1.50})$$

Diameter of the addendum circle. The radius r_{a_2} is dependent on the radius of the pins and the pitch diameter of the cyclo gear i.e.

$$r_{a_2} = r_2 - r_c \quad (\text{Eq 2.1.51})$$

After taking into consideration of equations (Eq 2.1.49) and (Eq 2.1.50), the radius and the diameter of addendum circle are:

$$r_{a_2} = \frac{m}{2}(z_2 - 2r_c^*) \quad (\text{Eq 2.1.52})$$

$$d_{a_2} = m(z_2 - 2r_c^*) \quad (\text{Eq 2.1.53})$$

Diameter of the working profile dedendum circle. This diameter is calculated only for gears which are like the one in Figure 17. The peaks of the teeth of the epicycloidal wheel should be in contact only with the pins and that can be achieved if the following inequality

$$r_{f_2} > r_{a_1} + a_w \quad (\text{Eq 2.1.54})$$

For the radius of the housing circle r_{f_2} except inequality (Eq 2.1.54) there is another one which also has to be taken into consideration

$$r_{f_2} < r_2 - \Delta \quad (\text{Eq 2.1.55})$$

$$\Delta = (0,15 \dots 0,3)r_c \quad (\text{Eq 2.1.56})$$

If those inequalities are not fulfilled then the attachment of the pins to the holes in the housing is not possible, because they will have the possibility to move radial. After applying equations (Eq 2.1.54) and (Eq 2.1.55) and expressing the basic parameters for the diameter of the housing circle we obtain :

$$d_{f_2} > m(z_1 + 3 - 2x - 2r_c^*) \quad (\text{Eq 2.1.57})$$

Coefficient of non-concentricity. From Figure 17 can be observed that the pins and the lobes of the epicycloidal gear are located out of their basic circles. That increase of their size is called coefficient of non-concentricity - l , it is defined as term of the following:

$$l = \frac{r_2}{r_{w_2}} \quad (\text{Eq 2.1.58})$$

After substitution of r_2 and r_{w_2} from equations (Eq 2.1.49) and (Eq 2.1.48) we receive :

$$l = \frac{1}{1-x} \quad (\text{Eq 2.1.59})$$

2.1.7. Action line. Contact Points

The epicycloid wheel is in contact with all of the pins all the time, but only half transmit the load. The forces F_2 , F_3 , F_4 and F_5 can be seen on Figure 17. Every force direction is formed by creating a line from point P to every pin centre. These forces are normal to every contact line (K_2 , K_3 , K_4 and K_5). If we assume that the epicycloid wheel is rotating anticlockwise with angular speed of ω_1 , it is obvious that the transmission pins would be pins number 2, 3, 4, and 5.

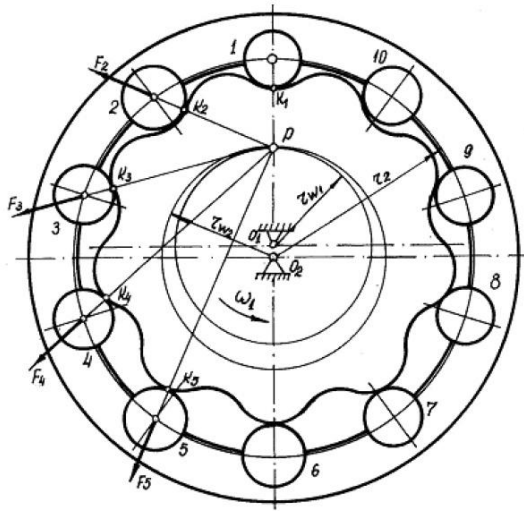


Figure 17. Transmission Forces (Alipiev, 1988)

The meshing circle is shown on Figure 18. Point A is the beginning point of the meshing circle and point B is the ending one. Also in the figure is shown that if housing with pins rotates with angle ψ , and that the epicycloid wheel is rotating with an angle $v = \frac{Z_2}{Z_1}\psi$. The point K is located on the line $\overline{O_cP}$ and radius r_c .

The exact location of point K can be found by looking at the triangle PCK and the following equation can be expressed:

$$X_k = \overline{PK} \cos \alpha_w = (\overline{PO_c} - r_c) \cos \alpha_w \quad (\text{Eq 2.1.60})$$

$$Y_k = r_{w2} + \overline{PK} \sin \alpha_w = r_{w2} + (\overline{PO_c} - r_c) \sin \alpha_w \quad (\text{Eq 2.1.61})$$

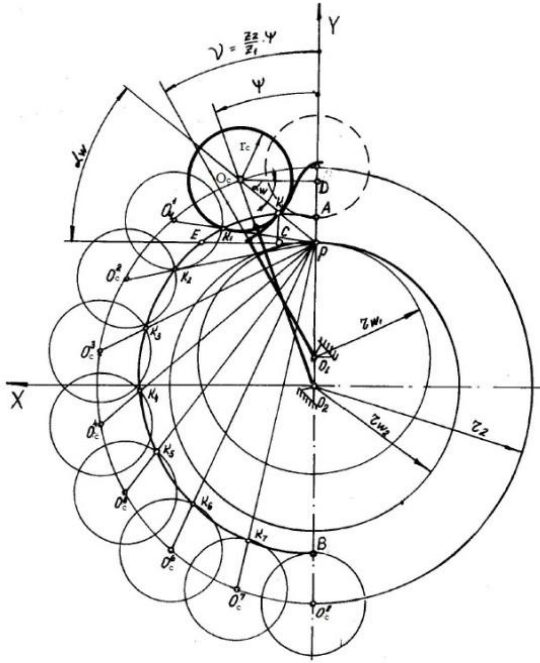


Figure 18. Meshing Circle (Alipiev, 1988)

The meshing circle equation can be found by calculating the relations between the triangles PO_2O_c , DO_2O_c and the lines $\overline{PO_c}$, $\overline{O_cD}$ and \overline{PD} :

$$X_k = \frac{m}{2} \left[z_2 - \frac{2r_c^*}{\sqrt{1+(1-x)^2-2(1-x)\cos\psi}} \right] \sin\psi \quad (\text{Eq 2.1.62})$$

$$Y_k = \frac{m}{2} \left[z_2(1-x) + z_2 - \frac{2r_c^*}{\sqrt{1+(1-x)^2-2(1-x)\cos\psi}} (\cos\psi - 1 + x) \right] \quad (\text{Eq 2.1.63})$$

The coordinates for each contact point from the action line can be obtained by solving (Eq 2.1.62), (Eq 2.1.63) and substituting the angle ψ from 0 to π .

2.1.8 Distinctive Meshing Angles

Table 8. Used Symbols

Symbol	Explanation	Dimension	Note
α_w	Pressure angle	deg	
θ	Angle equal to γ	deg	

- Angle of Meshing

The angle of meshing α_w is shown in Figure 19. It has a variable quantity, depending on the contact point in respect of the angle ψ . The value of α_w can be found by the following equation:

$$\alpha_w = \arcsin \left[\frac{\cos\psi + x - 1}{\sqrt{1+(1-x)^2-2(1-x)\cos\psi}} \right] \quad (\text{Eq 2.1.64})$$

This angle depends on the angle ψ and on the coefficient of displacement x .

In Figure 19 it has been build the relation of α_w in respect of ψ with different coefficient of displacement x . It is obvious that its maximum value is 90° and it can be as positive as negative.

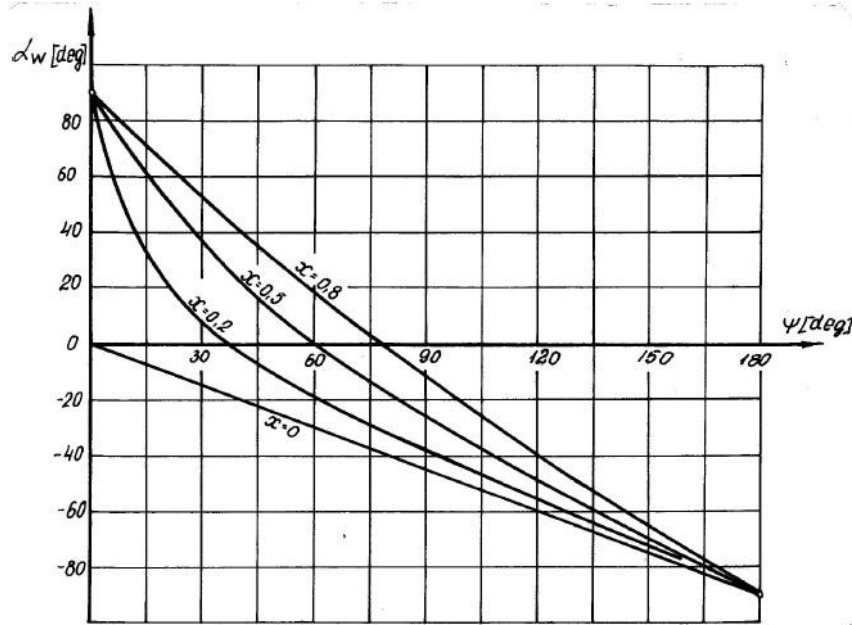


Figure 19. The Angle α_w in Respect of ψ (Alipiev, 1988)

- Transmitting Angles

The transmitting angle is between the directors of the force \vec{F}_{12} and the speed \vec{V}_{O_c} (see Figure 20). It is clear that this angle depends on ψ . The transmitting angle is important because of possible jamming and it must fulfil the following condition:

$$\theta_{max} \leq \theta_{allowable}$$

Sometimes it is better to use the angle γ instead of θ . The angle γ is called angle of motion transfer and it is the supplementary of θ to 90° . And in this case the equation will be:

$$\gamma_{min} \geq \gamma_{allowable}$$

Where the angle γ can be found by looking at triangle O_2O_cP and using the sine theorem:

$$\frac{\sin \gamma}{r_{w2}} = \frac{\sin \psi}{PO_c} : \quad \gamma = \arcsin \left[\frac{(1-x) \sin \psi}{\sqrt{1+(1-x)^2 - 2(1-x) \cos \psi}} \right] \quad (\text{Eq 2.1.65})$$

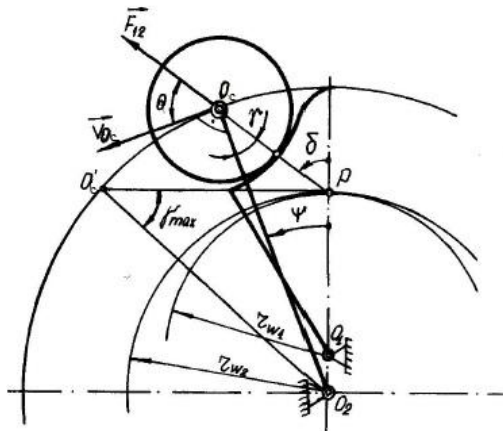


Figure 20. Transmitting Angles (Alipiev, 1988)

In Figure 21 it is shown the change of γ according different stages of x ($\gamma = \gamma(\psi)$). When $x \geq 0.5$ the angle γ starts to be less than 30° , which value is not appropriate for transmitting (Alipiev, 1988). The maximum value of x can be found by looking at O_2O_cP again:

$$\sin \gamma = \frac{r_{w2}}{r_2} \sin(\pi - \delta) \quad (\text{Eq 2.1.66})$$

Where the angle γ is in respect of δ (with values from 0 to π). After looking close to this equation - $\frac{r_{w2}}{r_2} = \text{const}$, the following can be expressed:

$$\delta = \frac{\pi}{2} \quad (\text{Eq 2.1.67})$$

And after calculating the above equations – the maximum value for γ is:

$$\gamma_{max} = \arcsin(1 - x) \quad (\text{Eq 2.1.68})$$

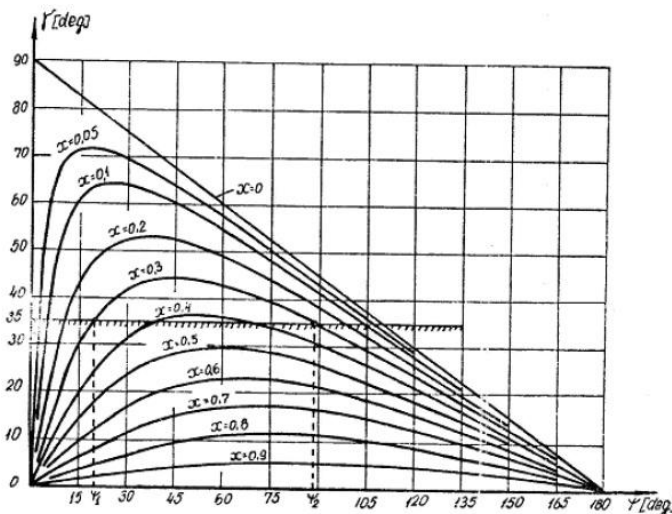


Figure 21. The Change of γ According Different Stages of x (Alipiev, 1988)

2.1.9 Contact ratio

Table 9. Used Symbols

Symbol	Explanation	Dimension	Note
ψ_n	Overlap ration angle	deg	
φ_1	angle	deg	
φ_2	angle	deg	
φ_k	Contact ratio angle	deg	
γ_a	allowable angle of transmitting	deg	
τ_2	Angle step	deg	
ε	Contact ratio	-	
ε_n	Optimal contact ratio	-	

- Angle of overlap ratio

The angle of beneficial overlapping Ψ_n is actually the angle of rotation of the gear, to which the contact between the teeth is done with transmitting angles higher than $\gamma_{allowable} = \gamma_a$. In initial position $\Psi = 0$ the angle of transmission is $\gamma = 0$. When the epicycloid gear starts to rotate the angle γ increases and when $\Psi = \Psi_1$ the angle becomes equal to the allowable angle of transmitting ($\gamma = \gamma_a$). If the rotating continues the angle increases but to a certain point where $\Psi = \arccos(1 - x)$. After that it starts to decrease and when $\Psi = \Psi_2$ the angle γ is equal to γ_a . The decrease will continue until $\Psi = \pi$ in that condition $\gamma = 0$. The formula for the angle of beneficial overlapping is :

$$\Psi_n = \Psi_2 - \Psi_1 \quad (\text{Eq 2.1.69})$$

Since some mistakes can occur while making the profile, there is another more accurate way to determine the angle. If we substitute Ψ_1 and Ψ_2 in (Eq 2.8.2) we have :

$$(1 - x)^2 \cos^2 \psi - 2(1 - x) \sin^2 \gamma_a \cos \Psi + (1 - x)^2 (\sin^2 \gamma_a - 1) + \sin^2 \gamma_a = 0 \quad (\text{Eq 2.1.70})$$

in which with γ_a is substituted γ .

The answers of the biquadratic equation - (Eq 2.1.70) are:

$$\cos \Psi_1 = \frac{\sin^2 \gamma_a + \cos \gamma_a \sqrt{(1-x)^2 - \sin^2 \gamma_a}}{1-x} \quad (\text{Eq 2.1.71})$$

$$\cos \Psi_2 = \frac{\sin^2 \gamma_a - \cos \gamma_a \sqrt{(1-x)^2 - \sin^2 \gamma_a}}{1-x} \quad (\text{Eq 2.1.72})$$

After substituting (Eq 2.1.71) and (Eq 2.1.72) in equation (Eq 2.1.69) for the angle of beneficial overlapping can be written :

$$\Psi_n = \arccos \left[\frac{\sin^2 \gamma_a - \cos \gamma_a \sqrt{(1-x)^2 - \sin^2 \gamma_a}}{1-x} \right] - \arccos \left[\frac{\sin^2 \gamma_a + \cos \gamma_a \sqrt{(1-x)^2 - \sin^2 \gamma_a}}{1-x} \right] \quad (\text{Eq 2.1.73})$$

Or after simplifying :

$$\Psi_n = 2\arccos\left(\frac{\sin\gamma_a}{1-x}\right) \quad (\text{Eq 2.1.74})$$

- Overlap ratio

The overlap ratio is related to the continual and smooth meshing of the teeth profiles. In order to have smooth meshing it is necessary to have as much as possible meshed pairs of teeth.

In epicycloidal gears half of the teeth in any moment are in contact with the pins, meaning that the coefficient of the overlapping should be equal to half of the pins. Since they are involved in transmitting the load. The overlap ratio is defined as a relation of the angle of overlapping $\psi_k = \pi$ to the angular pitch of the housing pins $\tau_2 = \frac{2\pi}{z_2}$. It can be expressed:

$$\varepsilon = \frac{\psi_k}{\tau_2} = \frac{z_2}{2} \quad (\text{Eq 2.1.75})$$

If the coefficient is defined like equation (Eq 2.1.75) it is not clear enough how many teeth pairs are engaged. Since that, a new term is introduced beneficial overlap ratio:

$$\varepsilon_n = \frac{\psi_n}{\tau_2} = \frac{\psi_n z_2}{2\pi} \quad (\text{Eq 2.1.76})$$

Where, ψ_n can be determined by equation (Eq 2.1.74).

If we take into consideration equations (Eq 2.1.74) and (Eq 2.1.76) for the coefficient of beneficial overlap ration can be written down the following:

$$\varepsilon_n = \frac{z_2}{\pi} \arccos\left(\frac{\sin\gamma_a}{1-x}\right) \quad (\text{Eq 2.1.77})$$

The coefficient is dependable on the number of pins z_2 , modification and the allowable angle of transmitting γ_a . If the number of pins z_2 increases then ε_n increases too, but if x increases then ε_n decreases.

- Boundary conditions of the modification

In the process of designing of corrected epicycloidal gears it is essential to take into consideration the modification of the profile cutting instrument x . The real range of variation of x is between x_{min} and x_{max} ($x_{min} < 1 < x_{max}$). The minimal values for x can be determined with the following equation:

$$x_{min} = 1 - \sqrt{1 - \frac{4(z_1+2)^3 r_c^{*2}}{27z_1(z_1+1)^2}} \quad (\text{Eq 2.1.78})$$

If x is increased that leads to decreasing the beneficial overlap ratio. To be sure that the transmission is working properly it is necessary the following to be fulfilled:

$$\varepsilon_n > \varepsilon_{n,min}, \quad (\text{Eq 2.1.79})$$

in which with $\varepsilon_{n,min}$ is designated the allowable minimal value of the beneficial overlap ratio. According to equation (Eq 2.1.77) for the maximum value of the coefficient of modification of the profile cutting instrument can be written :

$$x_{max} = 1 - \frac{\sin \gamma_t}{\cos\left(\frac{\pi \varepsilon_{n,min}}{z_1}\right)} \quad (\text{Eq 2.1.80})$$

2.2. Cycloid gearbox design

2.2.1 Forces and Force distribution in the cycloid gear

The cycloid reducer as a mechanical system is a statically indeterminate system. Therefore to obtain the stresses it is required to build a dynamic model in an appropriate software environment. The computer-aided approach will give very high accuracy.

Research made in National Academy of Sciences of Belarus (Tsetserukou D., 2012), presents force distribution among the transmission elements. In Figure 22 is shown how exactly the load is distributed among the housing pins. There can be seen that half of the pins are always in contact with the gear (colored with light blue) but the most loaded are less than half (colored with dark blue). These types of transmissions allow an overload of five times their rated torque. This is due to the fact that all the time while transmitting a large contact surface is provided.

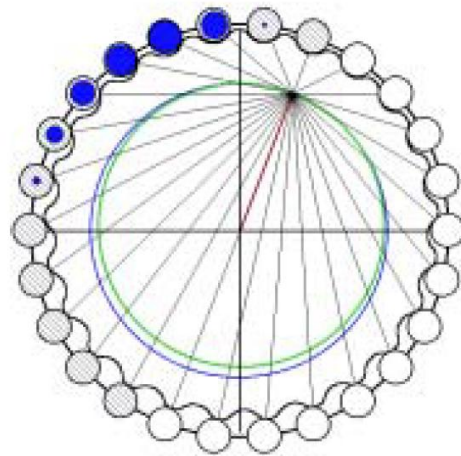


Figure 22. Force distribution between the gear and the pins (Tsetserukou D., BasinukV. ,2012)

Looking in depth a couple of forces will be acting on the main elements. Shown in Figure 23, below is a scheme how they are acting and their directions in a Cartesian coordinate system.

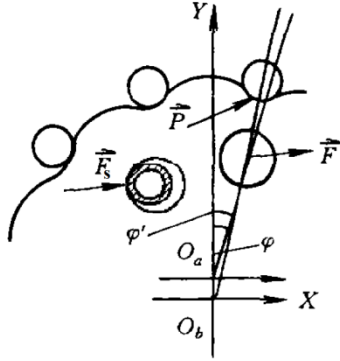


Figure 23. Forces (Yao & Zhang , 1997)

The acting forces here are:

-Force P is acting between the cycloid disc and the pins. Its value can be determined according to the following equation:

$$P = \sqrt[2]{(P_x^2 + P_y^2)} \quad (\text{Eq. 2.2.1})$$

With P_x is designated the force acting on axis x:

$$P_x = \frac{Z_4 M_1}{2 K_1 Z_3 r_2} \quad (\text{Eq. 2.2.2})$$

Where, Z_4 is the number of pins in the housing, M_1 is the input torque, K_1 - coefficient of width shortening of the epicycloid wheel, Z_3 - number of lobes and r_2 - pitch radius of pins.

The force P_y is on the Y axis:

$$P_y = \sum_{i=1}^{Z_4/2} \frac{2M_1 [\cos(\varphi - \frac{2\pi i}{Z_4}) - K_1] \sin(\varphi - \frac{2\pi i}{Z_4})}{K_1 Z_3 r_2 [1 + K_1^2 - 2K_1 \cos(\varphi - \frac{2\pi i}{Z_4})]} \quad (\text{Eq.2.2.3})$$

Force F is acting between the eccentric bearing and the cycloid disc (driving force) and its value can be determined by:

$$F_x = \frac{1}{n} \left(P_x + \frac{M_1 \sin \varphi'}{(Z_1 + Z_2)} \right) \quad (\text{Eq.2.2.4})$$

$$F_y = \frac{1}{n} \left(P_y + \frac{M_1 \sin \varphi'}{m(Z_1 + Z_2)} \right) \quad (\text{Eq.2.2.5})$$

And the total force can be determined:

$$F = \sqrt{F_x^2 + F_y^2} \quad (\text{Eq.2.2.6})$$

Force F_s is acting between the output shaft rollers and disc. Its value can be determined with equation (2.2.7).

2.2.2. Designing the holes and the thickness of the cycloid discs

-Diameter of output pins d'_p . In Figure 24 is shown where these diameters are situated.

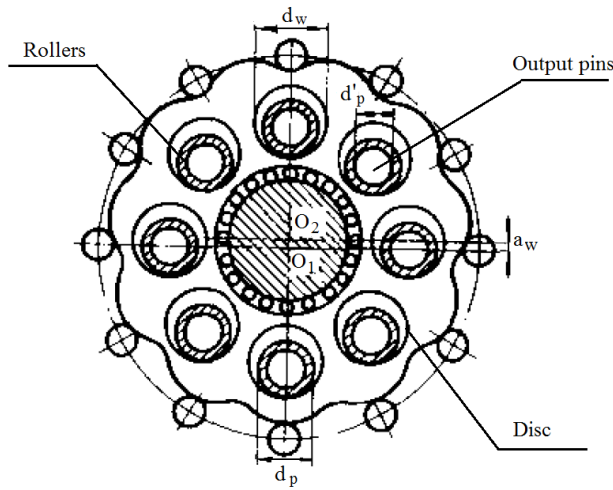


Figure 24. Corrected Cycloid Drive (Rao Zhengang, 1994)

Where: d'_p is the output pins' diameter, d_p is the roller diameter and with d_w is designated the disc's hole diameter. To calculate the diameter, first the force - F_s (acting on the rollers shown on figure below) should be taken into consideration. The force is calculated by the following equation:

$$F_{s \max} = \frac{4,8T_g}{Z_w r_2} \quad (\text{Eq2.2.7})$$

Where with T_g is designated the torque per cycloid disc. The number of holes in the gear for the output pins is presented with Z_w ; and r_2 is referred to the radius on which the pins are located.

According to (Zhengang, R., 1994) the output torque (T_2) is evenly distributed between the number of epicycloid discs (N), e.g.:

$$T_g = \frac{T_2}{N} \quad (\text{Eq 2.2.8})$$

On Figure 25 is shown a section cut of the reducer where the force is shown with a blue arrow.

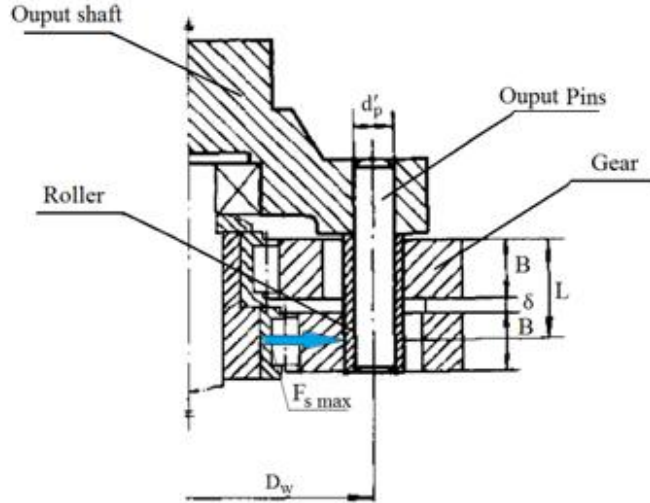


Figure 25. Reducer Section Cut (Zhengang, 1994)

The maximum bending stress in a pin is:

$$\sigma_F = \frac{F_{s \max} L}{W} \quad (\text{Eq 2.2.9})$$

Where with W is designated the section module:

$$W = \frac{\pi d'^3}{32} \quad (\text{Eq 2.2.10})$$

The distance L is the lever of the bending moment created from the force $F_{s \max}$ on the pin. It will be calculated using this equation:

$$L = 1,5B + \delta \quad (\text{Eq 2.2.11})$$

Where, B is the thickness of the disc and δ the distance between the discs. Also to calculate the pins for the output shaft the bending stress (σ_{FP}) is needed. It can be found by the following equation:

$$\sigma_{FP} = 0,43 \cdot \sigma_b \quad (\text{Eq 2.2.12})$$

With σ_b here is designated the tensile stress.

The equation for the diameter of the output pins:

$$d'_p \geq 36,6 \cdot \sqrt[3]{\frac{T_g(1,5B+\delta)}{Z_w R_w \sigma_{FP}}} \quad (\text{Eq 2.2.13})$$

When the diameter d'_p is known, d_p can be easily found according to the Table 10:

Table 10. Bush outer diameter d_w (Rao, 1994)

$d'_p [mm]$	12	14	17	22	26	32	35	45	55
$d_p [mm]$	17	20	26	32	38	45	50	60	75

When d_p is known the hole on the gear (d_w) can be calculated using this equation:

$$d_w = d_p + 2e \quad (\text{Eq 2.2.14})$$

The modern reducers have different output shaft pins. The shape is based on the area provided by the calculated diameter d_w . The better shape provides more contact surface and eliminates the roller element. Reducing the production cost per unit.

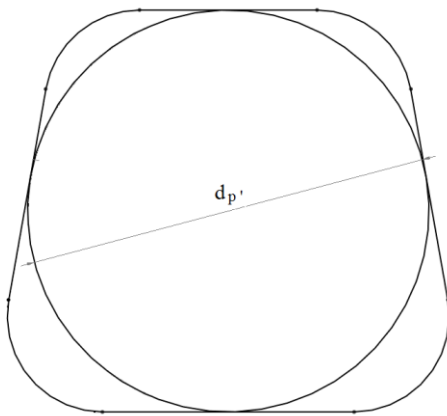


Figure 26. Pin Shape (Profile)

On Figure 26 is shown the shape, it is based on the inscribed in the trapezoid circle. This way the needed surface is provided. The edges are rounded and when the pins are offset inward with the value of the eccentricity, they can fluctuate in both of the discs. This provides a steady rotation of the output shaft.

- Disc thickness.

It is very important to determine the disc thickness with respect to the material and the contact forces. Here is shown a simplified equation, giving satisfactory result, but in the authors opinion more investigation in the area is needed for getting optimal designs.

Figure 27 shows section cut of the cycloid discs pins. With B is marked the thickness of the cycloid discs.

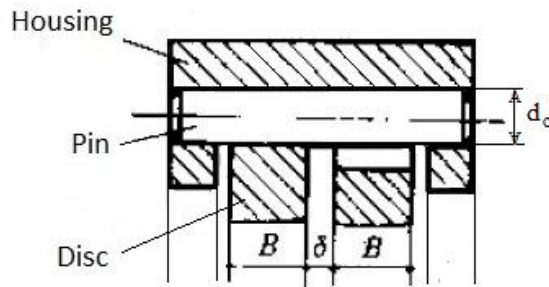


Figure 27. Section Cut (Rao , 1994)

The thickness can be calculated by the following equation:

$$B = (0,1 \div 0,2)r_2 \quad (\text{Eq 2.2.15})$$

Where r_2 is pitch radius of the housing.

3. Method

This chapter describes briefly and clearly the way of performing the work. Here will be explained how the computer software is used and the steps taken to receive the results.

3.1. Getting the results

- Examine the literature and theory

In order to find results and answers, first of all the literature and the theory in chapter 2 should be examined in details. The way of creating all the geometry and the relations should be clearly understood. Further knowledge in the engineering terminology, practical geometry and advanced computer skills in 3D modelling and simulations are also necessary due to the complexity of the material.

Before creating the 3D models and assembly, analytic calculations are needed. At the beginning the part geometry needs to be generated, using equations in chapter 2. Below is explained how this has been performed.

- Modeling in SolidWorks

SolidWorks software is a CAD (computer aided design) environment which gives the opportunity to create 3D solid body models. The whole process of creating a assembled product includes two steps: parts and making assemblies. The first and actually the basic step, creates parts (solid bodies) from already existing sketches, using ‘features’. The second step allows mounting the solid parts in particular order with the relations needed for the proper working of the mechanism. Using the Drawing module technical drawings from the parts or assemblies are created.

Using the potential that SolidWorks possess a prototype\model has been made and tested. Creating the working profile of the cycloidal gear and successfully assembling it with the other components. A special sketch feature called “equation driven curve” is used for establishing in the parametric equation for the needed curve or in this case profile. As a result a perfect epicycloidal curve is obtained. Using the feature extrude boss/base the epicycloidal wheel is created. For the simulation a feature called Motion Study is used, in which rotational speed is added on a certain axis.

- Parts creating

All of the components are built in Part files main data type file of SolidWorks. The output file format is *.SLDPRT. The most important step is making the epicycloid wheel (disc). Since SolidWorks does not have tools and commands for making epicycloid profiles, this specific profile has been built by “equation driven curve” command; the outcome is displayed in figure 28 (a) and (b). This command requires two parametric equations –for X and Y, which are functions of t. The equations for the working profile are from the theory chapter 2. They have been simplified and modified, in order to be understood by the software, as follows:

$$X_t = 2.5 * ((59 * \sin(t) - 0.7 * \sin(59 * t)) + ((2 * (0.7 * \sin(59 * t) - \sin(t)))) / (\sqrt{1 - (1.4 * \cos(58 * t))} + 0.49))$$

$$Y_t = 2.5 * ((59 * \cos(t) - 0.7 * \cos(59 * t)) + ((2 * (0.7 * \cos(59 * t) - \cos(t)))) / (\sqrt{1 - (1.4 * \cos(58 * t))} + 0.49))$$

Where the value of t is set to be from 0 to 2π .

After building the 2D sketch with the required profile, “Extruded Boss/Base” command has been used to build in 3D (Figure 28 (b)). The command “Extruded Cut” is used for making the holes in the disc.

Next step includes the housing. It has been built by the ordinary SolidWorks tools and commands, like: “sketch circle”, “sketch arc”, “Extruded Boss/Base”, ” Extruded Cut” etc.

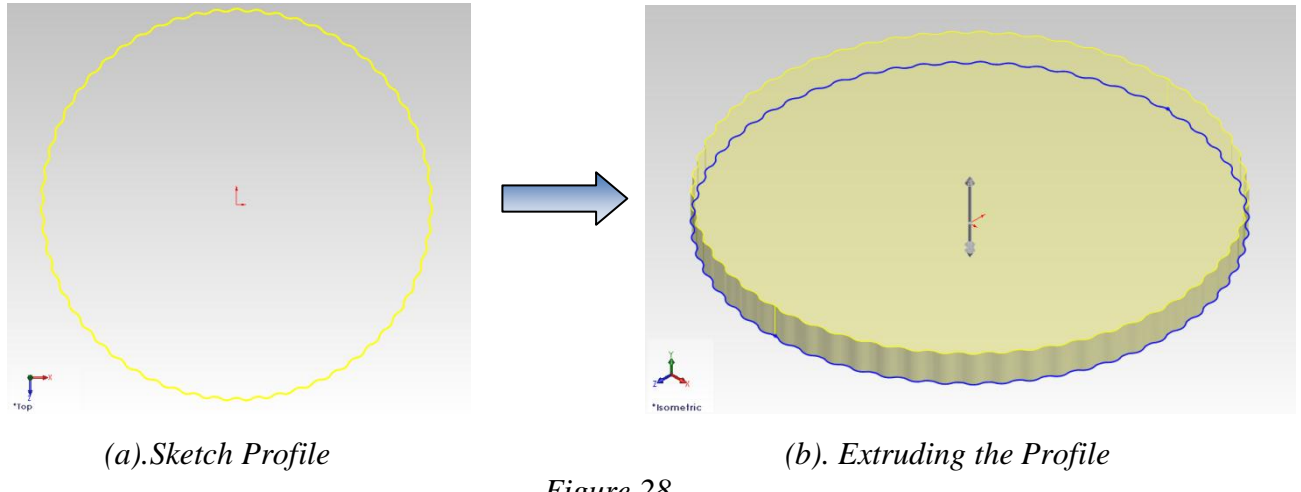


Figure 28

3.2. Making Assembly and Simulation

After all of the parts have been designed, they have been assembled. It can be made in Assembly module of SolidWorks. The output file format is *.SLDASM.

After importing the parts, only mates are added. Using the “Mate” command. We have made the entire assembly by the standard mates, available in SolidWorks: “Coincident”, “Parallel”, “Perpendicular”, “Tangent”, “Concentric”, etc ,except the case where the gears are mated using “Mechanical Mate”.

SolidWorks has a simulation package to set up virtual environments so that a test on a product can be tested before manufacture. Test against a broad range of parameters — like durability, static and dynamic analyses, motion of assemblies, heat transfer, fluid dynamics, etc.

To make the tests four steps have been accomplished:

1. The geometry has been defined
2. Material has been assigned
3. The Study has been specified
4. Environment has been set
5. The System processed the calculations and presented results

This modeling system offers a Von Mises – linear static analysis. Where the following assumptions are made by the software:

- The involved material is linear, when reacting to a force the displacement is proportional to the applied force, like the spring in figure 29 below (e.g. the material obeys Hooks law);
- Deformations are relative to the tested component or assembly's size;
- The loads do not change in time (e.g. the loads are static).

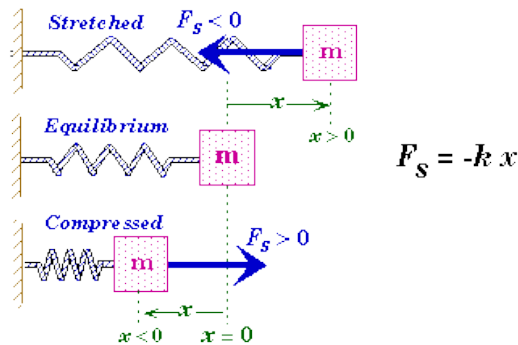


Figure 29. Force acting on a spring
[\(http://faculty.wwu.edu/vawter/PhysicsNet/Topics/Dynamics/gifs/Forces04.gif\)](http://faculty.wwu.edu/vawter/PhysicsNet/Topics/Dynamics/gifs/Forces04.gif)

The SolidWorks static analysis tool works with Von Mises yield criterion. According to this criterion the yield begins when the stresses (known as the yield strength) reaches a critical value. Also it is based on the octahedral shear stress. The Von Mises stress criterion is used to predict yielding under any loading condition from results of simple uniaxial tensile tests (Asaro R, 2004, page 463).

4. Results

This chapter presents the output data of this thesis. The results are reported simply and clearly. Most of the results are obtained by computer simulations with advanced software computations. In order to be understandable the results are simplified.

The results from the theory part are a new way of looking at the geometric shapes of the reducer. We have used Professor Ognian Alipiev's unique approach to design a product together with the group, working on the shafts, bearings etc. In order to fulfil the demands, we have designed the cycloid gear using standard values for the module, used in spur gears. As explained this is not typical when working with such transmissions. In this case this approach can be standardized in future for these kinds of gears. They can help the people working with cycloid transmissions.

All of the results are presented after examination and analysing the equations and the information in the theory chapter. The design process has been achieved from the output data given by SwePart Transmissions AB. What they required is the torque on the output shaft of the reducer should be 6300 Nm, ratio 240 and rotational speed of 4,3 rpm. To obtain these results, the forces and force distribution have been found.

4.1. Total ratio

The total ratio calculated with equation 1.1 in the background is as follows:

$$(1.1) \quad i = 1 + \frac{Z_2}{Z_1} \cdot Z_4 = 1 + \frac{69}{17} \cdot 59 = 240,47$$

4.2. Solidworks Simulation Results

Because of the complexity of the profile of the cycloid wheel we used computer simulation to get appropriate results. Also it is necessary to use the help of the computer software because the limitation of time, which is not enough for analytic calculations.

For this scheme the model of the gearbox has been simplified significantly, removing all the components except the housing, cycloid gear and eccentric shafts. Also the output, input and eccentric shaft are simulated separately without being connected with other parts of the cycloid reducer. These simplifications do not affect significantly the results. These assumptions and simplifications have been done to reduce the calculation time as such analyses take a lot of time if not simplified. The results are presented as figures, tables and diagrams for the model information, stress, displacement, strain and safety factor of the elements. Below are simulated the cycloid gear stage (cycloid disc and housing with pins), eccentric, output and input shafts.

4.2.1. Cycloid Gear Results – The results are presented in Appendix 1C.

4.2.2. Input Shaft Results - The results are presented in Appendix 2C.

4.2.3. Output Shaft Results - The results are presented in Appendix 3C.

4.2.4. Eccentric Shaft Results - The results are presented in Appendix 4C.

5. Analysis

Chapter analysis introduces principles, relationships or generalisations from the results. Sometimes the results speak for themselves. All of the results can be found in chapter 4. The function of the analysis chapter is to describe the ideas, models and theories with comparison of these with the computational data.

The Cycloid speed reducer has been studied, in details. Sufficient calculation process for the geometry of the cycloid gear has been presented. Using hi-end, up to date CAE software, the calculated model was studied showing the many benefits of the mechanism. In the future the need for such machines will continue to rise, as the reducer can be implemented almost in every mechanized solution.

Chapter 4.1 shows the total ratio (i) result. It has been calculated to be 240,47. According to the given input data in chapter 1.3 it should be 240. Comparing the two values - it is obvious that the designed reducer ratio is in theory as close as possible to the desired one. The result is based on analytic calculation, which makes it accurate and precise.

In the previous chapter are shown the graphical tables containing the outcome from the CAE software. For every tested model there are presented the following table types:

- Model info – shows general information about the tested model
- Study properties – they show information about the study conditions
- Units – the used units in the study
- Materials – there is displayed the type of material and its physical properties
- Loads and fixtures – information about the loads and the used fixtures
- Contact information – about how the software defines the contact conditions
- Mesh information – there can be observed a meshed view and detail about the meshing
- Stress – these are diagrams where with a color-graphic method is displayed the resultant stresses
- Displacement – it can be observed the linear displacements also in color-graphic
- Strain – strain level in the tested part
- Factor of safety – there with red color are designated the zones where safety factor is below 2 (e.g. $SF \leq 2$)

Here will be analyzed the stress/displacement/strain/factor of safety diagrams.

- Cycloid gear and housing

The model information given in Table 4.1 shows included parts (gear and housing) and the basic information about them like mass, volume, density and weight. Also with purple color can be seen the torque vectors that has been set. All the details (temperature, analysis types etc.) about the simulation and study properties are shown in Table 4.2. All of these simulations use *International System Units (SI)* (Table 4.3). This means that the pressure is in *MPa*, the temperature is in Kelvin etc.

The material properties are included in Table 4.4, where it is shown the yield and tensile strength of the used material. SolidWorks does not have the exact material as in our case (20 MnCr 6), this is the reason why we have set the material to be alloy steel (SS). It has lower yield and tensile strengths, comparison to 20 MnCr 6. This means that if the simulation is successful with this material, the design of the cycloid wheel would be good enough for material with higher values of yield and tensile stresses.

The applied torque in cycloid wheel is 3200Nm (Table 4.5).The simulation is set to be with global contact (Table 4.6), which means that contact will occur between the cycloid wheel and the housing. Also the mesh quality has been set to be high (Table 4.7), giving more accurate results.

Looking at the Table 4.8 can be observed that the developed stresses in the mechanical system do not exceed the yield strength of the material ($640,4MPa$). On the color scale at right, can be seen the meaning of every color occurred in details. With blue color and nuances of blue are colored the areas where the stresses have a low values (from 0 to $\approx 200MPa$) of the stresses. Respectively with red color the high values of the stresses. Fortunately when looking at the results for the cycloid gear design, it can be realized that overall the cycloid gear-housing has withstood the loads. There are not places with values more than $\approx 250MPa$ (only blue and some nuances of blue color). This means that all of the stress values are times lower than the yield strength of the material. In this case we are sure that the cycloid wheel and housing are designed properly, because in reality the gears and the pins will probably be tempered or/and galvanized.

In Table 4.9 is shown the displacement of the cycloid wheel. Analogically as stress analysis the color scale at right shows the value of the displacement (in mm). The minimum and maximum values are respectively 0 and $27,66\mu m$. Most of the displacements in the cycloid wheel are between $10\mu m$ and $20\mu m$, except one area with values more than $20\mu m$ (indicated with yellow color). These values are still under the nominal values in which case no problems will occur.

With Table 4.10 is shown the permanent strains after unloading the components. As can be read from the diagram, all strains are in elastic zone (low values are colored in blue).

The safety factor is shown in Table 4.11. There is not color scale in this diagram. The reason is that only two colors exist in this type of analysis. With blue are colored the areas with safety factor bigger than two, and with red are colored the areas with safety factor less than two (red $< SF=2 <$ blue). As easily can be seen in the figure – all zones of the cycloid wheel and the housing have safety factor bigger than two (zones with blue color).

These static analyses give a satisfactory accuracy as the conditions simulated by the software are very similar to the real working condition.

- Input Shaft

Analogically this analysis provides the same information in tables from 4.12 to 4.17 as tables from 4.1 to 4.7 (as in the previous analysis). The most significant deference is in tables from 4.18 to 4.21.

In table 4.18 can be observed that the developed stresses in the mechanical system do not exceed the yield strength of the material ($220,6MPa$). On the color scale at right, can be seen the meaning of every color occurred in the details. With blue color and nuances of blue are colored the areas where the stresses have a low values (from 0 to $\approx 100MPa$) of the stresses. Respectively with red color are colored the high values of the stresses. Fortunately when looking at the results for the input shaft, it can be realized that it has withstood the loads. There are no places where the values are more than $\approx 115MPa$ (only blue and some nuances of blue color). This means that all of the stress values are times lower than the yield strength of the material. In this case we are sure that the input shaft is designed properly.

In Table 4.19 is shown the displacement of the input shaft. Analogically as stress analysis the color scale at right shows the value of the displacement (in mm). The minimum and maximum values are respectively 0 and $45,62\mu m$.

With Table 4.20 is shown the permanent strains after unloading the components. As can be read from the diagram, all strains are in elastic zone (low values are colored in blue and green).

The safety factor is shown in Table 4.21. There is not color scale in this diagram. The reason is that only two colors exist in this type of analysis. With blue are colored the areas with safety factor bigger than two, and with red are colored the areas with safety factor less than two (red $< SF=2 <$ blue). As easily can be seen in the figure – all zones of the input shaft have safety factor bigger than two (zones with blue color).

- Output Shaft

In table 4.22 is displayed the model information, such as volumetric properties, view etc. In the next table 4.23 are the details about the properties of the study and the used features by the software. The next two tables 4.24 and 4.25 prove units and material information.

In Table 4.26 are shown the used fixtures when doing the simulation and also the loads. Here one face is fixed, there is one that is where the bearings will be and its status is made Roller/Slider to simulate the bearing effects. The opposite to the fixed face is the loaded face subjected to a torque of 6400Nm, the actual output torque.

Looking down to the next Table 4.27. It includes a lot of data about the mesh and mesh control. There is also a picture showing the meshed detail, there can be observed that the meshing is quite fine, which will help generate a very accurate calculation process.

On the stress color-diagram in Table 4.28, can be seen the resultant stresses from the simulated twisting. The deformed state of the model is magnified by the software, only to help the viewer to imagine how this will happen in reality. Again here can be seen that the stresses do not exceed the yield strength of the material as the colors show. Also the next three figures (4.29,4.30,4.31) show that overall the design will withstand the static loads.

- Eccentric Shaft

The following tables have the similar information, they provide information how the study was conducted and etc., from Table 4.32 up to 4.37.

In Table 4.38 is shown the stress color-diagram. Looking at the colors and the color legend, it can be said that the stress does not exceed the material yield strength. Also the same can be said for the other color-diagrams presenting the displacement, strain and factor of safety.

6. Conclusion

This study shows the geometry and designing and calculating process in a second stage of a cycloidal reducer. The cycloidal gear capacity can be estimated by computer aided software like SolidWorks, as shown in this work. All of the theory and the equations are based on advanced work of many high qualified scientists in this area of study. By this thesis we have created SolidWorks assembly models, which can be used for further analysis by recalibrating the materials and model settings. These models have been simulated in software environment, in order to get results.

The results included in chapter 4 are accurate enough for making predictions and important conclusions. The designing process in Appendix 1 and theory chapter is shown in clear way. By following the equations it is easy to find all dimensions and designing the cycloid gear components.

As the results and analysis present, this type of gear reducers are more reliable and profitable than the conventional spur gears reducers. More researches and examinations are required in this area. Our team hopes that this work will help for future studies and standardization of the cycloid reducer.

7. References

- Alipiev O. (1988), “Geometry and Forming of Epi- and Hypo-Cycloidal Toothed Wheels in Modified Cyclo-Transmission”, Ph.D. Dissertation, Ruse, pp.1-36 (in Bulgarian).
- Ashby M. (2005), How to Write a Paper 6rd Edition, Engineering Department, University of Cambridge, Cambridge
- Darali drives, (2012) homepage, <http://www.darali.com/page17.html>
- D'Amico J., (2012), <http://machinedesign.com/article/comparing-cycloidal-and-planetary-gearboxes-0203>
- Sumitomo Drives, (2012) homepage,
http://www.smcycle.com/modules.php?name=Product&op=productBrand&brand_id=7
- TsetserukouD., V. Basinuk (2012), CONTACT FORCE DISTRIBUTION AMONG PINS OF TROCHOID TRANSMISSIONS, Department of vibroprotection of machines, Institute of Mechanics and Reliability of Machines of the National Academy of Sciences of Belarus (IMRM of NAS of Belarus), Akademicheskaya 12, 220072 Minsk, Belarus
- Yao W.,Zhang Z. (1997), Journal of Beijing, Institute of Machinery Industry(In Chinese)
- Rao Z., (1994),"Planetary transmission mechanism design"(in Chinese)
- Robert J. (2004), V. Lubarda , Mechanics of Solids and Materials, University of Cambridge, Cambrige
- <http://www.nabtescomotioncontrol.com/pdfs/RVseries.pdf>
- <http://machinedesign.com/article/comparing-cycloidal-and-planetary-gearboxes-0203?page=0%2C0>
- http://fluid.ippt.gov.pl/ictam04/CD_ICTAM04/SM2/10540/SM2_10540_new.pdf
- <http://www.rmhoffman.com/faqs/engineering/cycloidal.html>

8. Appendix

Appendix 1 – Geometry Design

Appendix 2 – Figures

Appendix 3 – Linear Static Analyses with SolidWorks

Appendix 4 - Drawings

Appendix 1 - Geometry Design

1A. Basic Parameters

2A. Epicycloidal Wheel Dimensions

3A. Pin Wheel Dimensions

4A. Epicycloidal Gear Parameters

Appendix 1- Geometry Design

1A. Basic Parameters

The calculation process starts with determination of the four basic parameters of the epicycloidal wheel:

$$\text{Number of teeth - according to (Eq 1) and (Eq 1.1)} \quad z_1 = 58$$

$$\text{Module - by standard value:} \quad m = 5$$

$$\begin{aligned} \text{Coefficient of the radius of the profile generating circle:} & \quad r_c^* = 1 \\ (\text{recommended by (Alipiev, 1988)}) \end{aligned}$$

coefficient displacement of the profile cutting instrument*:

$$1 - \frac{\sin\gamma_t}{\cos\left(\frac{\pi\varepsilon_{n,min}}{z_1+1}\right)} \geq x \geq 1 - \sqrt{1 - \frac{4(z_1 + 2)^3 r_c^{*2}}{27z_1(z_1 + 1)^2}}$$

where $\gamma_t = 30^\circ$, what else is not known is $\varepsilon_{n,min}$.

$$\varepsilon_{n,min} = \frac{z_2}{\pi} \arccos\left(\frac{\sin\gamma_t}{1 - x_{max}}\right) = \frac{59}{\pi} \arccos\left(\frac{\sin 30}{1 - 0,49}\right) = 213,4356$$

In the formula x_{max} is substituted with 0,49 which is the maximum coefficient of modification of the profile cutting instrument for this kind of gears. Finally for x we have

$$0,49 > x > 0,083$$

$$x = 0.3$$

2A. Epicycloidal Wheel Dimensions

2.1. Diameter of pitch circle:

$$(Eq 2.1.11) \quad d_1 = m \cdot z_1 = 5 \cdot 58 = 290 \text{ mm}$$

2.2. Diameter of the theoretical dedendum circle:

$$(Eq 2.1.13) \quad d_{Tf_1} = m(z_1 + x) = 5(58 + 0,3) = 291,5 \text{ mm}$$

2.3. Diameter of theoretical addendum circle:

$$(Eq 2.1.16) \quad d_{Ta_1} = m(z_1 + 2 - x) = 5(58 + 2 - 0,3) = 298,5 \text{ mm}$$

2.4. Diameter of dedendum circle:

$$(Eq 2.1.19) \quad d_{f_1} = m(z_1 + x - 2 \cdot r_c^*) = 5(58 + 0,3 - 2 \cdot 1) = 281,5 \text{ mm}$$

2.5. Diameter of addendum circle:

$$(Eq\ 2.1.22) \quad d_{a_1} = m(z_1 + 2 - x - 2 \cdot r_c^*) = 5(58 + 2 - 0,3 - 2,1) = 288,5\ mm$$

2.6. Teeth height:

$$(Eq\ 2.1.23) \quad h_1 = m(1 - x) = 5(1 - 0,3) = 3,5\ mm$$

2.7. Addendum curvature radius*:

$$\rho_f = \frac{m}{2} \left[\frac{(z_1 + 1)x^2}{z_1 - x(z_1 + 1)} + 2 \cdot r_c^* \right] = \frac{5}{2} \left[\frac{(58 + 1)0,3^2}{58 - 0,3(58 + 1)} + 2,1 \right] = 5,3294\ mm$$

2.8. Dedendum curvature radius*:

$$\rho_a = \frac{m}{2} \left[\frac{(z_1 + 1)(2 - x)^2}{(z_1 - x)^2(z_1 + 1) + 1} - 2 \cdot r_c^* \right] = \frac{5}{2} \left[\frac{(58 + 1)(2 - 0,3)^2}{(58 - 0,3)^2(58 + 1) + 1} - 2,1 \right] = 4,998\ mm$$

2.9. Minimal teeth curvature radius*:

$$\rho_{min} = \frac{m}{2} \left[\frac{3(z_1 + 1)\sqrt{3z_1x(2 - x)}}{(z_1 + 2)^{\frac{3}{2}}} - 2 \cdot r_c^* \right] = \frac{5}{2} \left[\frac{3(58 + 1)\sqrt{3 \cdot 58 \cdot 0,3(2 - 0,3)}}{(58 + 2)^{\frac{3}{2}}} - 2,1 \right] = 3,969\ mm$$

2.11. Coefficient of shortening of the epicycloid:

$$(Eq\ 2.1.26) \quad \lambda = 1 - x = 1 - 0,3 = 0,7$$

1.12. Disc Thickness

$$(Eq\ 2.2.9) \quad B = (0,1 \div 0,2) \cdot R_p = 0,1 \cdot 147,5 = 14,75\ mm$$

3A. Pin Wheel Dimensions.

3.1. Number of teeth of the pin wheel:

$$z_2 = z_1 + 1 = 58 + 1 = 59$$

3.2. Diameter of the pitch circle:

$$d_2 = mz_2 = 5,59 = 295\ mm$$

3.3. Diameter of the pins:

$$(Eq.2.1.50) \quad d_c = 2r_c^*m = 2 \cdot 1,5 = 10\ mm$$

3.4. Diameter of the addendum circle:

$$(Eq\ 2.1.53) \quad d_{a_2} = m(z_2 - 2r_c^*) = 5(59 - 2.1) = 285\ mm$$

3.6. Contact angle*

$$\beta = \arcsin(1 - x) = \arcsin(1 - 0,3) = 44,427$$

4A. Epicycloidal Gear Parameters.

4.1. Centre distance

$$a_w = \frac{m}{2}(1 - x) = \frac{5}{2}(1 - 0,3) = 1,75\ mm$$

4.2. Diameters of initial circles:

-epicycloidal wheel	$d_{w_1} = mz_1(1 - x) = 5.58(1 - 0,3) = 203\ mm$
-pins wheel	$d_{w_2} = mz_2(1 - x) = 5.59(1 - 0,3) = 206,5\ mm$

4.3. Coefficient of non centoroidity

$$l = \frac{d_2}{d_{w_2}} = \frac{d_1}{d_{w_1}} = \frac{1}{1 - x} = \frac{1}{1 - 0,3} = 1,4285\ mm$$

4.4. Maximum angle of transmitting movement

$$\gamma_{max} = \arcsin(1 - x) = \arcsin(1 - 0,3) = 44,427$$

4.5. Angle of beneficial overlapping

$$\psi_n = 2\arccos\left(\frac{\sin\gamma_{allowable}}{1 - x}\right) = 2\arccos\left(\frac{\sin 30}{1 - 0,3}\right) = 88,83$$

4.6. Coefficient of beneficial overlapping

$$\varepsilon_n = \frac{z_2}{\pi} \arccos\left(\frac{\sin\gamma_{allowable}}{1 - x}\right) = \frac{60}{\pi} \arccos\left(\frac{\sin 30}{1 - 0,3}\right) = 848,26$$

* - Equations marked with * symbol are taken directly from (Alipiev, 1988), based on the theory in chapter 2.

Appendix 2 - Figures

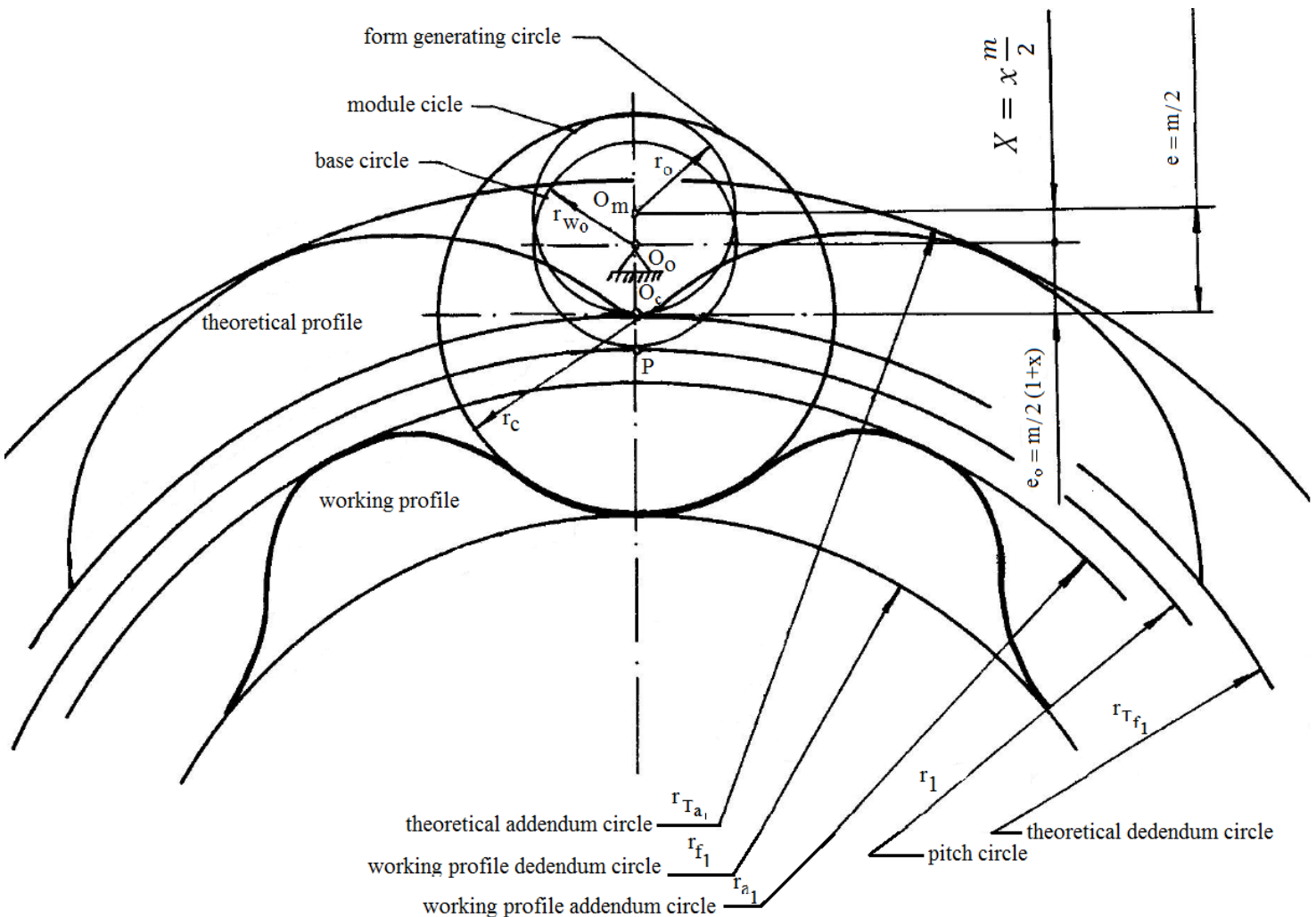
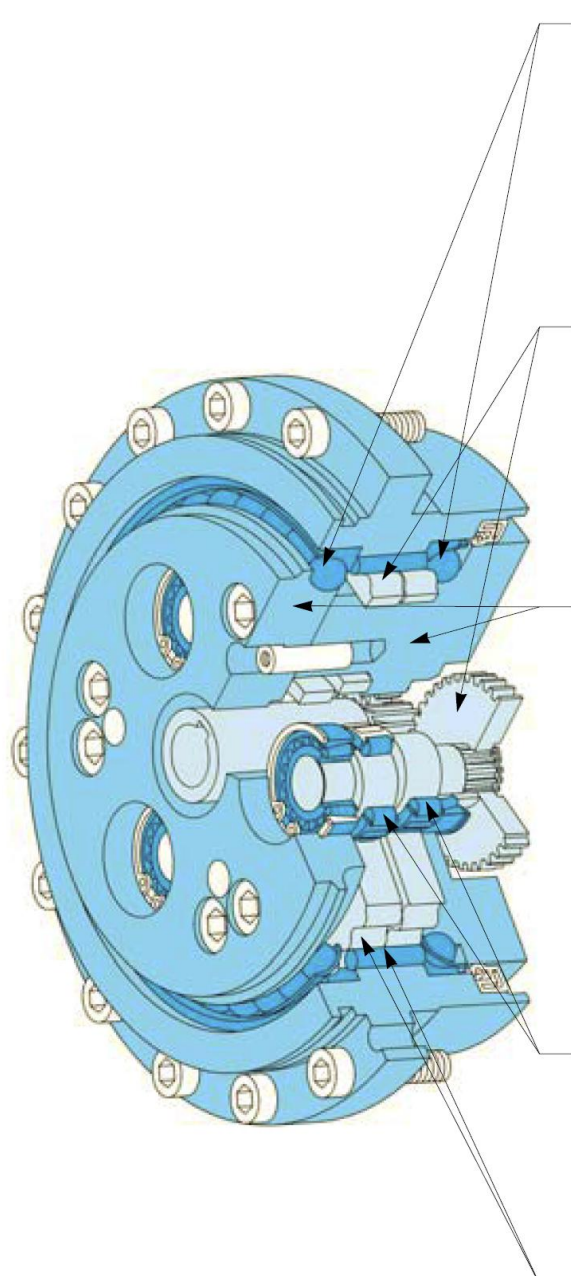


Figure 1. Gear dimensions (Alipieva, 1988)

FEATURES AND BENEFITS



INTEGRATED ANGULAR BALL BEARINGS

Benefits:

- Increases reliability
- Reduces overall cost

Attributed to:

- Built-in angular ball bearing construction improves ability to support external loads, increases moment rigidity and maximum allowable moment.
- Reduces the number of components required.
- Simplifies installation and maintenance.

2 STAGE REDUCTION

Benefits:

- Reduces vibration
- Reduces inertia (GD^2)

Attributed to:

- Low speed rotation of the RV gear reduces vibration.
- Reduced size of the motor coupling part (input gear) lowers inertia.

ALL MAIN ELEMENTS ARE SUPPORTED ON BOTH SIDES

Benefits:

- Higher torsional stiffness
- Less vibration
- High shock load capability (5 times rated torque)

Detail:

- Crankshafts are supported on both sides of the reduction gear as shown below.

Shaft + hold flange Crankshaft bearing supports Crankshaft through hole

Rigid supporting structure Clearance hole for rigid supporting structure RV gear

ROLLING CONTACT ELEMENTS

Benefits:

- Excellent starting efficiency
- Low wear and longer life
- Low backlash (Less than 1 arc. min.)

Attributed to:

- Use of roller bearings throughout.

PIN & GEAR STRUCTURE

Benefits:

- Very low backlash (Less than 1 arc. min.)
- Higher shock load capability (5 times rated torque)

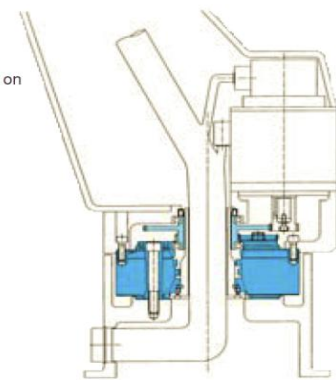
Attributed to:

- Synchromeshing of many RV gear teeth and pins.

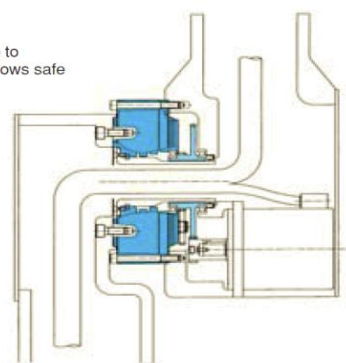
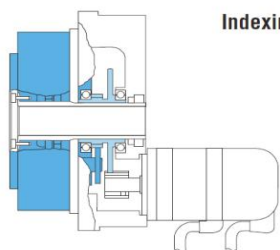
Figure. 2 Features and Benefits of the RV (Nabtesco, 2012 homepage)

Robot Swing Axis

- Allows space-saving design
- Main bearing is not required on robot side.

**Robot arm**

- Greater internal resistance to adverse environments-allows safe throughput of cables.
- Wider operating angle.

**Indexing Table****Robot Wrist Axis**

As shown in the figure(right), the input gear can also be supported within the reduction gear mechanism.
Please contact Nabtesco for more details.

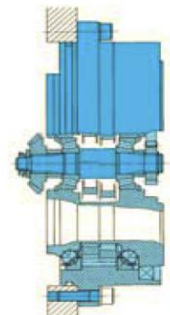
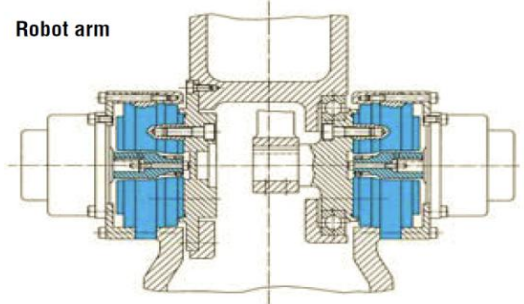
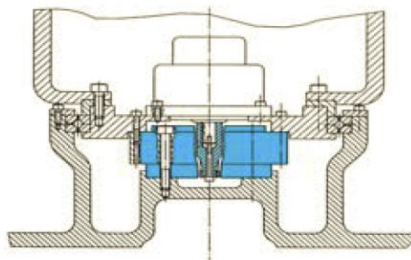
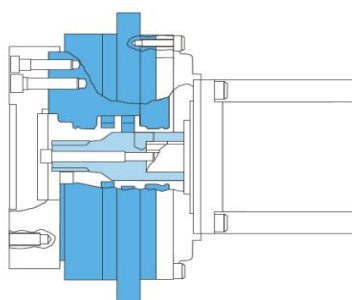
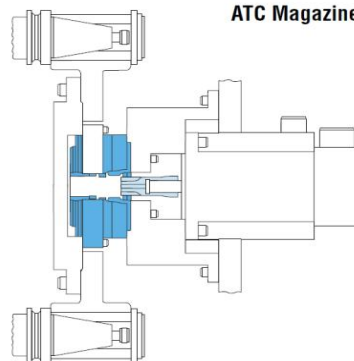
**Robot arm****Robot Swing Axis****Positioner****ATC Magazine**

Figure 3. Cycloid Implementation Examples (Nabtesco, 2012 homepage)

Appendix 3 – Linear Static Analyses with SolidWorks

1C. Cycloid Gear Results

2C. Input Shaft Results

3C. Output Shaft Results

4C. Eccentric Shaft Results

1C. Cycloid Gear Results

Table 4.1 Model Information

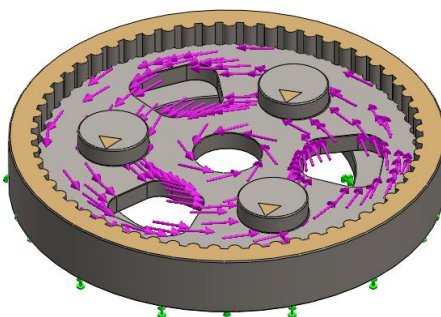
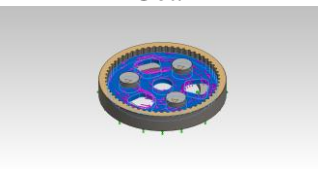
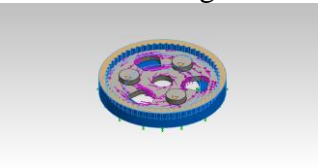
 Model name: Cycloid Gear Model Current Configuration: Default			
Solid Bodies			
Document Name and Reference	Treated As	Volumetric Properties	Document Path/Date Modified
Gear 	Solid Body	Mass:5.11346 kg Volume:0.000664086 m ³ Density:7700 kg/m ³ Weight:50.1119 N	C:\Users\DELLi7\Desktop\epicycloid\Part1.SLDP RT May 23 11:50:18 2012
Housing 	Solid Body	Mass:11.1377 kg Volume:0.00144645 m ³ Density:7700 kg/m ³ Weight:109.149 N	C:\Users\DELLi7\Desktop\epicycloid\Part2.SLDP RT May 23 11:51:10 2012

Table 4.2 Study Properties

Study name	Static Study 1
Analysis type	Static
Mesh type	Solid Mesh
Thermal Effect:	On
Thermal option	Include temperature loads
Zero strain temperature	298 Kelvin
Include fluid pressure effects from SolidWorks Flow Simulation	Off
Solver type	FFEPlus
Inplane Effect:	Off
Soft Spring:	Off
Inertial Relief:	Off
Incompatible bonding options	Automatic
Large displacement	Off
Compute free body forces	On
Friction	Off
Use Adaptive Method:	Off

Table 4.3 Units

Unit system:	SI (MKS)
Length/Displacement	mm
Temperature	Kelvin
Angular velocity	Rad/sec
Pressure/Stress	N/m ² (Mpa)

Table 4.4 Material Properties

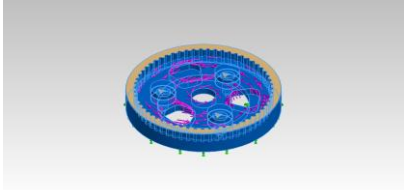
Model Reference	Properties	Components
	<p>Name: Alloy Steel Model type: Linear Elastic Isotropic Unknown Default failure criterion: Yield strength: 6.20422e+008 N/m^2 Tensile strength: 7.23826e+008 N/m^2 Elastic modulus: 2.1e+011 N/m^2 Poisson's ratio: 0.28 Mass density: 7700 kg/m^3 Shear modulus: 7.9e+010 N/m^2 Thermal expansion coefficient: 1.3e-005 /Kelvin</p>	SolidBody - Gear SolidBody - Housing
Curve Data:N/A		

Table 4.5 Load

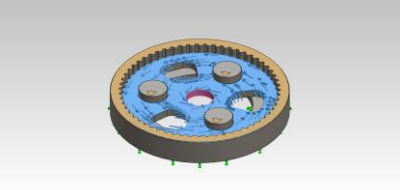
Load name	Load Image	Load Details
Torque-1		Entities: 1 face(s) Reference: Face< 1 > Type: Apply torque Value: 3200 N·m

Table 4.6 Contact Information

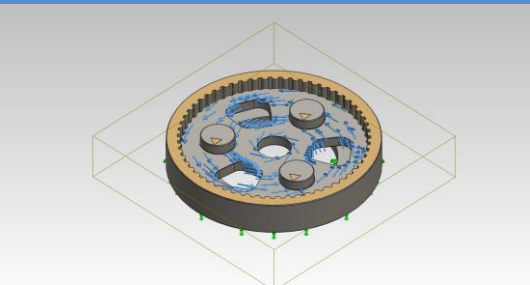
Contact	Contact Image	Contact Properties
Global Contact		Type: Node to node Components: 1 component(s)

Table 4.7 Mesh Information

Mesh type	Solid Mesh
Mesher Used:	Curvature based mesh
Jacobian points	4 Points
Maximum element size	13.292 mm
Minimum element size	2.65841 mm
Mesh Quality	High

Table 4.8 Stress

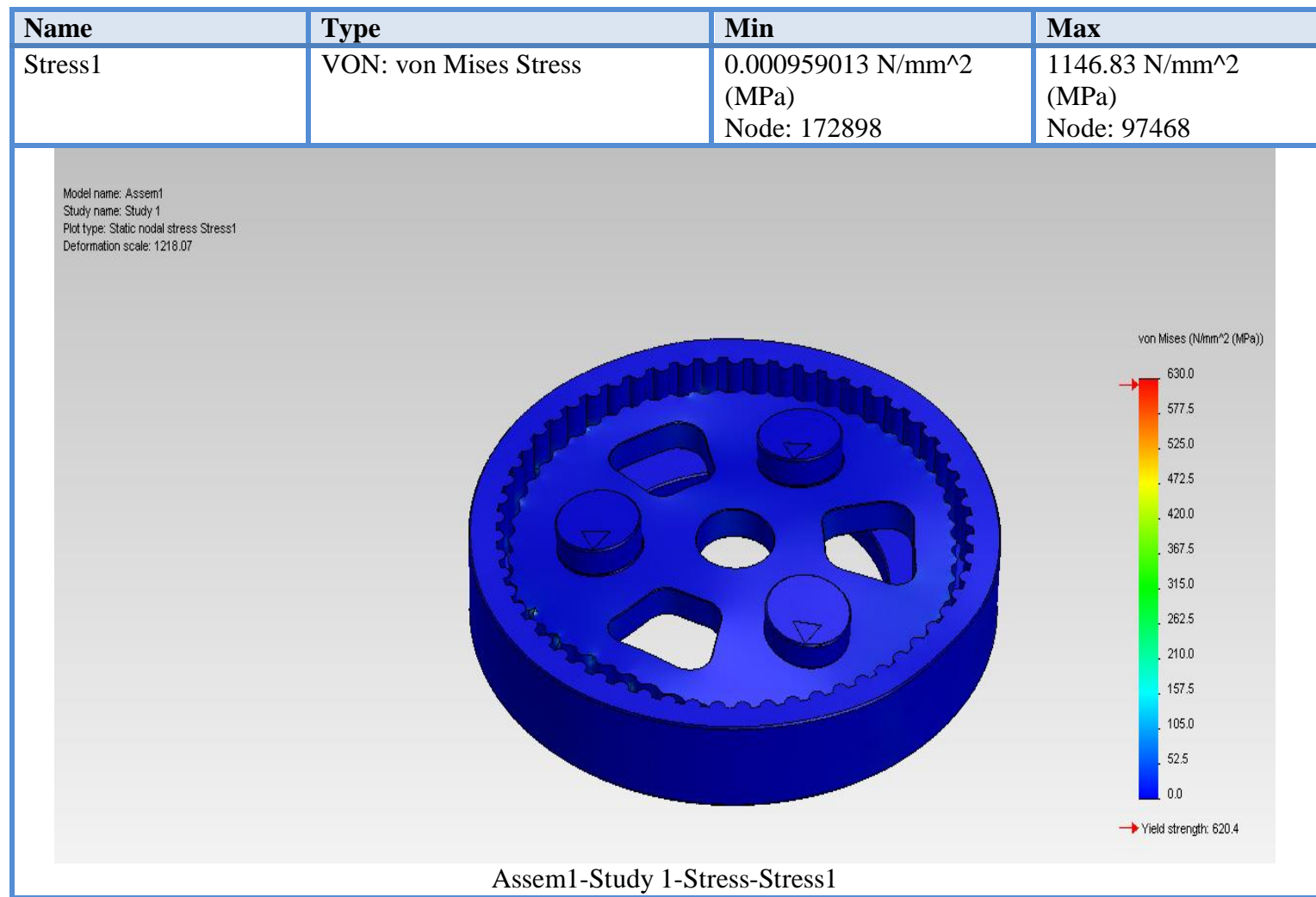


Table 4.9 Displacement

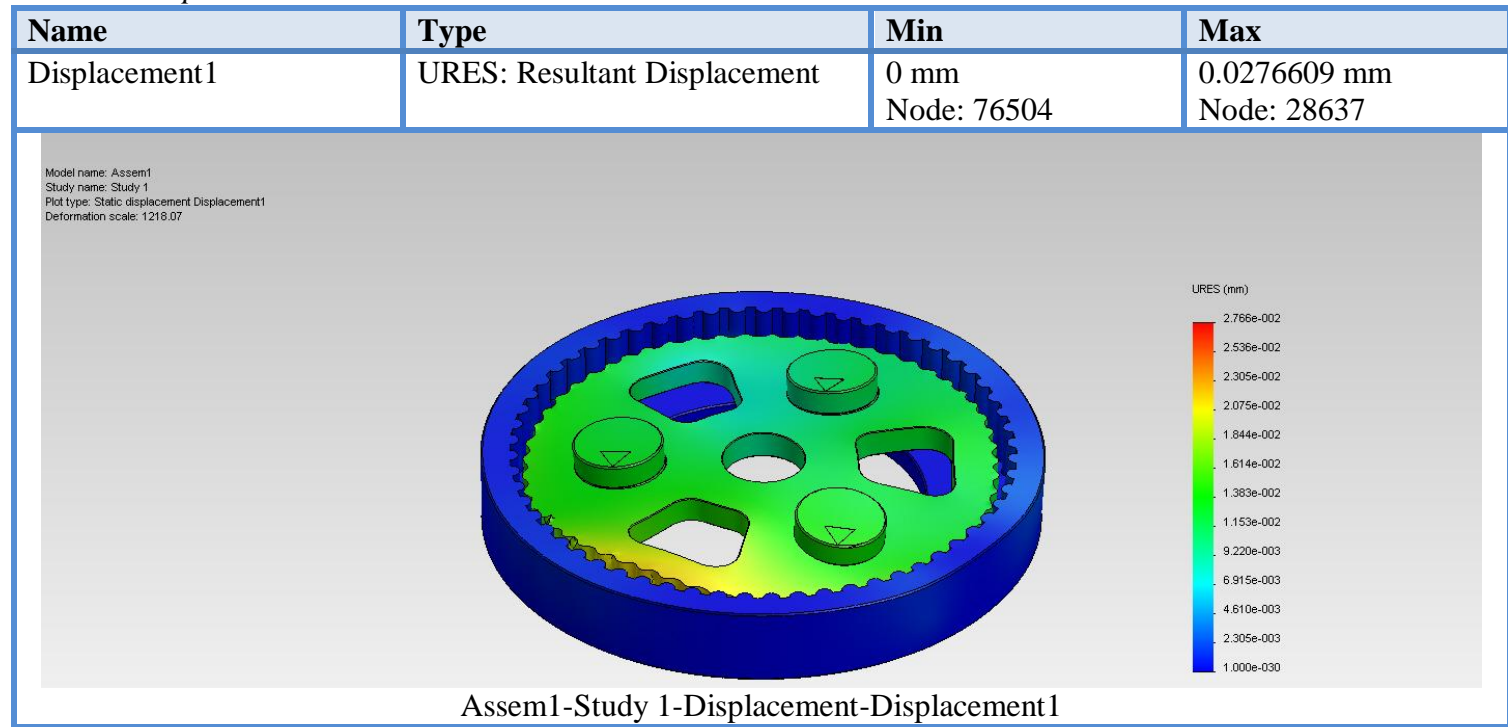


Table 4.10 Strain

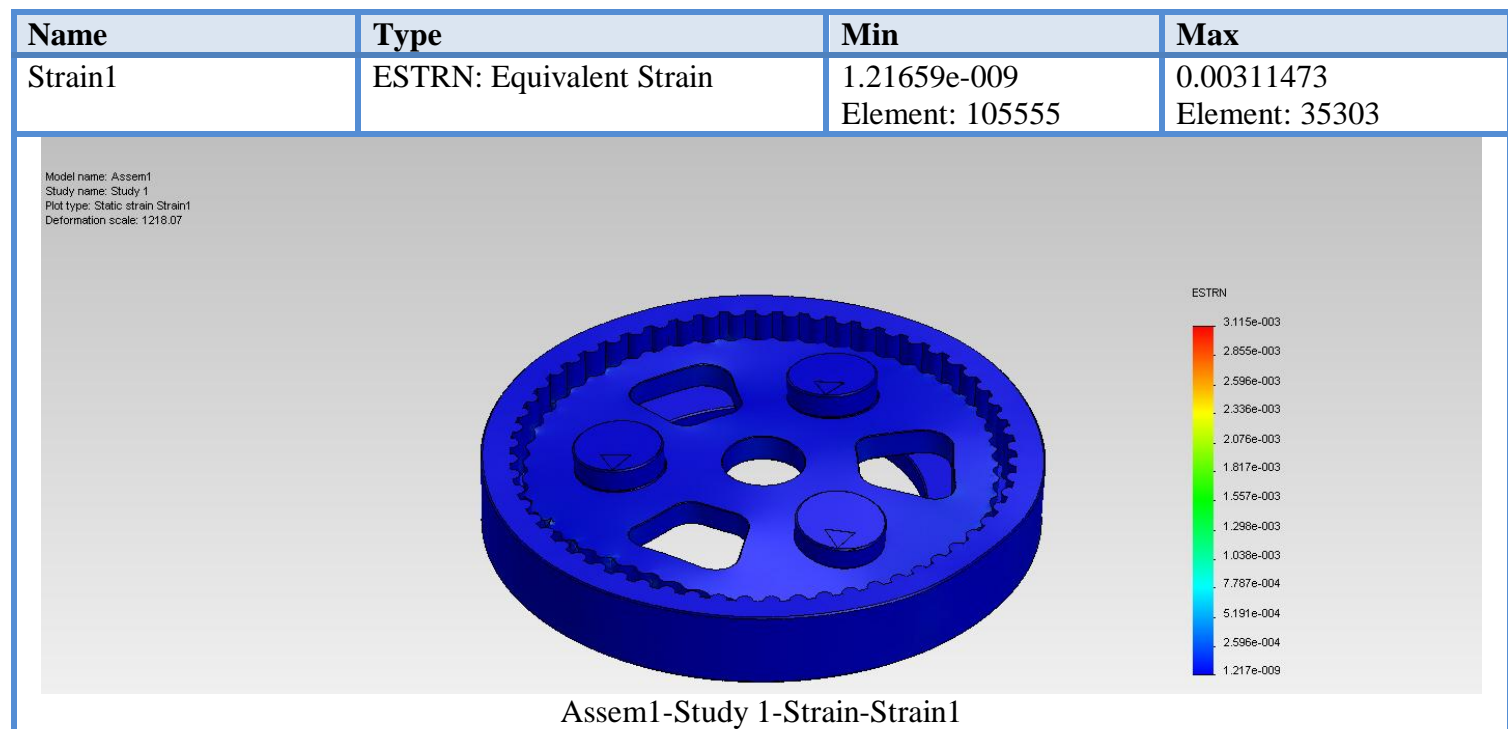


Table 4.11 Factor of Safety



2C. Input Shaft Results

Table 4.12. Model Information

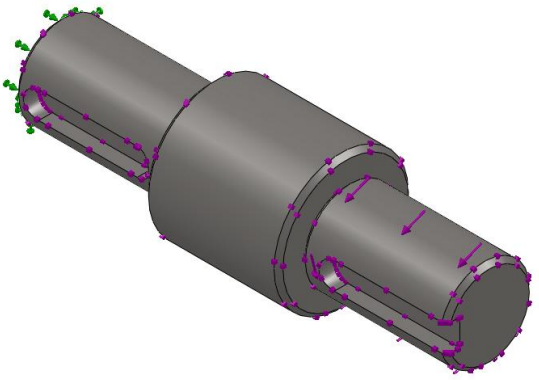
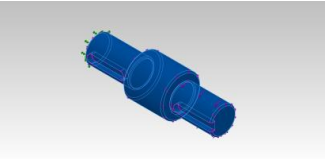
			
Model name: InputShaft Current Configuration: Default			
Solid Bodies			
Document Name and Reference	Treated As	Volumetric Properties	Document Path/Date Modified
Chamfer3 	Solid Body	Mass:0.31655 kg Volume:4.05834e-005 m^3 Density:7800 kg/m^3 Weight:3.10219 N	C:\Users\DELLi7\Desktop\I mputShaft.SLDPRT May 24 18:06:48 2012

Table 4.13. Study Properties

Study name	Study 1
Analysis type	Static
Mesh type	Solid Mesh
Thermal Effect:	On
Thermal option	Include temperature loads
Zero strain temperature	298 Kelvin
Include fluid pressure effects from SolidWorks Flow Simulation	Off
Solver type	FFEPlus
Inplane Effect:	Off
Soft Spring:	Off
Inertial Relief:	Off
Incompatible bonding options	Automatic
Large displacement	Off
Compute free body forces	On
Friction	Off
Use Adaptive Method:	Off
Result folder	SolidWorks document (C:\Users\DELLi7\Desktop)

Table 4.14. Units

Unit system:	SI (MKS)
Length/Displacement	mm
Temperature	Kelvin
Angular velocity	Rad/sec
Pressure/Stress	N/m ²

Table 4.15. Material Properties

Model Reference	Properties	Components
	<p>Name: Plain Carbon Steel Model type: Linear Elastic Isotropic Default failure criterion: Unknown Yield strength: 2.20594e+008 N/m² Tensile strength: 3.99826e+008 N/m² Elastic modulus: 2.1e+011 N/m² Poisson's ratio: 0.28 Mass density: 7800 kg/m³ Shear modulus: 7.9e+010 N/m² Thermal expansion coefficient: 1.3e-005 /Kelvin</p>	SolidBody 1(Chamfer3)(InputShaft)
Curve Data:N/A		

Table 4.16. Load

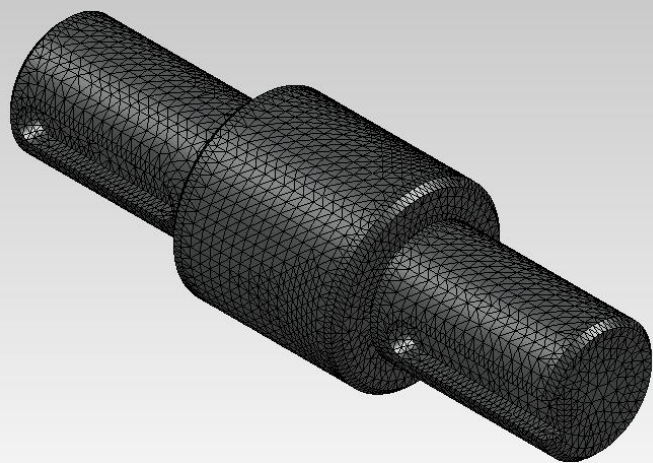
Load name	Load Image	Load Details
Torque-1		<p>Entities: 1 face(s) Type: Apply torque Value: 26.3 N-m</p>

Table 4.17. Mesh Information

Mesh type	Solid Mesh
Mesher Used:	Standard mesh
Automatic Transition:	Off
Include Mesh Auto Loops:	Off
Jacobian points	4 Points
Element Size	1.71883 mm
Tolerance	0.0859414 mm
Mesh Quality	High
Total Nodes	122152

Total Elements	84271
Maximum Aspect Ratio	52.914
% of elements with Aspect Ratio < 3	99.5
% of elements with Aspect Ratio > 10	0.00119
% of distorted elements(Jacobian)	0
Time to complete mesh(hh:mm:ss):	00:00:07
Computer name:	DELLI78GB

Model name: InputShaft
 Study name: Study 1
 Mesh type: Solid mesh



Mesh Control Name	Mesh Control Image	Mesh Control Details
Control-1		Entities: 36 edge(s) Units: mm Size: 0.859414 Ratio: 1.5

Table 4.18. Stress

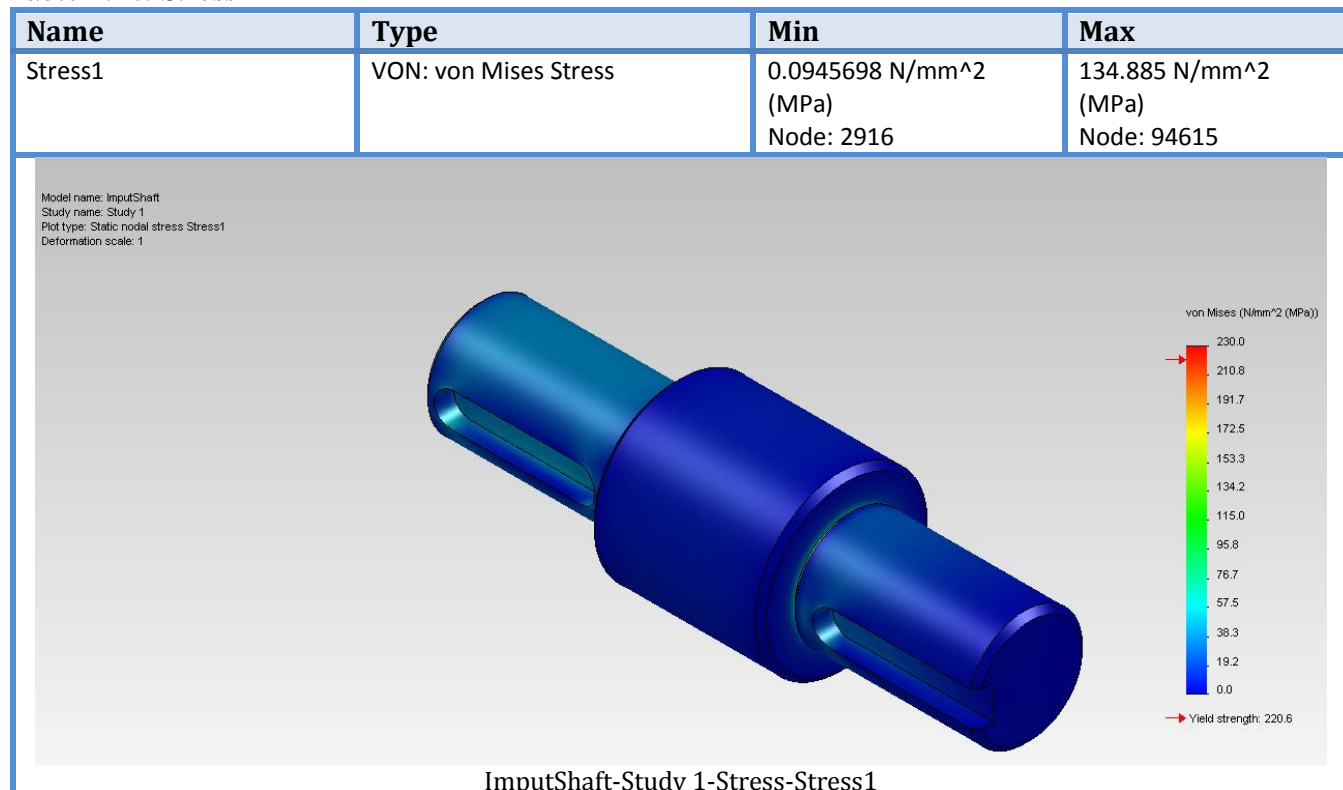


Table 4.19. Displacement

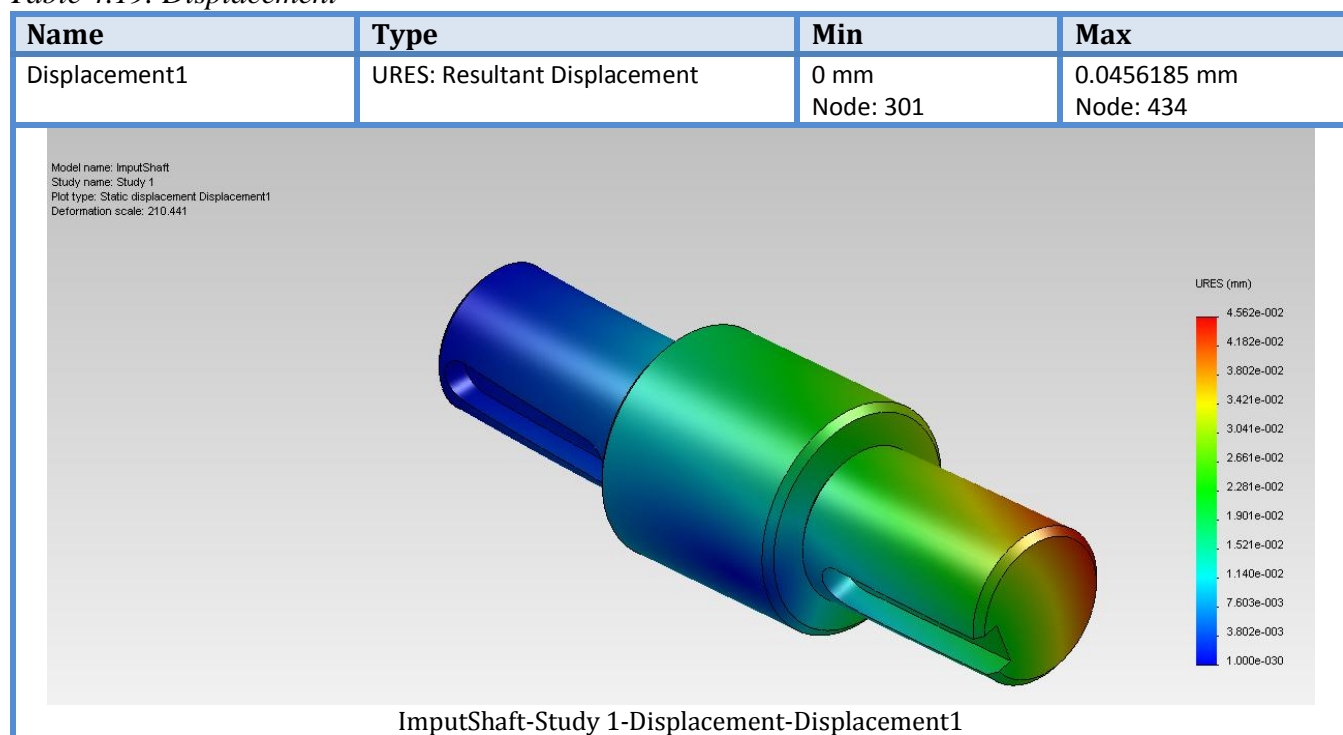


Table 4.20. Strain

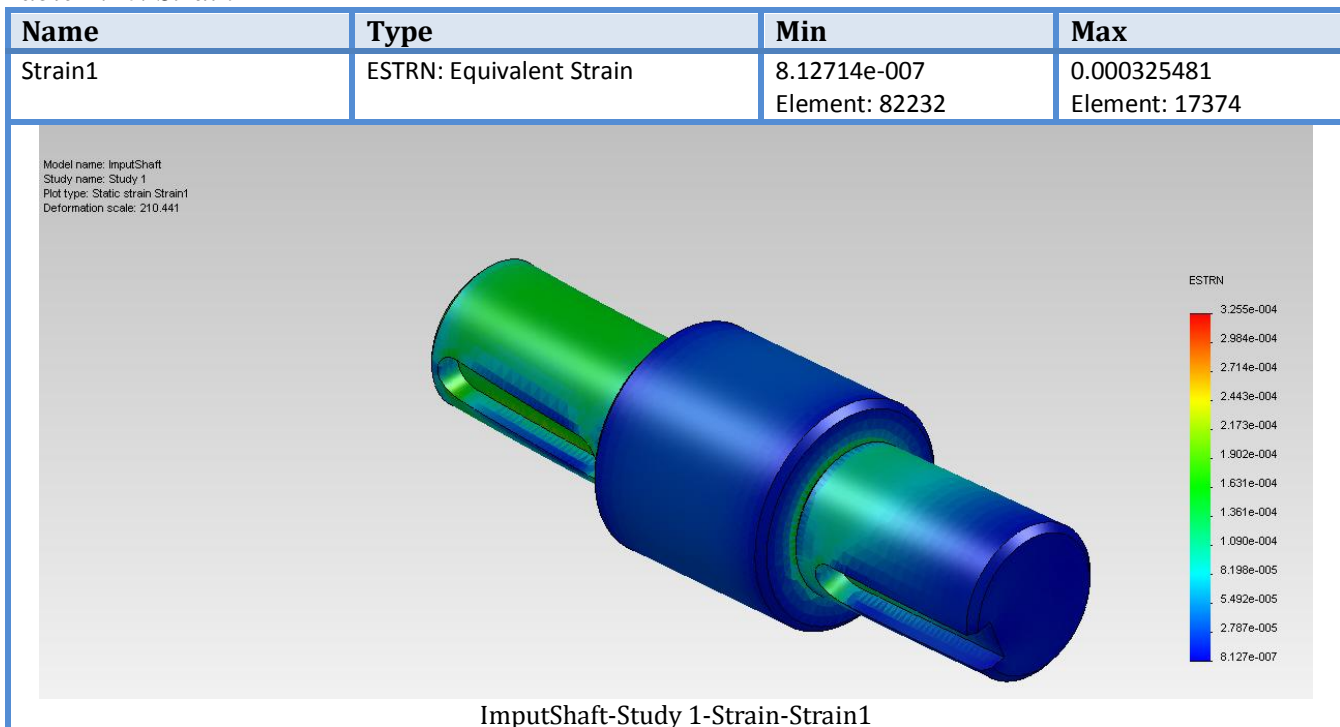
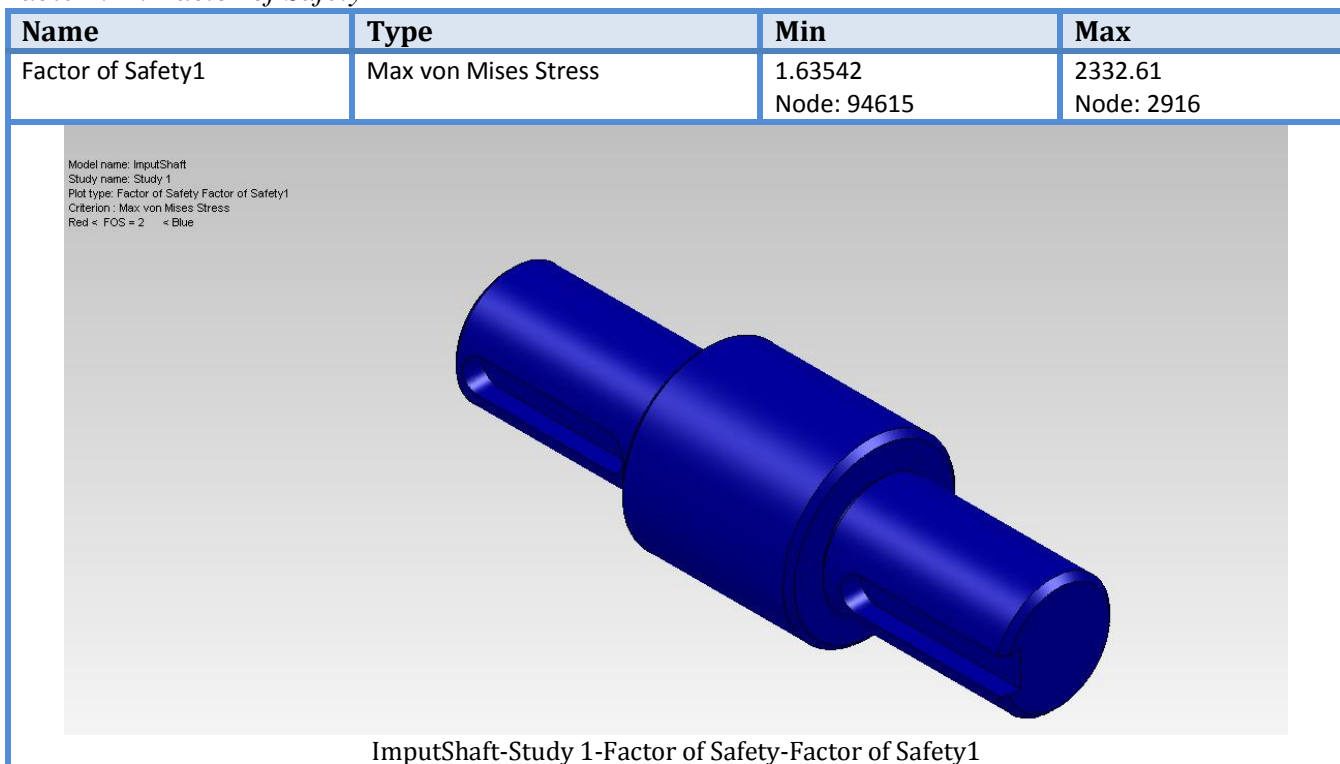


Table 4.21. Factor of Safety



3C. Output Shaft Results

Table 4.22. Model Information

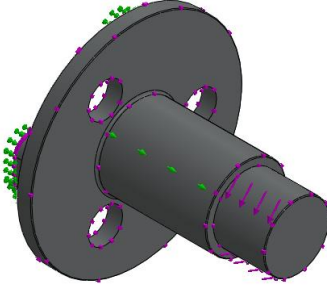
			
Model name: Output Shaft Current Configuration: Default			
Solid Bodies			
Document Name and Reference	Treated As	Volumetric Properties	Document Path/Date Modified
Chamfer3 	Solid Body	Mass:26.5767 kg Volume:0.00340727 m ³ Density:7800 kg/m ³ Weight:260.452 N	C:\Users\DELLi7\Desktop\Solid\Part10.SLDPRT May 24 18:20:17 2012

Table 4.23. Study Properties

Study name	Study 1
Analysis type	Static
Mesh type	Solid Mesh
Thermal Effect:	On
Thermal option	Include temperature loads
Zero strain temperature	298 Kelvin
Include fluid pressure effects from SolidWorks Flow Simulation	Off
Solver type	FFEPlus
Inplane Effect:	Off
Soft Spring:	Off
Inertial Relief:	Off
Incompatible bonding options	Automatic
Large displacement	Off
Compute free body forces	On
Friction	Off
Use Adaptive Method:	Off
Result folder	SolidWorks document (C:\Users\DELLi7\Desktop\Solid)

Table 4.24. Units

Unit system:	SI (MKS)
Length/Displacement	mm
Temperature	Kelvin
Angular velocity	Rad/sec
Pressure/Stress	N/m ²

Table 4.25. Material Properties

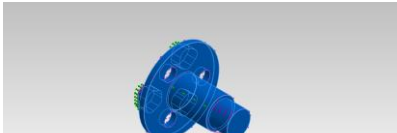
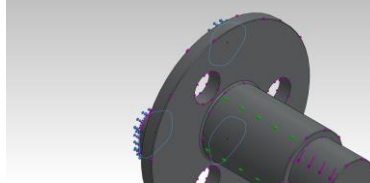
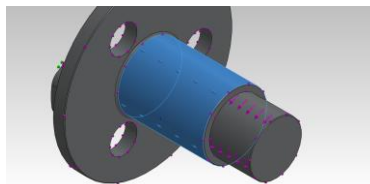
Model Reference	Properties	Components
	<p>Name: Plain Carbon Steel Model type: Linear Elastic Isotropic Default failure criterion: Unknown Yield strength: 2.20594e+008 N/m² Tensile strength: 3.99826e+008 N/m² Elastic modulus: 2.1e+011 N/m² Poisson's ratio: 0.28 Mass density: 7800 kg/m³ Shear modulus: 7.9e+010 N/m² Thermal expansion coefficient: 1.3e-005 /Kelvin</p>	SolidBody 1(Chamfer3)(Part10)
Curve Data:N/A		

Table 4.26. Loads and Fixtures

Fixture name	Fixture Image	Fixture Details		
Fixed-1		<p>Entities: 3 face(s) Type: Fixed Geometry</p>		
Resultant Forces				
Components	X	Y	Z	Resultant
Reaction force(N)	13.7777	0.888504	-0.321193	13.8101
Reaction Moment(N-m)	0	0	0	0
Roller/Slider-1				
		<p>Entities: 1 face(s) Type: Roller/Slider</p>		
Resultant Forces				
Components	X	Y	Z	Resultant
Reaction force(N)	-16.1683	124.928	15.6023	126.932
Reaction Moment(N-m)	0	0	0	0

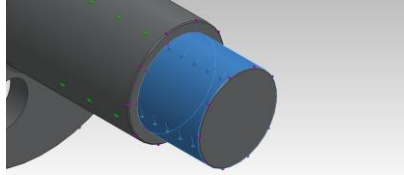
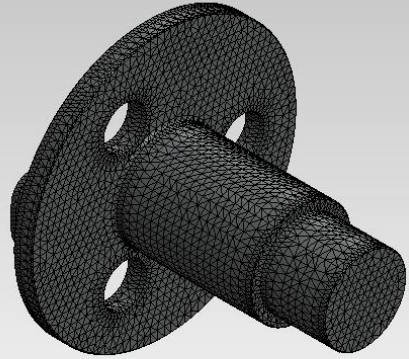
Load name	Load Image	Load Details
Torque-1		Entities: 1 face(s) Type: Apply torque Value: 6400 N·m

Table 4.27. Mesh Information

Mesh type	Solid Mesh
Mesher Used:	Standard mesh
Automatic Transition:	Off
Include Mesh Auto Loops:	Off
Jacobian points	4 Points
Element Size	7.52525 mm
Tolerance	0.376263 mm
Mesh Quality	High

Total Nodes	111439
Total Elements	73128
Maximum Aspect Ratio	9.584
% of elements with Aspect Ratio < 3	97.5
% of elements with Aspect Ratio > 10	0
% of distorted elements(Jacobian)	0
Time to complete mesh(hh:mm:ss):	00:00:08
Computer name:	DELLI78GB

Model name: Part10
Study name: Study 1
Mesh type: Solid mesh



Mesh Control Name	Mesh Control Image	Mesh Control Details
Control-1		Entities: 73 edge(s) Units: mm Size: 3.76263 Ratio: 1.5

Table 4.28. Stress

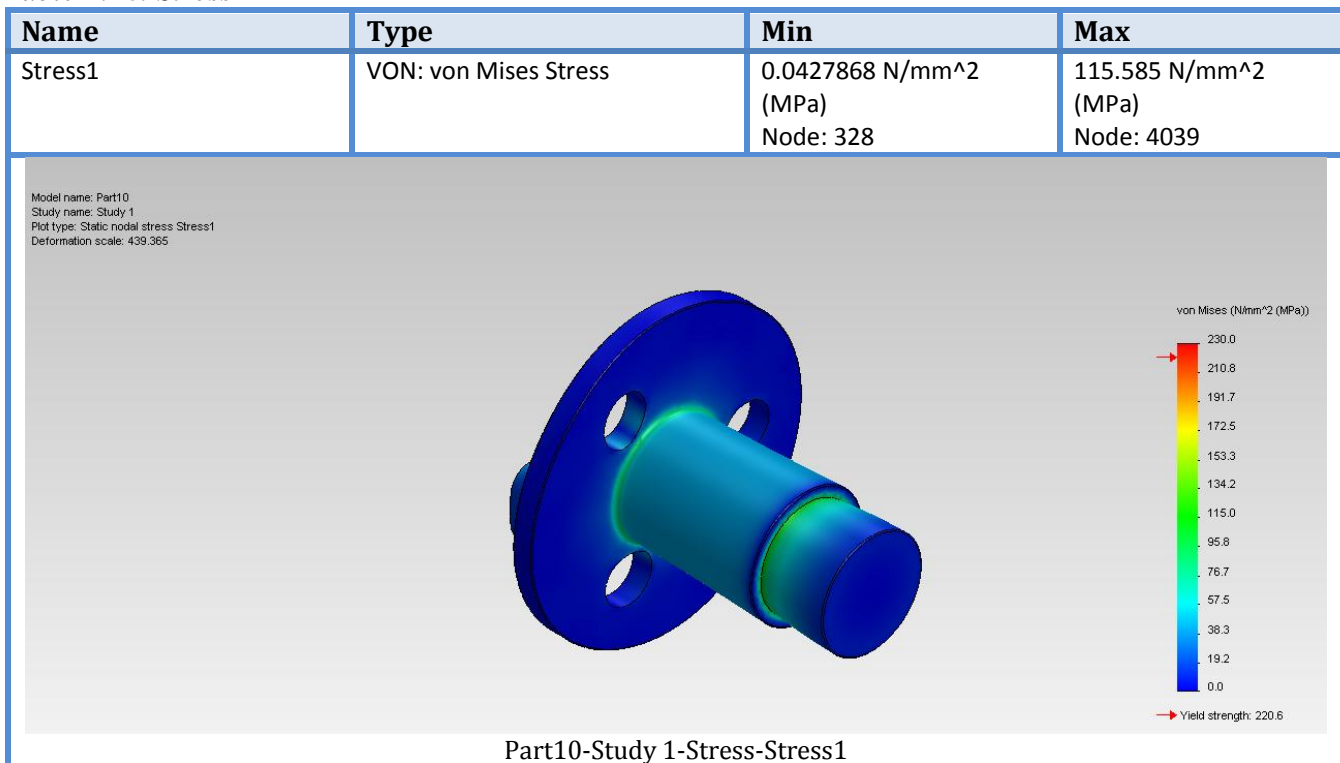


Table 4.29. Displacement

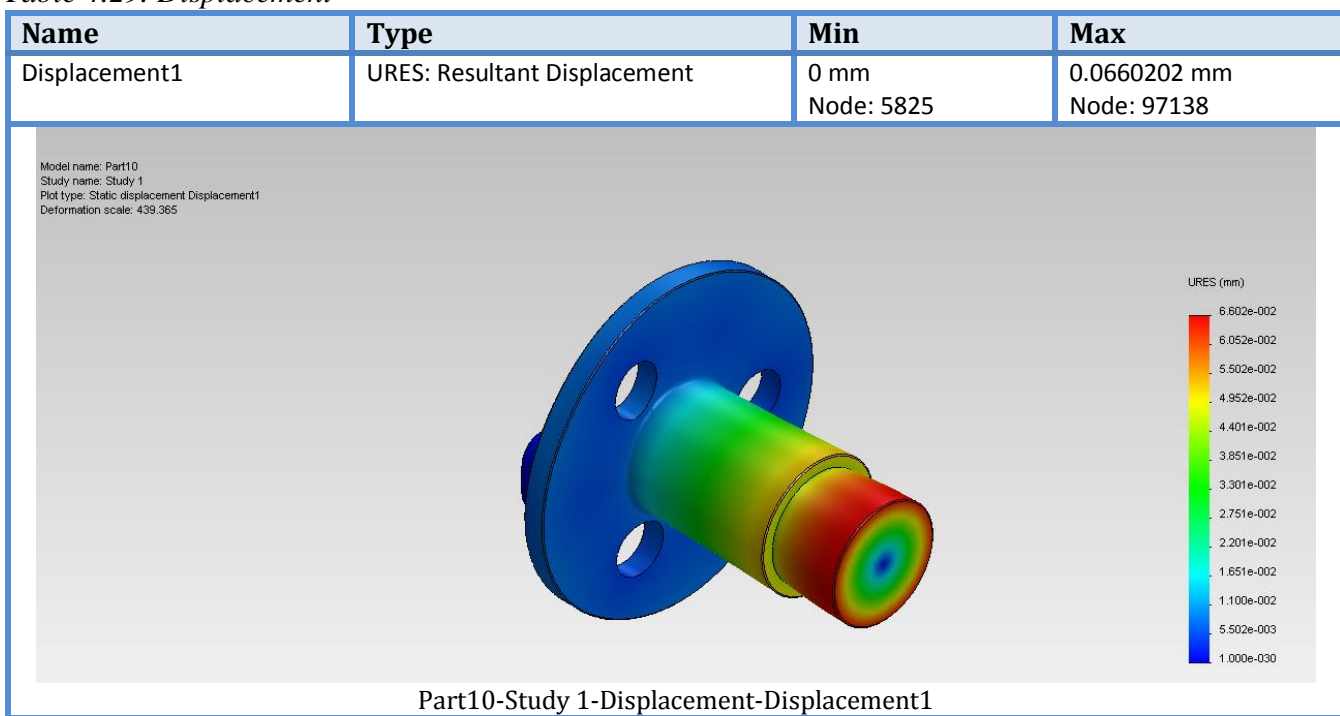


Table 4.30. Strain

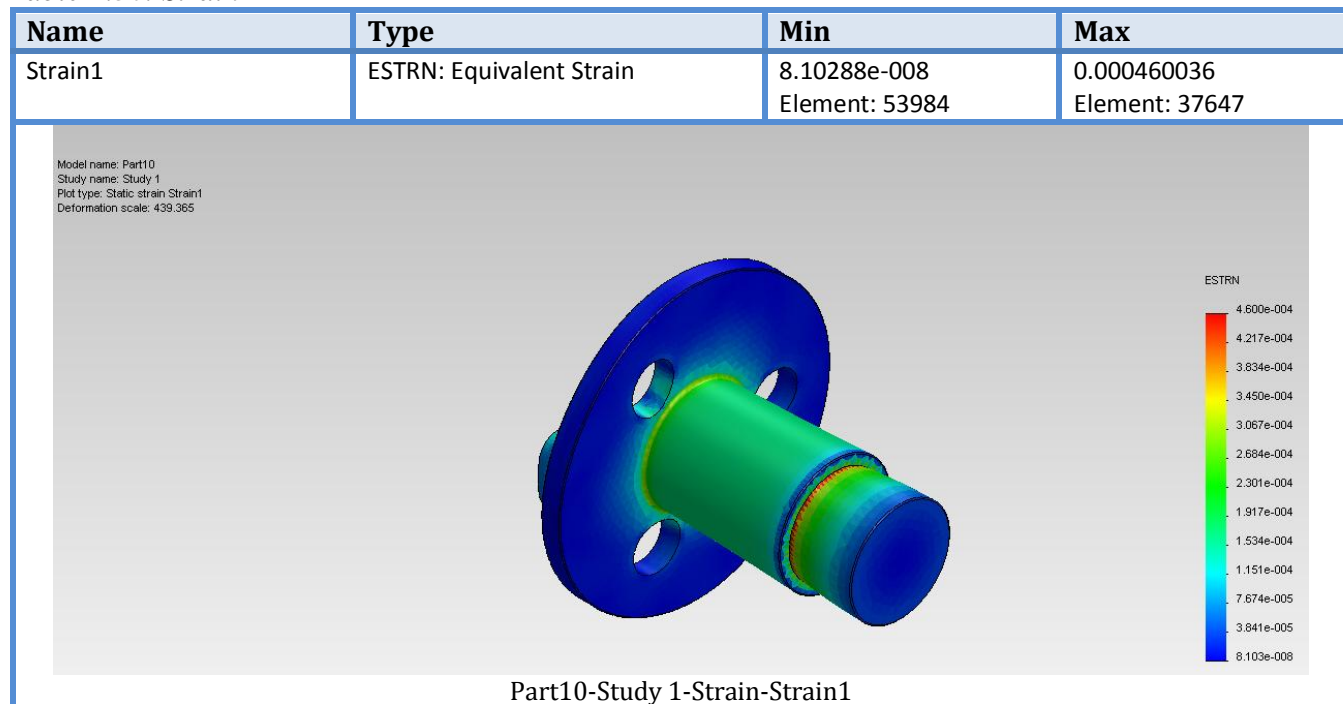
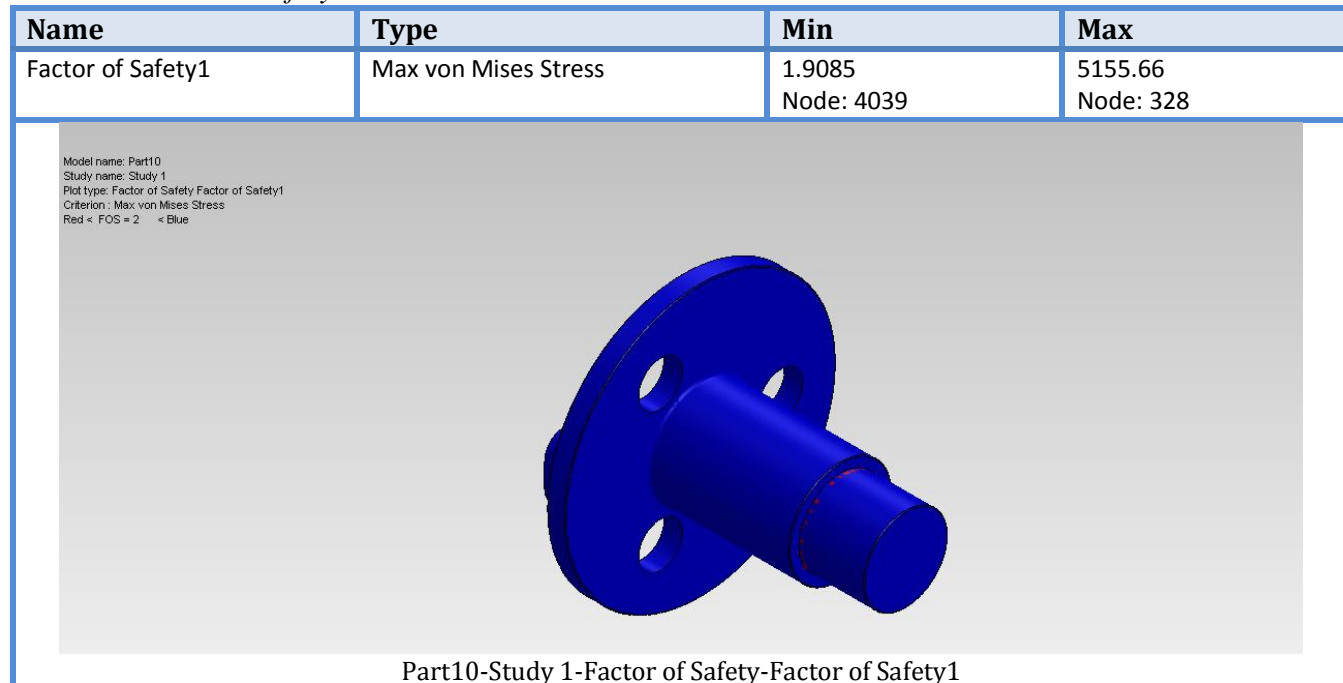


Table 4.31. Factor Safety



4C. Eccentric Shaft Results

Table 4.32. Model Information

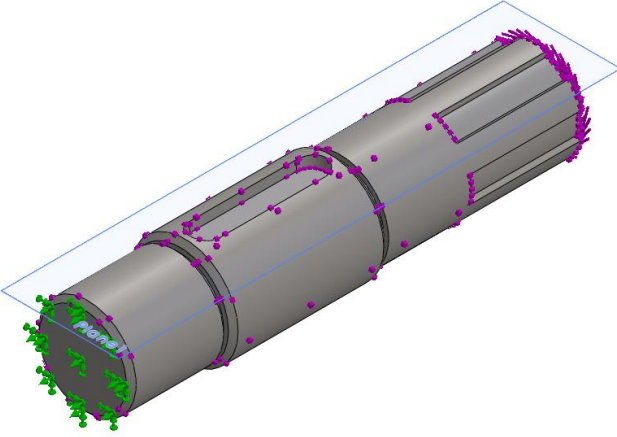
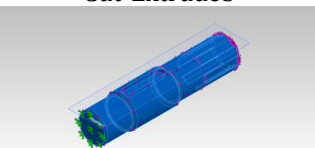
			
Model name: shaft Current Configuration: Default			
Solid Bodies			
Document Name and Reference	Treated As	Volumetric Properties	Document Path/Date Modified
Cut-Extrude3 	Solid Body	Mass:0.236455 kg Volume:3.03147e-005 m ³ Density:7800 kg/m ³ Weight:2.31726 N	C:\Users\DELLi7\Desktop\Solid\shaft.SLDPRT May 23 18:36:44 2012

Table 4.33. Study Properties

Study name	Study 1
Analysis type	Static
Mesh type	Solid Mesh
Thermal Effect:	On
Thermal option	Include temperature loads
Zero strain temperature	298 Kelvin
Include fluid pressure effects from SolidWorks Flow Simulation	Off
Solver type	FFEPlus
Inplane Effect:	Off
Soft Spring:	Off
Inertial Relief:	Off
Incompatible bonding options	Automatic
Large displacement	Off
Compute free body forces	On
Friction	Off
Use Adaptive Method:	Off
Result folder	SolidWorks document (C:\Users\DELLi7\Desktop\Solid)

Table 4.34. Units

Unit system:	SI (MKS)
Length/Displacement	mm
Temperature	Kelvin
Angular velocity	Rad/sec
Pressure/Stress	N/m ²

Table 4.35. Material Properties

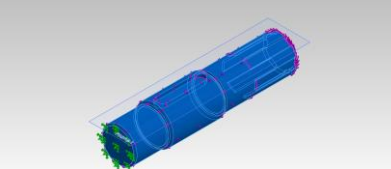
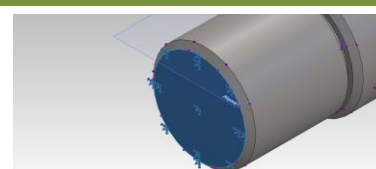
Model Reference	Properties	Components
	<p>Name: Plain Carbon Steel Model type: Linear Elastic Isotropic Default failure criterion: Unknown Yield strength: 2.20594e+008 N/m² Tensile strength: 3.99826e+008 N/m² Elastic modulus: 2.1e+011 N/m² Poisson's ratio: 0.28 Mass density: 7800 kg/m³ Shear modulus: 7.9e+010 N/m² Thermal expansion coefficient: 1.3e-005 /Kelvin</p>	SolidBody 1(Cut-Extrude3)(shaft)
Curve Data:N/A		

Table 4.36. Loads and Fixtures

Fixture name	Fixture Image	Fixture Details															
Fixed-1		<p>Entities: 1 face(s) Type: Fixed Geometry</p>															
Resultant Forces																	
<table border="1"> <thead> <tr> <th>Components</th><th>X</th><th>Y</th><th>Z</th><th>Resultant</th></tr> </thead> <tbody> <tr> <td>Reaction force(N)</td><td>0.101737</td><td>-0.0974712</td><td>0.0701776</td><td>0.157404</td></tr> <tr> <td>Reaction Moment(N-m)</td><td>0</td><td>0</td><td>0</td><td>0</td></tr> </tbody> </table>			Components	X	Y	Z	Resultant	Reaction force(N)	0.101737	-0.0974712	0.0701776	0.157404	Reaction Moment(N-m)	0	0	0	0
Components	X	Y	Z	Resultant													
Reaction force(N)	0.101737	-0.0974712	0.0701776	0.157404													
Reaction Moment(N-m)	0	0	0	0													

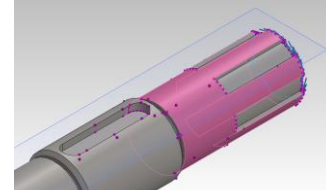
Load name	Load Image	Load Details
Torque-1		<p>Entities: 1 face(s) Reference: Face< 1 > Type: Apply torque Value: 36 N-m</p>

Table 4.37. Mesh Information

Mesh type	Solid Mesh
Mesher Used:	Curvature based mesh
Jacobian points	4 Points
Maximum element size	1.55957 mm
Minimum element size	0.519852 mm
Mesh Quality	High

Total Nodes	288067
Total Elements	199071
Maximum Aspect Ratio	4.6466
% of elements with Aspect Ratio < 3	99.8
% of elements with Aspect Ratio > 10	0
% of distorted elements(Jacobian)	0
Time to complete mesh(hh:mm:ss):	00:00:11
Computer name:	DELLI78GB



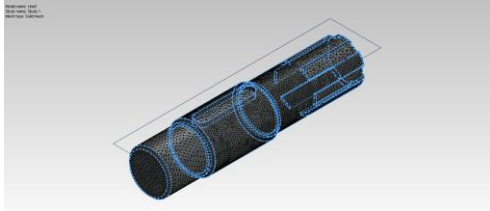
Mesh Control Name	Mesh Control Image	Mesh Control Details
Control-1		Entities: 116 edge(s), 2 face(s) Units: mm Size: 0.779785 Ratio: 1.5

Table 4.38. Stress

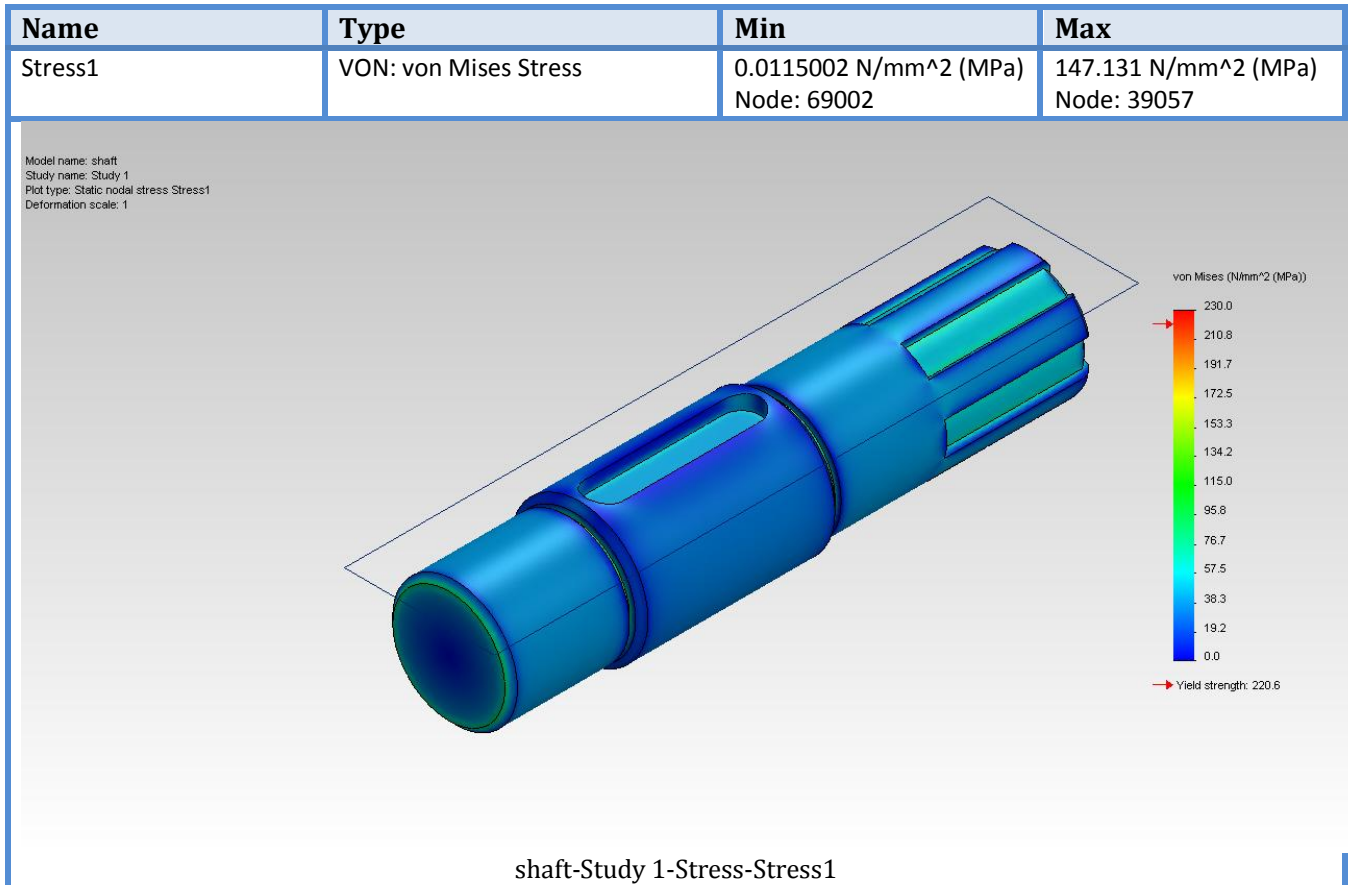


Table 4.39. Displacement

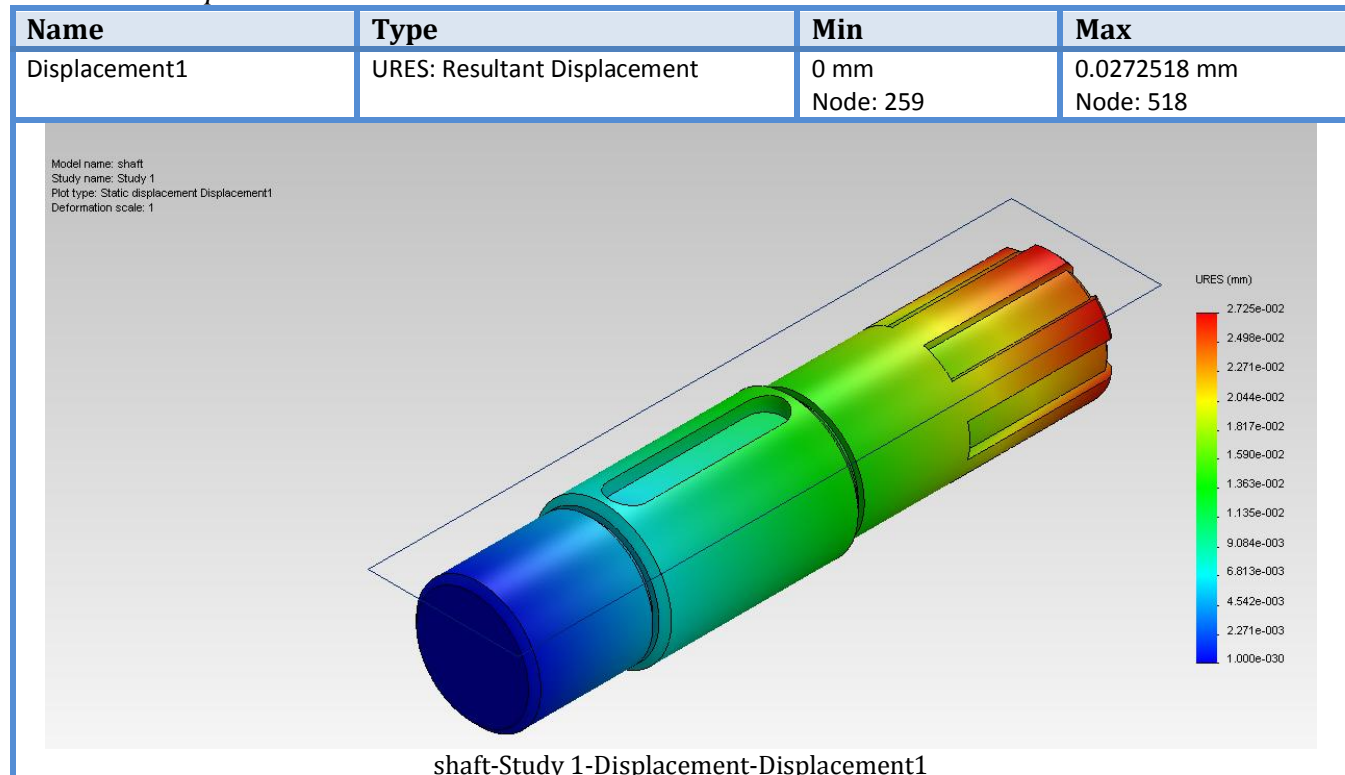


Table 4.40. Strain

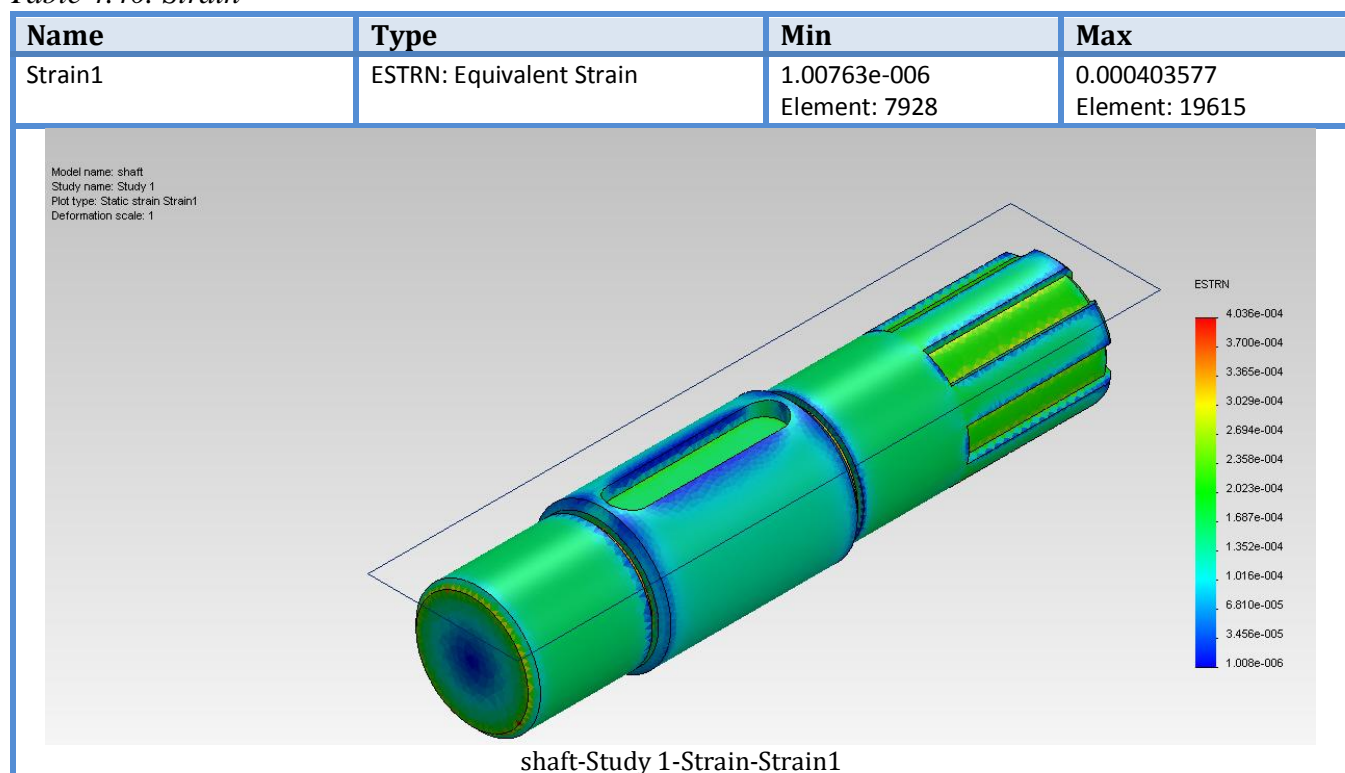
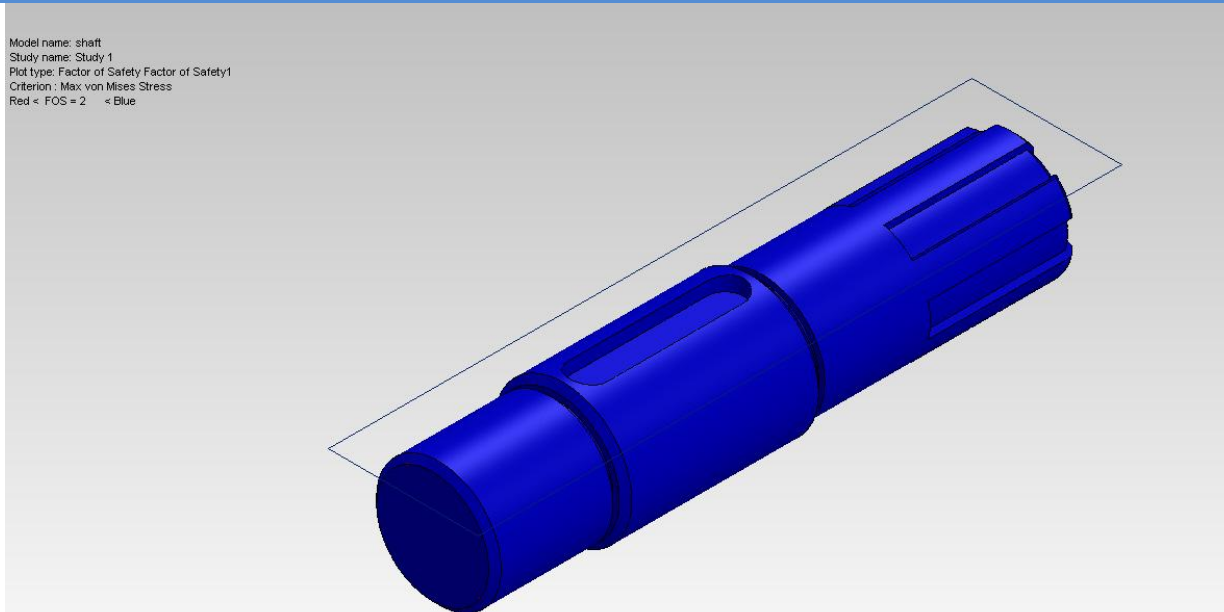


Table 4.41. Table Factor of Safety

Name	Type	Min	Max
Factor of Safety1	Max von Mises Stress	1.4993 Node: 39057	19181.7 Node: 69002



shaft-Study 1-Factor of Safety-Factor of Safety1

Appendix 4 - Drawings

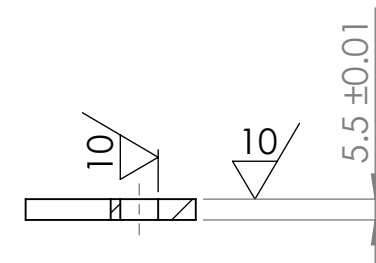
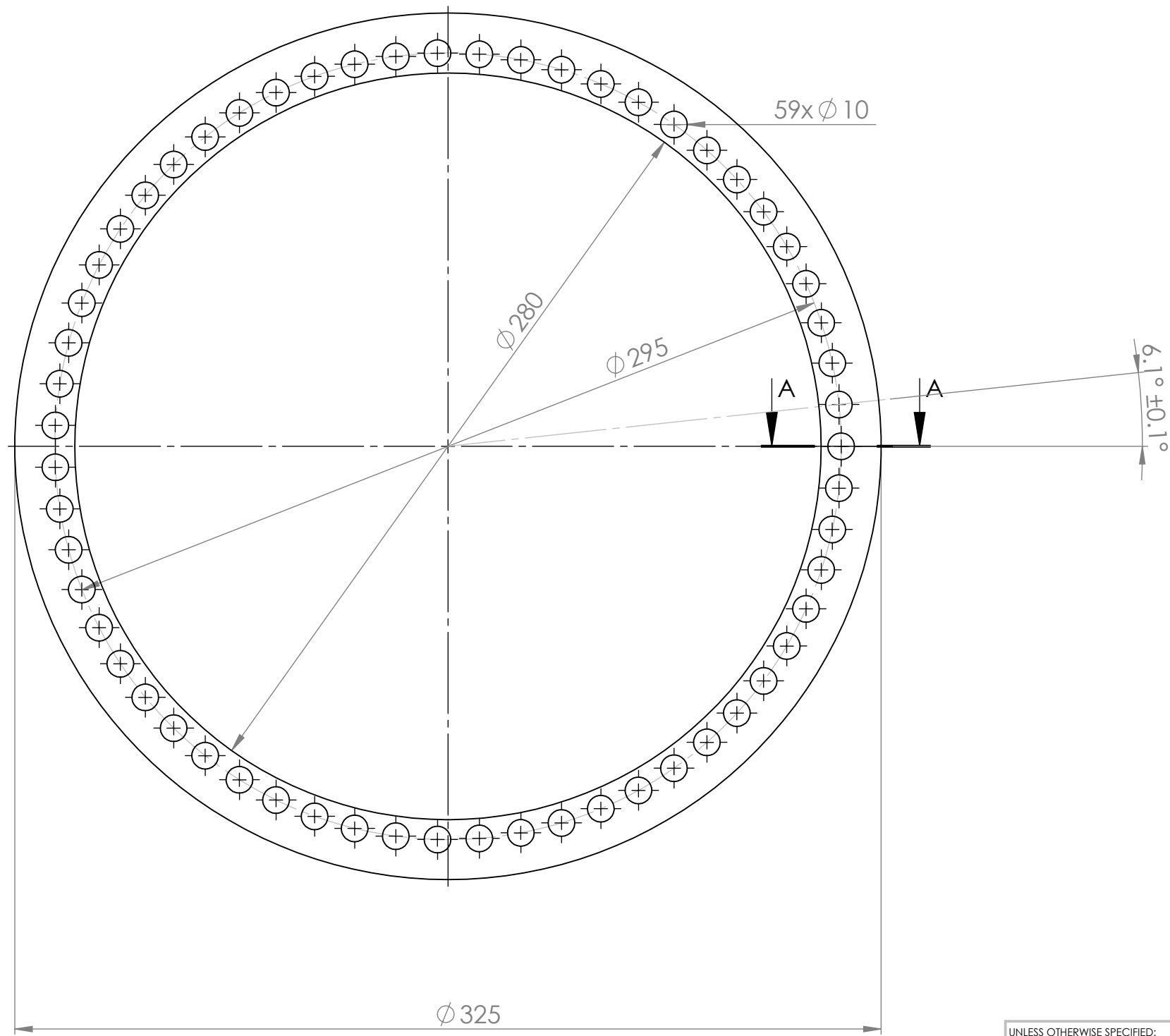
DWG No. 1/5 – Gasket

DWG No. 2/5 – Cycloid Wheel

DWG No. 3/5 – Pin

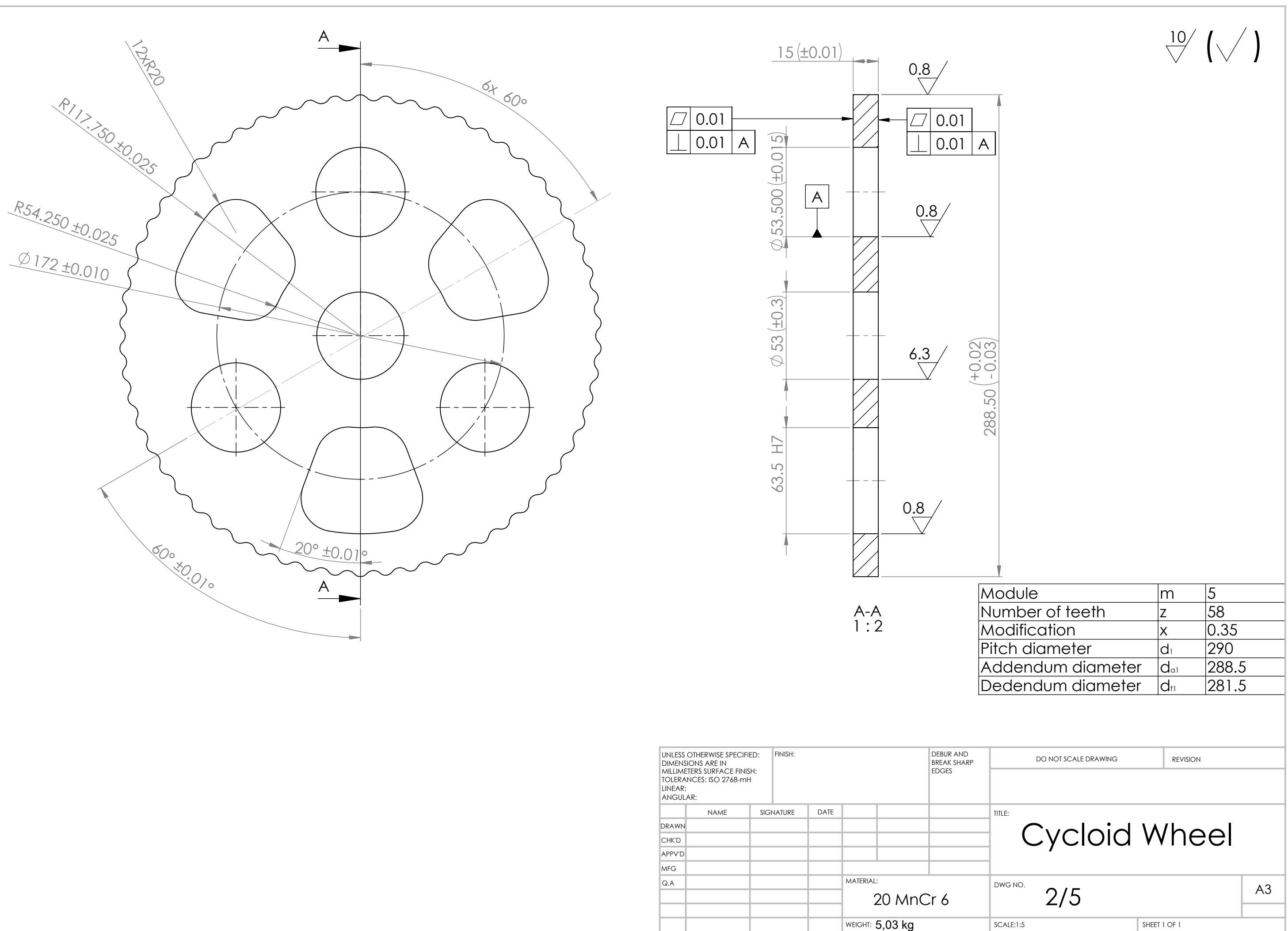
DWG No. 4/5 – Housing

DWG No. 5/5 – Cycloid Stage

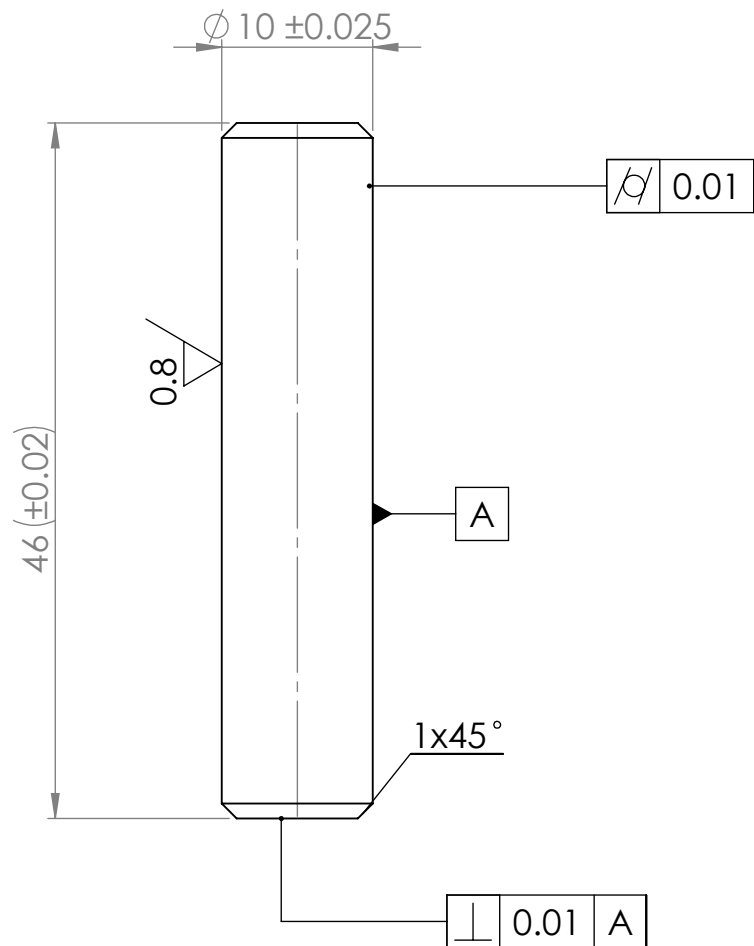


A-A
1:2

UNLESS OTHERWISE SPECIFIED: DIMENSIONS ARE IN MILLIMETERS SURFACE FINISH: TOLERANCES: LINEAR: ISO 2768-mH ANGULAR:		FINISH:	10 /		DEBUR AND BREAK SHARP EDGES	DO NOT SCALE DRAWING	REVISION
<p style="text-align: center;">Linnaeus University, Vaxjo</p> <p style="text-align: center;">Gasket</p>							
DRAWN	NAME	SIGNATURE	DATE			TITLE: DWG NO.	
CHK'D							
APPV'D							
MFG							
Q.A	MATERIAL: Cast Alloy Steel				1/5	A3	
	WEIGHT: 0,67 kg				SCALE:1:5	SHEET 1 OF 1	



10/ (✓)



UNLESS OTHERWISE SPECIFIED:
DIMENSIONS ARE IN
MILLIMETERS SURFACE FINISH:
TOLERANCES:ISO 2768-mH
LINEAR:
ANGULAR:

FINISH:

DEBUR AND
BREAK SHARP
EDGES

DO NOT SCALE DRAWING

REVISION

Linnaeus University, Vaxjo

DRAWN

CHK'D

APP'D

MFG

Q.A

TITLE:

Pin

MATERIAL:

Plain Carbon Steel

DWG NO.

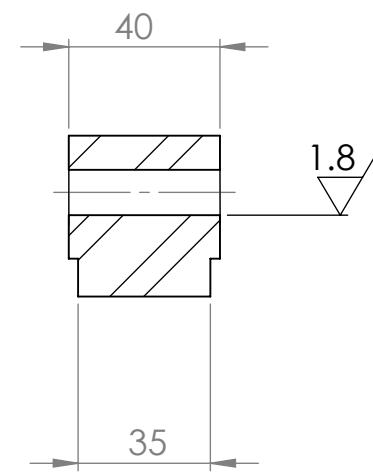
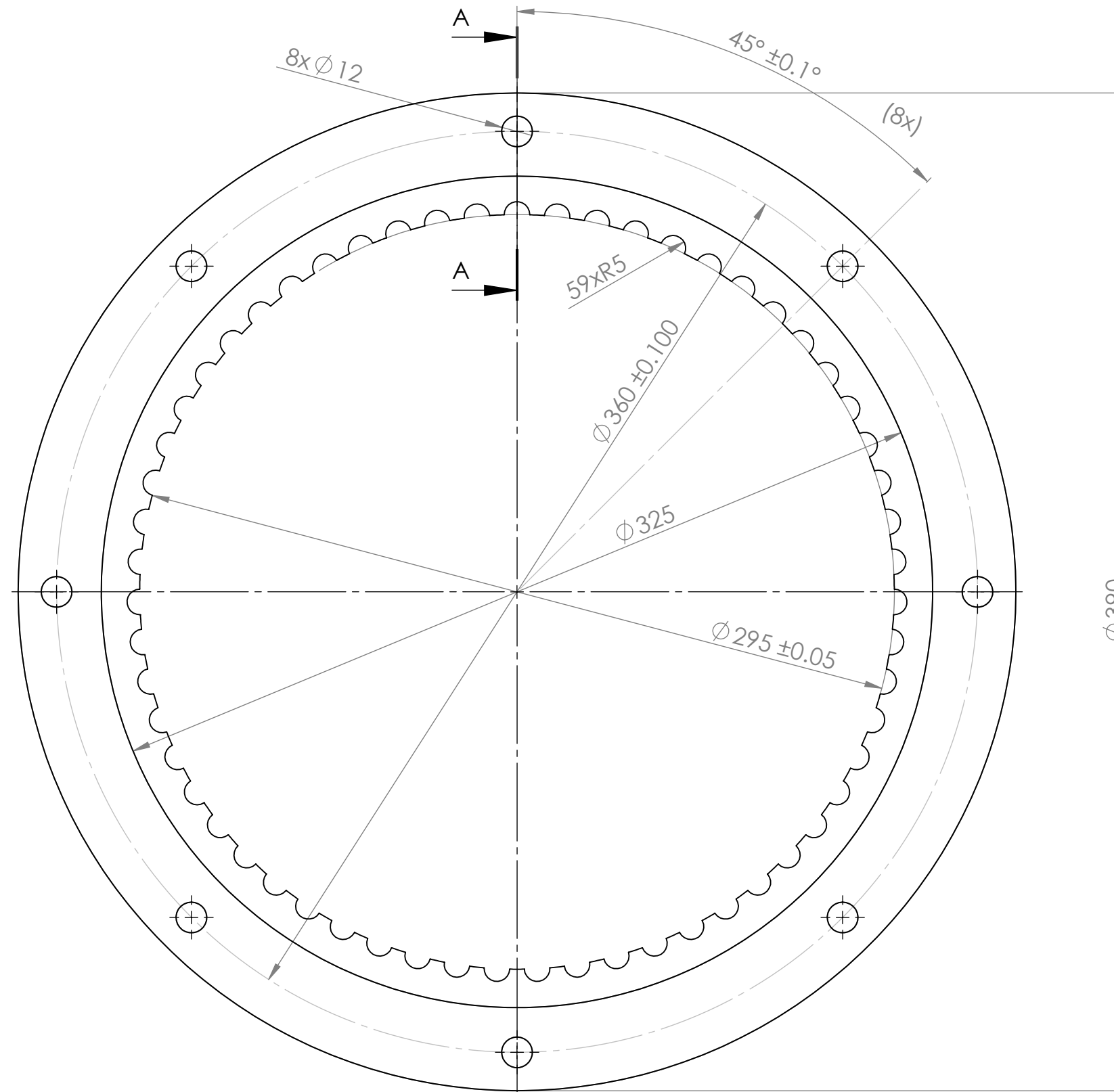
3/5

A4

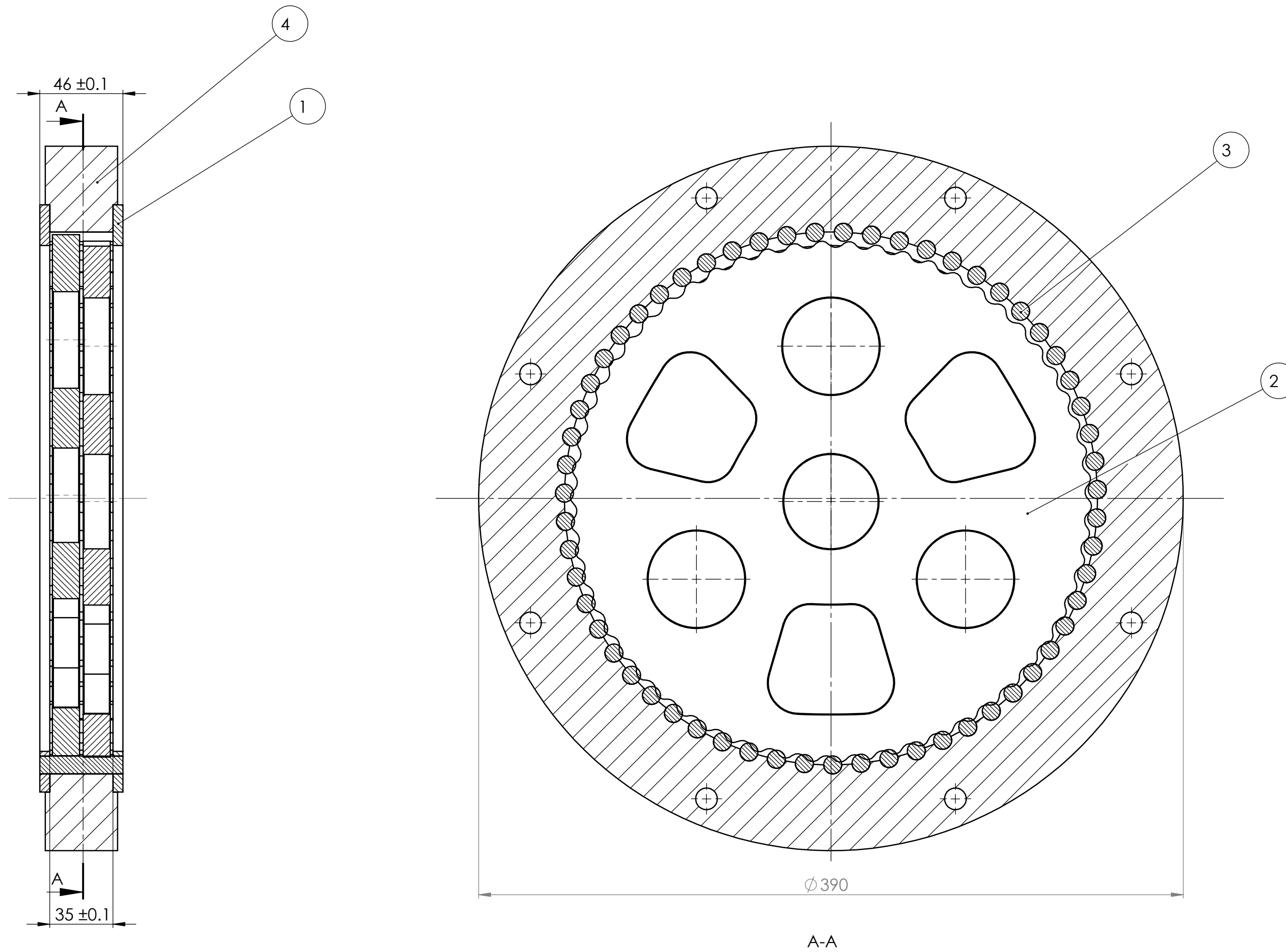
WEIGHT: 0.028 kg

SCALE:2:1

SHEET 1 OF 1



UNLESS OTHERWISE SPECIFIED: DIMENSIONS ARE IN MILLIMETERS SURFACE FINISH: TOLERANCES:ISO 2768-mH LINEAR: ANGULAR:		FINISH:			DEBUR AND BREAK SHARP EDGES	DO NOT SCALE DRAWING	REVISION
DRAWN		NAME	SIGNATURE	DATE			
CHK'D							
APPV'D							
MFG							
Q.A							
			TITLE:				
Linnaeus University, Vaxjo			Housing				
			DWG NO.			A3	
			4/5				
			SCALE:1:5			SHEET 1 OF 1	
			WEIGHT: 13.5 kg				



4 Housing
 3 Pin x59
 2 Cycloid Wheel
 1 Gasket

- DWG NO. 4/5
 - DWG NO. 3/5
 - DWG NO. 2/5
 - DWG NO. 1/5

UNLESS OTHERWISE SPECIFIED: DIMENSIONS ARE IN MILLIMETERS SURFACE FINISH: TOLERANCES: LINEAR: ANGULAR:		FINISH:	DEBUR AND BREAK SHARP EDGES	DO NOT SCALE DRAWING		REVISION
DRAWN	NAME	SIGNATURE	DATE			
CHKD						
APPV'D						
MFG						
Q.A.				MATERIAL:		
				WEIGHT:		
DWG NO.		5/5		SCALE 1:2		Sheet 1 of 1
						A2

TITLE: Linnaeus University, Vaxjo
Cycloid stage